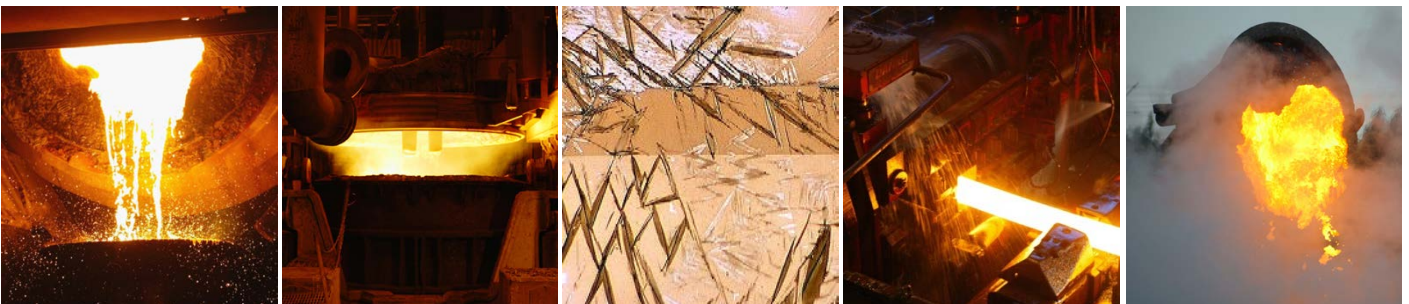


# Optimization of the Geometric Design of Moulds, in order to reduce the Energy Consumption for Continuous Casting of Slabs

(Energimyndighetens projektnr. 35337-1)

S. Peter Andersson, Swerea KIMAB  
Pavel E. Ramirez Lopez, Swerea MEFOS  
Tomas Sohlgren, SSAB EMEA, Oxelösund  
Arashk Memarpour and Bo Rogberg, Sandvik Materials  
Technology

Slutrapport JK 24055, utgiven 2013-12-20



**Foto:** Stig-Göran Nilsson och Mats Hillert

## Abstract

A full review of previous mould design work within the research programs of Jernkontoret has been carried out. Based on these design principles an Excel spreadsheet methodology has been developed. This resulted in two moulds being engineered and manufactured, one designed for blooms and one designed for slabs. The moulds have been instrumented with thermocouples. All the experiments were successfully carried out at SSAB EMEA Oxelösund and Sandvik Materials Technology. At SSAB EMEA the main activity was focused on improving the plate results. For SMT the main focus was to decrease or completely eliminate the appearance of corner cracks. The experiments at SMT as well as SSAB EMEA did not, however, show the expected and wanted results.

No improvements at and near the corners of the blooms and no improvement of the plate results could be found. The design of moulds is much more difficult than expected and several factors may have interacted to the outcome. The project generated, though, new ideas and gave a strong base of competence on how to proceed with mould design optimisation with good hope of success in the future regarding defect free continuous casting of advanced steel grades. This will be used in a continuation project within the member program of Swerea KIMAB.

*The project was funded by the Swedish Energy Agency, project 35337-1, the participating industrial companies and Technical area 24, Casting and solidification at Jernkontoret.*

**Keywords:** Mould design, slabs, blooms, mould, IMMODCO, continuous casting, corner angle contraction, solidification

## Sammanfattning

En fullständig översyn och genomgång av tidigare arbeten avseende design för stränggjutningskokiller inom Jernkontorets forskningsprogram har genomförts. Baserat på de principer som utvecklats inom dessa projekt har en metodik för kokilldesign i form av ett Excel-ark utvecklats. Med detta som underlag har två designade kokiller tagits fram och tillverkats, en avsedd för blooms hos Sandvik Materials Technology och en för slabs hos SSAB EMEA Oxelösund. Kokillerna har instrumenterats med termoelement. Alla experiment som utförts har varit lyckade med noggrann uppföljning av processen. Hos SSAB EMEA var det huvudsakliga arbetet inriktat på att förbättra plåtresultaten och för SMT att minska eller helt eliminera hörnsprickor.

Experimenten gav inte de förväntade och önskade resultaten. Inga förbättringar i eller nära hörnet för blooms och ingen förbättring av plåtresultat kunde påvisas. Att förbättra designen för stränggjutningskokiller visade sig vara mycket svårare än förväntat och flera faktorer kan ha samverkat till att de önskade resultaten inte kunde uppnås. Projektet genererade dock nya idéer och en stark kompetensbas om hur man kan gå vidare med förbättrad kokilldesign. Detta ger goda förhoppningar att i en framtid lyckas med defektfri stränggjutning av avancerade stålsorter som kommer att användas i ett fortsättningsprojekt inom Swerea KIMAB:s medlemsprogram.

*Projektet har finansierats av Energimyndigheten, projekt 35337-1, deltagande industriföretag samt Jernkontorets Teknikområde 24, Gjutning och stelning*

**Sökord:** Kokilldesign, slabs format, blooms format, IMMODCO, stränggjutning, hörnvinkelkontraktion, stelning

# TABLE OF CONTENTS

1. Introduction .....	6
2. Goals of the project .....	7
3. Summary of work carried out.....	7
4. The project has delivered .....	8
5. Development of a simulation program.....	9
5.1. Literature review (Pavel Ramirez Lopez) .....	9
5.2. Current design including IMMODOCO concept.....	10
5.3. Design principles for the new mould .....	11
5.3.1. Strand perimeter shrinkage concept .....	11
5.3.2. Deduction of $\Delta T$ .....	13
5.3.3. Thermal expansion coefficient treatment.....	16
5.3.4. Thickness shrinkage and bending (convex mould).....	17
5.3.5. Separate face design concept.....	20
5.3.6. Combining shrinkage predictions and dimensioning.....	20
5.4. Design program and spreadsheet layout.....	22
5.5. Mould design for SSAB Oxelösund.....	24
5.5.1. Modifications to design due to machining .....	30
5.6. Mould design for SMT .....	33
5.6.1. Description of the SMT blooms machine equipped with a plate mould.....	33
5.6.2. New design of parallel plates to obtain an improved corner angel distribution.....	35
5.6.3. Change of reference design radius .....	36
5.6.4. Parabolic design of the fixed and loose wide side .....	38
5.6.5. Machining of the mould .....	39
6. Experiments and evaluation of optimal mould for SMT in Sandviken.....	39
6.1. Instrumentation of the design mould.....	39
6.2. Thermocouples .....	44
6.2.1. Numbering of thermocouples.....	44
6.3. Results SMT.....	45
6.3.1. Heat Number 537742 (single, stainless steel). .....	45
6.3.2. Heat Number 537740 and 537741 (sequence, stainless steel) .....	47
6.3.3. Heat Number 537766 and 53767 (sequence, carbon steel).....	47
6.3.4. Heat Number 537731 (single, stainless steel high Ni).....	49
6.3.5. Heat Number 537738 and 537739 (sequence, stainless steel) .....	50
6.3.6. Heat Number 537766 (carbon steel, new design) and Heat Number 537944 (carbon steel, old design).....	52

6.3.7. Heat Number 537731 (stainless steel high Ni, new design) and Heat Number 537399 (stainless steel high Ni, old design).....	53
6.4. Conclusions and future work for SMT.....	54
7. Experiments and evaluation of optimal mould for SSAB EMEA Oxelösund .....	55
7.1. Instrumentation of the design mould.....	55
7.2. Logger, calibration and inaccuracy .....	56
7.2.1. Logger .....	56
7.2.2. Calibration of type K thermocouples with SCXI logger.....	56
7.2.3. Temperature error using the SCXI-1125 with SCXI-1600 device (inaccuracy)....	56
7.3. Results from the temperature measurements .....	58
7.3.1. Numbering of thermocouples.....	58
7.3.2. Sequence Number 25733 (single) .....	59
7.3.3. Sequence Number 25735 .....	61
7.3.4. Sequence number 25737 .....	63
7.3.5. Sequence number 25740 .....	64
7.3.6. Tilting trials sequence number 25740 .....	65
7.3.7. Sequence number 25742 .....	67
7.3.8. Sequence number 25745 (single).....	68
7.3.9. Sequence number 25747 .....	69
7.3.10. Sequence number 25749 .....	70
7.3.11. Sequence number 24751 and 25753.....	71
7.4. Summary of measurements of temperature in the mould .....	71
7.5. Plate quality results .....	76
7.6. Conclusions .....	76
8. Potentials of energy savings by using optimised CC moulds .....	81
9. Suggestions for further research and implementation efforts .....	82
10. Acknowledgement.....	82
11. References .....	83

## **Bilaga 1**

Projektorganisation och deltagare

# 1. INTRODUCTION

The main purpose of the project is to avoid surface cracks for crack sensitive steel grades; for example, steels undergoing the peritectic transformation during solidification. For these steel grades, there is both a need to reduce the solidification and cooling rates, as well as to develop as uniform heat transfer as possible to avoid crack formation.

The mould in a continuous casting machine is the "heart" of the process, where all the surfaces of the slabs or blooms are formed and its quality is determined. During solidification the steel shell grows and shrinks. These effects are particularly strong near the corners. The shrinkage has to be compensated by the mould taper or mould design in order to avoid poor thermal contact between the shell (strand) and mould. This is mainly done by setting a correct taper of the wide and narrow faces which could match the shrinkage of the steel for a given casting speed. Casting speed is the dominant parameter for shell growth, but also the heat flow to the mould through the slag film is an important factor to be taken into account. Additionally, the mould needs to be optimal in a geometrical sense to avoid poor thermal contact between the mould and strand corners where shrinkage is higher; which could result in re-heating, abnormal grain growth, tension-building and increased risk of cracking. To crack sensitive grades, a poor support in the corners leads to increased risk of breakout and limits the casting speed and by that the productivity.

Surface distributed cracks require surface conditioning (flame scarfing or grinding), or in the worst case scenario, scrapping of the whole slab. The benefits of avoiding or reducing surface cracks include reduced energy and labour costs by lowering material losses due to re-melting, grinding and casting again to reach the required steel throughput. Moreover, lowering the waste is equal to lowering the cost of producing sensitive, difficult and advanced steel grades giving an overall higher competitive opportunity for the steel companies as well as allowing a more environmentally friendly production.

Extensive work has been carried out between 1997 and 2005 at Jernkontoret (Technical area 24, Casting and solidification) regarding improvements in the mould design. This extensive work has been mainly focused on how the corner region of the solidifying product shrinks and what adjustments of the mould shape should be made to account for this shrinkage. The work has been conducted by the former Institute for Metals Research, now Swerea KIMAB.

The outcome of that work was a mould with corner angles more than 90 degrees at the top that gradually change to exactly 90 degrees at the mould end (straight corners). Since the wide faces were not altered; the whole contribution of angle was concentrated to the narrow faces. This design was called IMMODOCO (IM MOuld Design Concept). Several trials with IMMODOCO have been conducted and the design has proven successful in improving the surface quality of slabs and blooms. There is little or no additional cost to manufacture IMMODOCO moulds and no increased mould wear could be detected. There were only benefits using a better mould support in the corner region, which has been confirmed through long-term use of these moulds for bloom casting at Sandvik Materials Technology and slab casting for the 220 mm thickness at SSAB EMEA Oxelösund. However, translating the successful results to thicker slabs has not been straightforward and IMMODOCO didn't produce the desired results for 290 mm slab thickness at SSAB EMEA.

This can be attributed to the fact that the increased angle on top should be different for thicker slabs as well as the taper along the mould length which is linear for the IMMODOCO concept. Several full-scaled experiments have been made to further validate the mould design concept (IMMODOCO) after the project was closed. However, linking the IMMODOCO concept to parabolic taper and other variations in the mould shape has not so far been investigated.

The current project is a follow-up to include further aspects of a mould design, which relate how the horizontal shape between the corner regions should be constructed in the mould. Another important design feature is how the built-in mould taper should be distributed along the mould length. Both design aspects have been analysed in the current project. Additionally, from a design point of view; it is important to develop the local know-how to construct a mould which follows and balances the shrinkage of the strand and exhibits uniform heat transfer along the whole length, without shaping the mould for only one steel grade.

## **2. GOALS OF THE PROJECT**

The overall goal of the project is to reduce the energy consumption for continuous casting by reducing the need of surface treatment and the amount of wasted material due to surface defects. The following milestones were defined to achieve this:

- Develop a design program based on Excel spreadsheets that calculate the optimal geometrical design of the mould for selected steel grades and casting speeds for both slabs and blooms.
- Conduct trials at SSAB EMEA Oxelösund (Hereafter SSAB) with a mould design based on the previously developed program for casting 290 mm thick slabs. Verify the expected improvement in terms of surface quality regarding off-corner cracks.
- Conduct trials at Sandvik Materials Technology (Hereafter SMT) using an optimally designed bloom mould based on the design program. Verify that the thermal contacts and the surface quality are improved compared to ordinary moulds. A successful outcome of the trials of an optimal geometrical CC mould may also give opportunities to cast steel grades which are currently produced by ingot casting.

## **3. SUMMARY OF WORK CARRIED OUT**

For both SSAB and SMT:

- A design program based on Excel spreadsheets for designing slab and bloom moulds has been developed.
- Design of moulds for slab and bloom casting based on the Excel program has been carried out.
- Both mould designs have been machined and instrumented with thermocouples.

Summary of SSAB trials:

- 15 heats have been casted with the new designed moulds.
- Thermocouple readings and samples of the as cast material have been taken.
- Analysis of the heats was performed with the following results:

- The thermocouple temperatures during casting at the narrow face centreline was very low compared to thermocouple temperatures at the corners.
- The heat extraction through the narrow sides in relation to the heat extraction through the wide sides was lower than normal, probably due to air gap at the gullwing body.
- The new mould design has not produced entirely the expected results since the microstructure in the centre of the narrow face is coarser than expected (due to lack of contact). This also produced significant bulging in the narrow face.
- The microstructure in the corners is more fine grained and better contact has been achieved in upper parts of mould. The fine grained structure in the vicinity of the corners has to be expanded.

SSAB considered the first trial as a good first step since a methodology to design, manufacture, instrument and test new mould designs has been put into place. However, further work is required and further experiments will be made within a continuation project within the member program of Swerea KIMAB.

#### Summary of SMT trials:

- Swerea MEFOS and SMT have discussed a changed of the present mould design. Due to the tricky way of machining the mould performed by the subcontractor, SMT decided to go ahead with its own mould design based on the proposed design of a parabolic mould made by Swerea MEFOS.
- SMT has redesigned a mould for better corner angle distribution and at the same time changed the reference design line from the fixed side of the caster to the center of the bottom parallel side. By that all 4 plates had to be re-machined.
- Holes for thermocouples were drilled in the four corner regions. The thermocouples were fastened by a simple clip for easy change.
- In the new mould 8 heats of 3 different alloy types were cast and followed. It could be concluded that the temperature varies from the fixed side to the loose side. Still the duplex stainless steel exhibited longitudinal corner cracks on the first blooms in the sequence.

## **4. THE PROJECT HAS DELIVERED**

- A design program based on Excel spreadsheets for the design of optimum mould shapes taking into account the 3 criteria: an increased corner angle (IMMODCO concept=concave mould), a perimeter concept based on the shrinkage produced along the width of the mould plates and a shell shrinkage concept produced along the thickness of the strand.
- The design program has been used to generate suitable 3D coordinates and/or drawings/CAD suitable for machining the mould design. These designs have been translated into CNC coordinates for machining the moulds for SSAB Oxelösund.
- Sandvik Materials Technology has chosen to go ahead with their own mould design and has made extensive geometrical models to fulfil their mould supplier demands for machining of new moulds.

- Experiments have been carried out for the newly manufactured optimum moulds for both slab and bloom format. Evolution of surface quality, on rolled plate results and temperature in the moulds have been carried out for the newly manufactured optimum moulds for both slabs and blooms format at SSAB and SMT.
- The project has provided mixed results with successful implementation of the thermocouple measurements and possible operation with the moulds, but not the expected results regarding improved surface quality.

## **5. DEVELOPMENT OF A SIMULATION PROGRAM**

All previous Jernkontoret reports were reviewed while experimental results and tests of previous mould designs were discussed in detail for each steel plant. The quality of input data regarding steel properties was identified as an important factor, since the review of the reports showed a lack of input data for the chosen peritectic steel grades. 3 design principles were used as a basis for the design: IMMODCO concept, Perimeter concept and shell thickness concept. Based on these principles and taking into account the lack/availability of input data, a modelling approach was developed in an iterative stepwise manner.

The first design proposal was made for SSAB EMEA, Oxelösund. This design was converted to CAD and CNC coordinates and moulds were manufactured based on these designs. Machining of the mould was carried out including adjustments to the initial shape. The manufactured mould was subsequently instrumented with thermocouples and tested for 15 heats. The main measurements concerned temperatures of the mould and the output of the rolled plate results.

A proposal for mould design was also carried out for Sandvik Materials Technology, but SMT chose to go ahead with a different design. SMT has made geometrical modelling to fit the conditions for its respective supplier of machined moulds and performed its own instrumentation of the mould with thermocouples.

A calculation methodology and a simulation program based on Excel have been developed for designing the optimal mould shape to be tested at SSAB and SMT. The development of the simulation program consisted of several stages that go from reviewing the design methods available and documented by Jernkontoret to the development of new calculation routines for the strain and shrinkage that finalized with a new design. The development of the simulation program is based on the following stages:

- Literature review
- Current design including IMMODCO concept
- Design principles for the new mould
- Model development and spreadsheet layout
- Mould design for SSAB
- Mould design for SMT

### **5.1. Literature review**

An extensive literature review was carried out by Swerea MEFOS analysing around 20 documents including reports, journal papers, thesis and internal documents provided by

Jernkontoret, SMT, SSAB and Swerea KIMAB. A summary of the most important documents used for the new design and keywords about their content is given below:

JK 2417/90 [ref.1]	Basic 2D model for stress-strain and mould simulator.
Patent WO 96/35532 [ref. 2]	Description of parabolic mould.
Patent WO 96/35533 [ref. 3]	Description of increased corner mould.
JK 2430/94 [ref. 4]	Main design features described including increased corner angle and parabolic taper.
TO24-144 [ref. 5]	Taper treatment description and taper model. Description of corner shrinkage experiment.
TO24-121 [ref. 6]	IMMODCO design 1 for SSAB Oxelösund – Linear taper
TO24-122 [ref. 7]	IMMODCO design 2 for SSAB Oxelösund – Parabolic taper
TO24-141 [ref. 8]	IMMODCO initial design and implementation at Avesta Polarit
TO24-142 [ref. 9]	Master Thesis on modelling the Corner Shrinkage experiment in FEM
TO24-154 [ref. 10]	Final report of IMMODOCO.
Kristiansson, J-O [ref. 11]	PhD Thesis, Stress and strain during solidification. Principles for shrinkage analysis.
JK 24050 D835 [ref. 12]	Development of a CC mould with soft cooling properties.

## 5.2. Current design including IMMODOCO concept

Basically, the IMMODOCO concept was developed around the patent WO 96/35532 with an increased angle in the corners (higher than 90 degrees) which changes towards the mould's end to form a 90 degree angle at the corners. The current design for the IMMODOCO mould at SSAB Oxelösund is based in the prior findings of reports JK 24045/02 and KIMAB (IM) 2001-258.

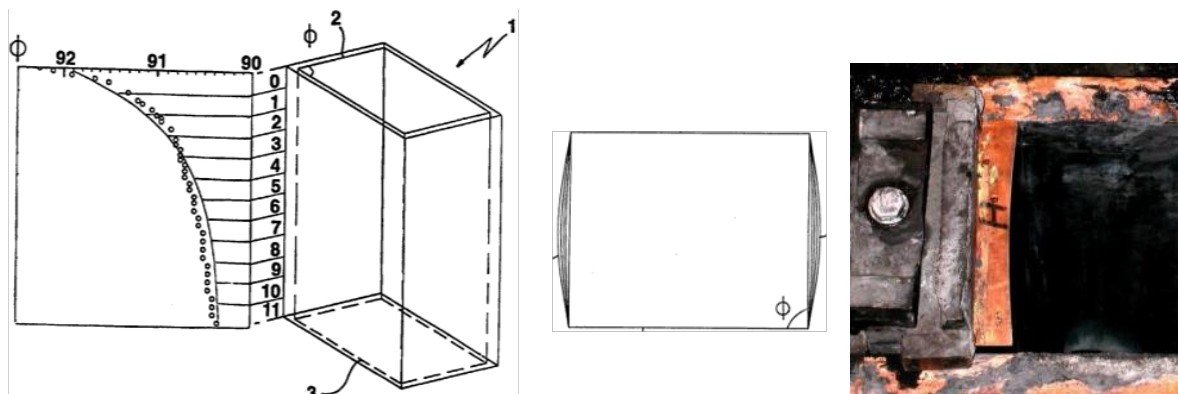


Figure 1. IMMODOCO schematics and implementation in the caster.

Originally, calculations were performed to describe the variation in angle (decrease) as a function of mould length providing an initial estimate on how this angle should change along the mould length. Moreover, a series of efforts and projects to accurately describe the effect of

different steel grades on the shrinkage behaviour at the corners were performed by KIMAB: JK 2417/90 and JK 2441/97. However, an accurate description of the behaviour at the corner was elusive; so, when the actual design was applied to a slab mould, the predicted angle was deemed too soft to correct the shrinkage behaviour at the corners. Thus an empirical approach was used to approximate a functional corner angle.

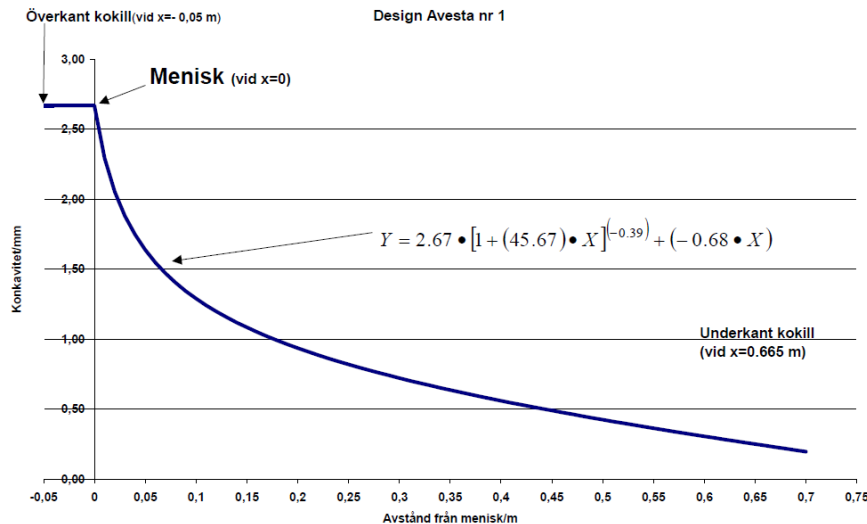


Figure 2. Parabolic taper for IMMODOCO (after TO24-157).

### 5.3. Design principles for the new mould

#### 5.3.1. Strand perimeter shrinkage concept

The first design principle for the mould is based on the shrinkage of the shell. From the general formulation for strain (eq 20, Brolund, IM-3442):

$$\varepsilon = \varepsilon^e + \varepsilon^T + \varepsilon^B$$

Without considering bending, the strain due to temperature gradient and phase transformation\* (eq 22, Brolund, IM-3442) is:

$$\varepsilon^T(x, t^*) - \varepsilon^T(x, t_a) = \alpha(T_s - T)$$

Where  $T_s$  is the surface temperature of the strand. If we assume that the shrinkage for the phase transformation and thermal gradient is included in  $\alpha$  (thermal expansion coefficient). The actual dimensionless strain can be simplified to:

$$\varepsilon = \alpha(T_s - T) = \alpha(\Delta T)$$

But we also know that strain is:

$$\varepsilon = \frac{\text{change in length}}{\text{initial length}} = \frac{\Delta L}{L_{\text{initial}}}$$

Substituting:

$$\frac{\Delta L}{L_{\text{initial}}} = \alpha(\Delta T)$$

So, the actual change in length is:  $\Delta L = \alpha(\Delta T)L_{\text{initial}}$

Assuming that the strand perimeter suffers the maximum shrinkage (which is justified since the surface is the coldest region of the strand during casting), it is possible to extend the perimeter as a line or even compare it to a beam suffering shrinkage in only one direction as in Figure 3. This change of length is equivalent to the shrinkage suffered by the strand. So, now it is possible to define an Initial length for the strand perimeter and a final length. But, we also know that the final length is equal to the initial length minus the shrinkage.

Thus:  $L_{final} = L_{initial} - \text{change in length} = L_{initial} - \Delta L$

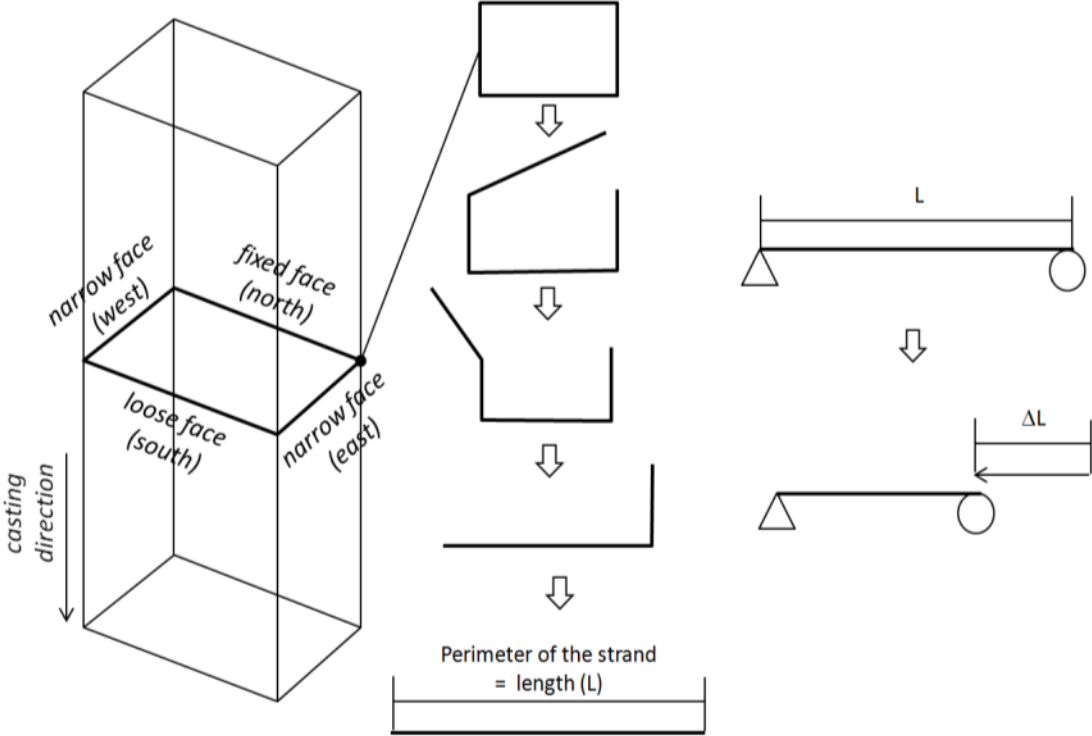


Figure 3. Strand perimeter design concept.

Then, the actual mould design could be based on the initial perimeter on top. However, this means that the strand length will go from the original perimeter to whatever final length it reaches after shrinkage. This would represent a problem since the support rolls and rest of the machine would have to be modified to account for this change and the size of the product will not be the desired one. Therefore, the best option is to take the final perimeter of the strand as basis. So, rearranging:  $L_{initial} = L_{final} + \Delta L$

Substituting:  $L_{initial} = L_{final} + (\alpha \cdot \Delta T \cdot L_{final})$

Reducing:  $L_{initial} = L_{final}(1 + \alpha \cdot \Delta T)$

Moreover, this method can be used to confirm if the overall strand perimeter fits the mould or for the shrinkage of every side separately. See figure 4.

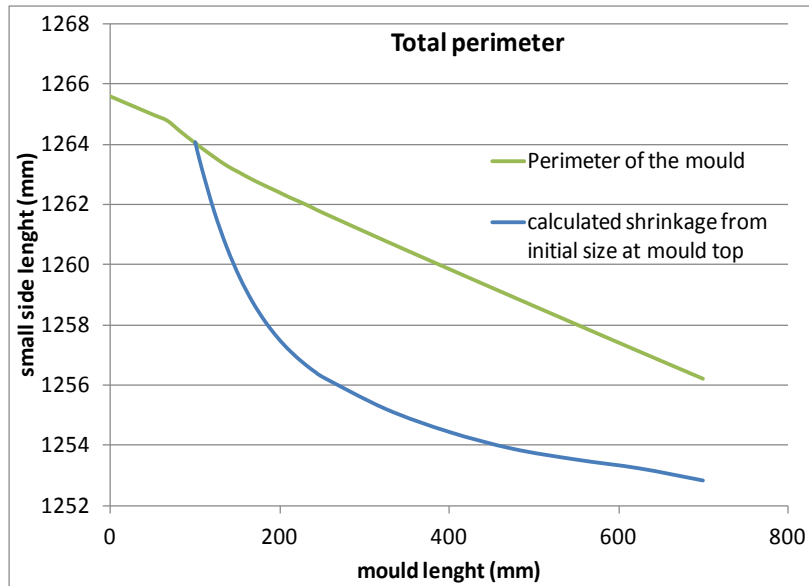


Figure 4. Difference between predicted shrinkage and taper along the mould length.

### 5.3.2. Deduction of $\Delta T$

The election of  $\Delta T$  is not trivial and requires considerable background information. The normal procedure for deducing the temperature is based on readings from thermocouples embedded in the mould. Unfortunately, the temperature provided cannot be directly assigned to the strand surface, since this reading also includes the effect of the slag film and gas gap between strand and mould. Thus, an assumption of the slag film thickness and the resistance it provides should be made. Moreover, a shell thickness growth function is also necessary to have the complete system of thermal resistances in the mould as shown below:

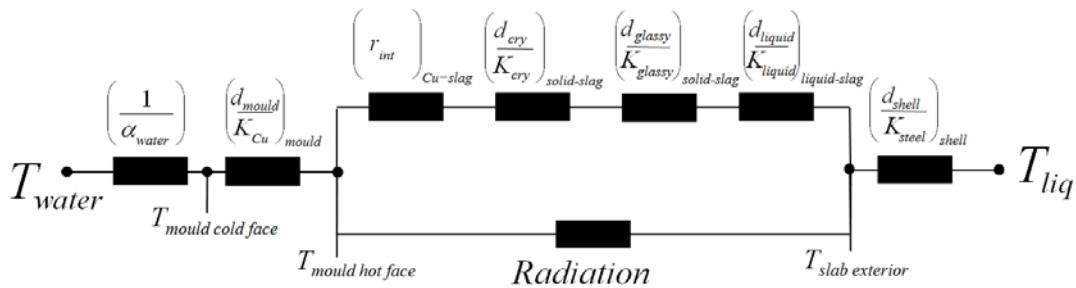
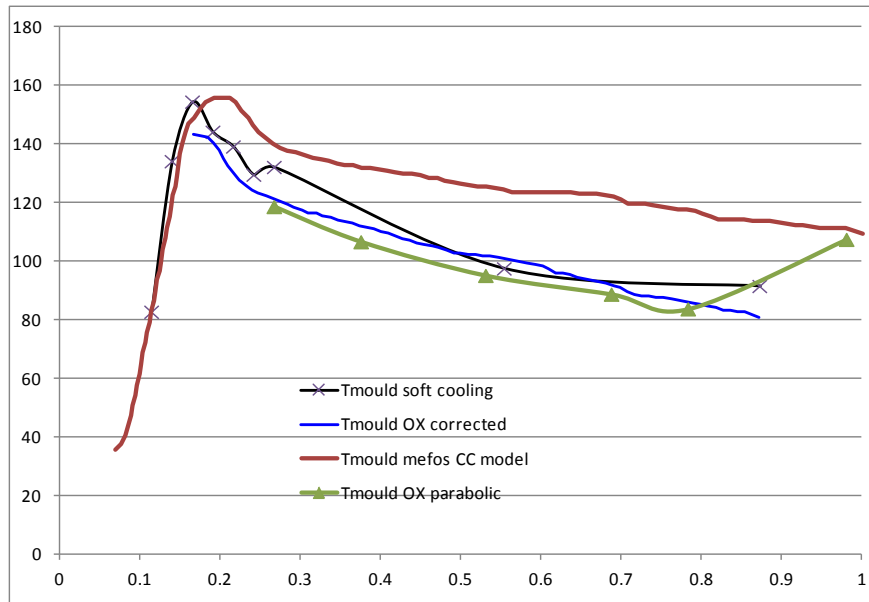
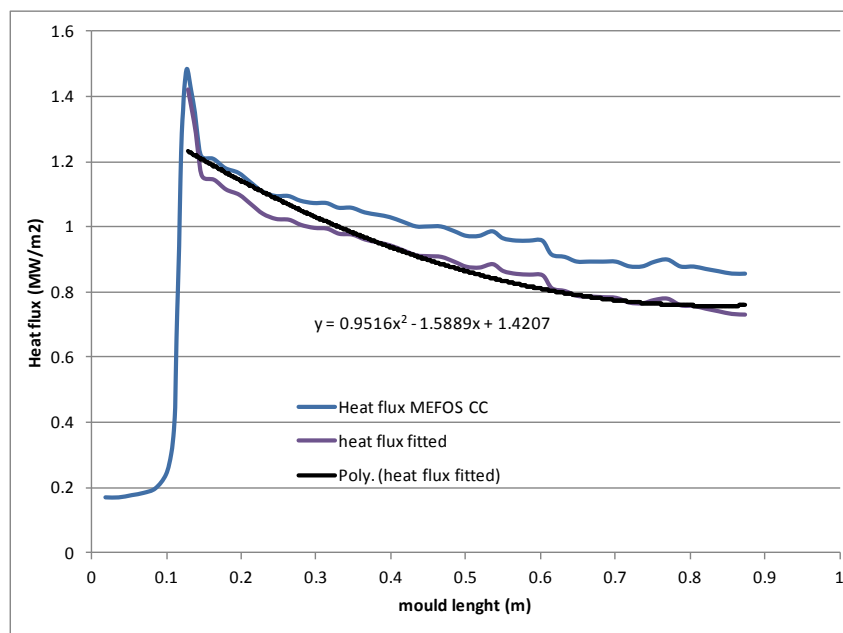


Figure 5. Thermal resistances through the shell, slag film and mould during CC.

The current design abandons these limitations by using statistical results from a numerical model for CC that includes slag infiltration effects combined with temperature measurements from thermocouples in the mould. Unfortunately, the model was not applied directly to any of the industrial casters involved due to budget constraints; but prior statistics of several casters were used to provide typical mould temperatures and heat flux curves; these were named  $T_{mould}$  MEFOS CC model and Heat flux MEFOS CC model respectively (Figure 6 and 7).



**Figure 6.** Mould temperatures during CC predicted by MEFOS model vs thermocouple measurements for fitting of SSAB Oxelösund data.



**Figure 7.** Heat fluxes during CC predicted by MEFOS model and fitting of SSAB Oxelösund data.

The statistic average was then multiplied by a factor to match the measured Thermocouple temperatures from a prior project [ref. 12] and shown in the figure as  $T_{mould}$  soft cooling. This same factor was used to multiply the statistic heat flux curve from MEFOS CC model to produce a “fitted” heat flux curve for the industrial case, since no information regarding heat flux was available. MEFOS CC model was also able to provide a statistic average for the shell thickness. The predicted shell thickness was also compared to empirical models of shell growth.

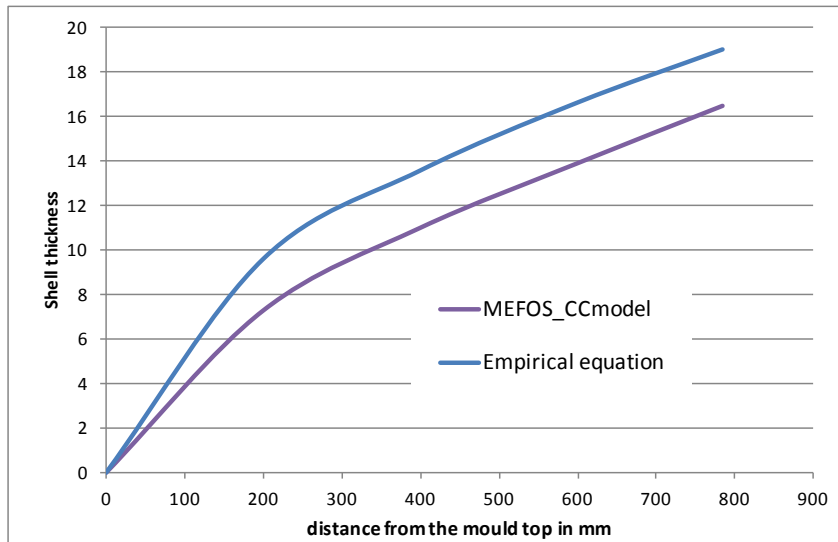


**Figure 8.** Shell growth during CC predicted by MEFOS model vs empirical equation for fitting of SSAB Oxelösund data.

So, now is possible to predict the actual strand surface temperature and the expected  $\Delta T$  by using the inverse heat flux equation:

$$q = \frac{k(T_s - T)}{\text{shell thickness}}$$

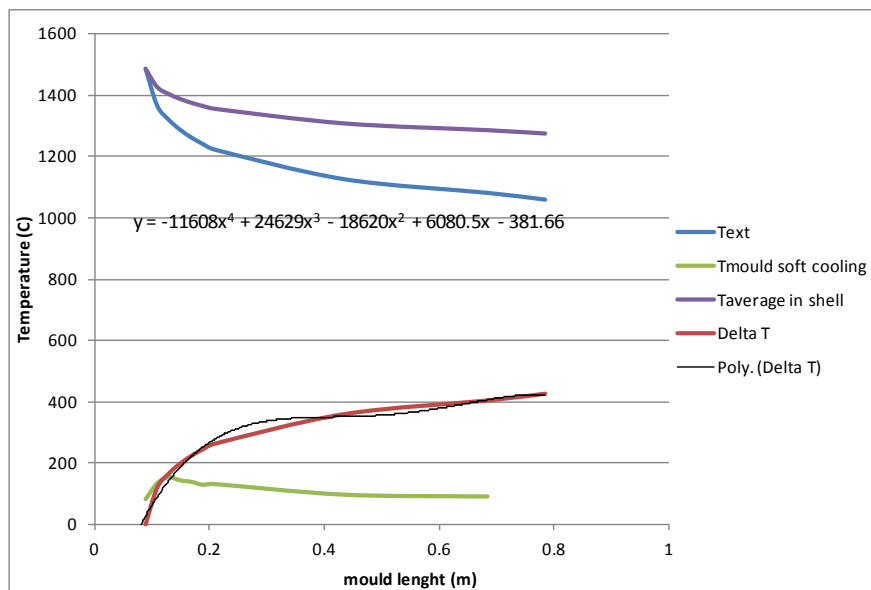


**Figure 9.** Temperature fittings for SSAB Oxelösund data.

An obvious problem is that  $\Delta T$  is now higher at the end of the mould than at the top (which is logic since the thickest and coldest shell occurs at the mould exit, so the largest shrinkage amount occurs at the mould exit). However, this suffers from the same problem as the perimeter calculation, so  $\Delta T$  needs to be reversed to be used with the perimeter formulation to provide zero shrinkage at the exit (i.e. to match a pre-defined format size). This has been done accordingly in the spreadsheet for the mould design.

### 5.3.3. Thermal expansion coefficient treatment

A fitted function based on the density changes was used to produce the thermal expansion coefficient (Figure 10) due to lack of data on the thermal expansion coefficient for the desired peritectic grades. For exactly isotropic materials, and for small expansions, the volumetric thermal expansion coefficient is three times the linear coefficient:  $\alpha_v = 3\alpha_L$ .

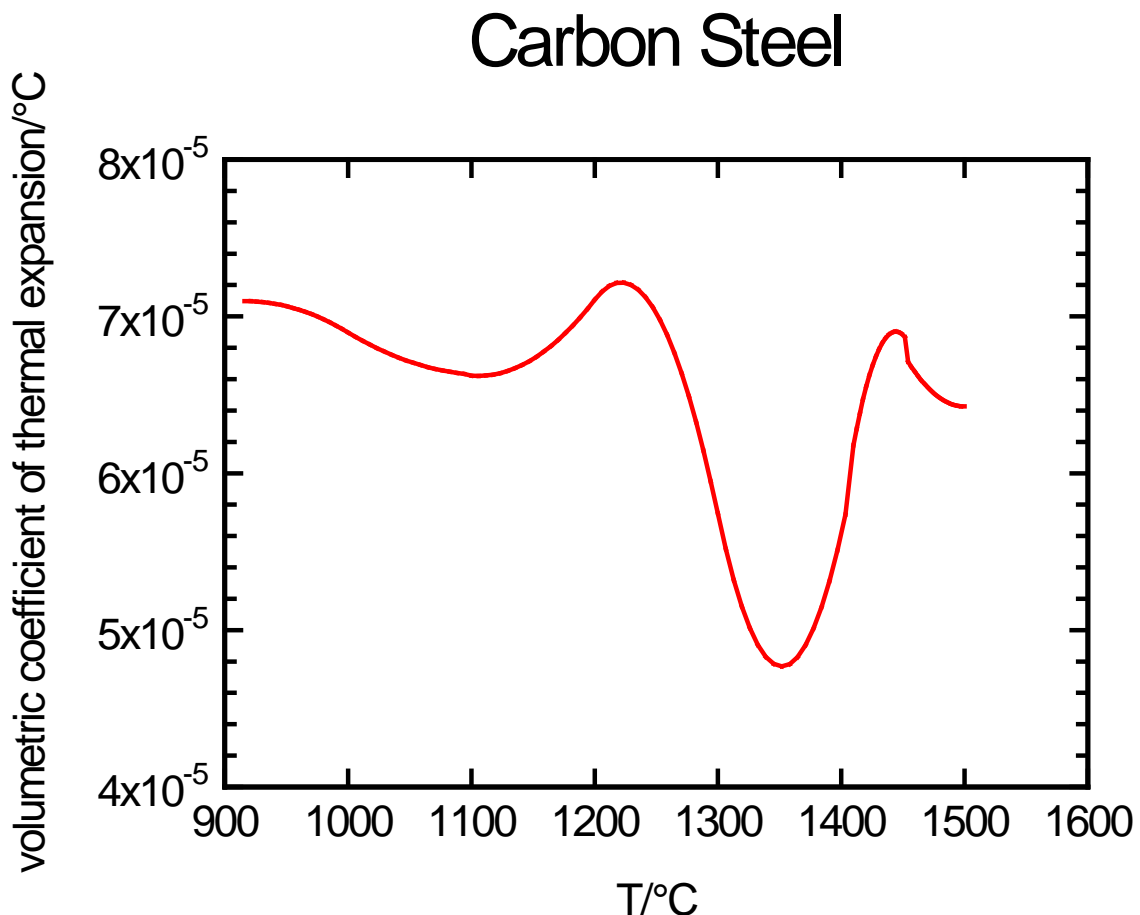


Figure10. Thermal expansion as  $f(T)$ .

Naturally, the thermal expansion coefficient is a function of temperature. Yet, the shell undergoes different temperatures in all directions (along the casting direction, mould width and through its thickness). Thus, average alpha functions were produced to have representative values across all directions in the shell. For instance, if the external shell temperature is now known and the internal temperature is assumed to be the liquidus temperature, the average temperature can be calculated as:

$$T_{average} = \frac{T_{exterior} - T_{liquidus}}{2}$$

If the value of alpha for that average temperature is known, a new function with the average alpha for a given shell thickness can be produced:

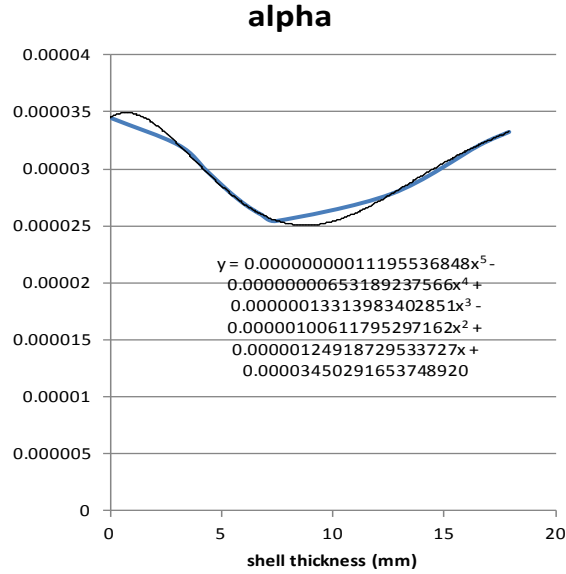


Figure 11. Thermal expansion coefficient as a function of shell thickness.

### 5.3.4. Thickness shrinkage and bending (convex mould)

A separate model has been developed to account for the shrinkage along the thickness of the strand and the effects of an additional curvature to compensate for the shrinkage when using an angle in the mould corners higher than 90°. The model is based on the strain distribution model by Brolund (eq 24, IM-3442):

$$\varepsilon^e(x,t) = \alpha(T_s - T_y) \left( \frac{1}{2} \ln \left( \frac{x}{x_s} \right) - \frac{x}{x_s} + 1 \right)$$

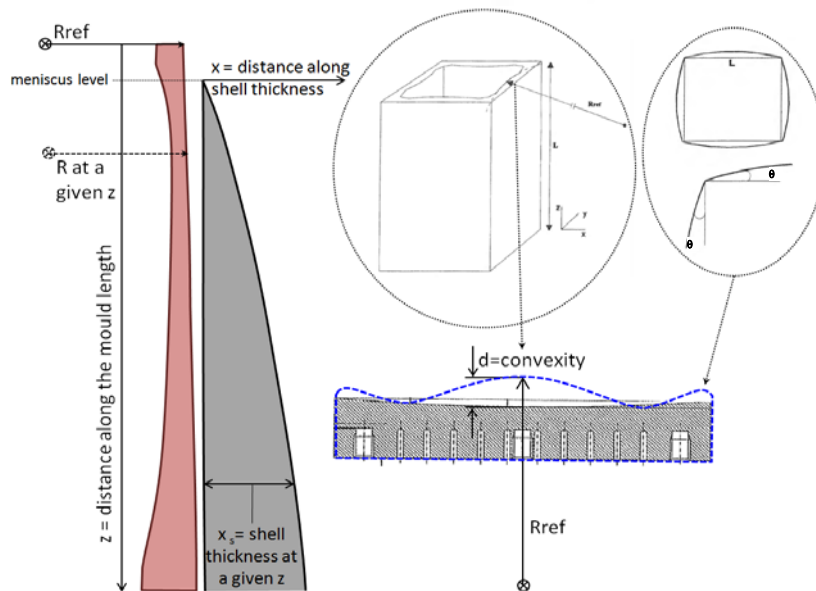
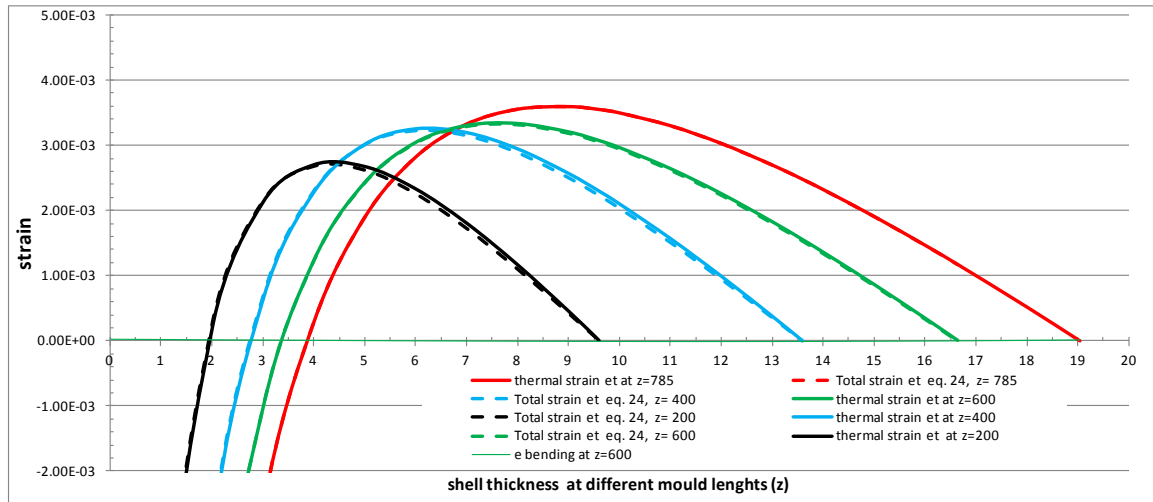


Figure 12. Shrinkage along the shell thickness and bending concept through convexity and shell growth.

By replacing  $(T_s - T_y) = \Delta T$  and taking  $x_s$  as the shell thickness at a given mould height, it is possible to calculate the shrinkage for any given thickness along the mould.



**Figure13.** Strain along the shell thickness for different positions along the mould length.

The plot shows how the strain goes from compression (negative) at the surface of the strand (0.0 thickness) to tension at the interior of the strand for a given thickness value (strain becomes zero at the solidification front when  $T = T_{liquidus}$ ). It is possible to obtain the Total strain for the shell ( $\varepsilon_t$ ) by integrating the strain along the thickness. It is also possible to deduct the actual shrinkage from this by using the shell thickness at a given mould height as initial length. Thus:

$$\varepsilon_t = \frac{\Delta x}{x_s} \Rightarrow \Delta x = \varepsilon \cdot x_s$$

Brolund proposed a model where bending of the shell could compensate for the strain produced by using the following equation (eq 22, IM-3442):

$$\varepsilon^e(x,t) = \alpha(T_s - T_y) \left( \frac{1}{2} \ln \left( \frac{x}{x_s} \right) - \frac{x}{x_s} + 1 \right) + \frac{1}{3} \frac{v}{k^2 L R_{ref}} (x_s^2 (x_s - 3x) + 2x^3)$$

Then, a new calculation of the bending required to reduce the actual strain can be made.  $L$  is the mould length and  $R_{ref}$  is the initial reference radius on the mould top to counteract the effect of shrinkage. The Radius can be normalized by using the expressions:

$$R' = \frac{R}{R_{ref}} \quad z' = \frac{z}{L}$$

Where  $z$  is a function of the casting speed ( $v$ ) and time ( $t$ ):

$$z = vt$$

Any desired function for the normalized  $R'$  can be chosen to produce a linear or non-linear increase of the Radius (i.e. linear or parabolic taper). This means that the reference Radius on top will increase to become infinite at the mould exit (since the corners are now at  $90^\circ$ ). For instance, the functions for a linear or parabolic taper are:

$$R' = \frac{1}{1 - z'} \quad R' = \frac{1}{(1 - z')^2}$$

Finally, the actual radius as a function of the mould length for a circular section based on an increased angle (defined in the equations by Brolund as  $\alpha$  but redefined here as  $\theta$  to avoid confusion with the thermal expansion coefficient  $\alpha$ ) can be defined through:

$$d(\alpha, L) := R(\alpha, L) - \frac{1}{2} \cdot \sqrt{4 \cdot R(\alpha, L)^2 - L^2} \quad R(\alpha, L) := \sqrt{\frac{L^2}{4} + \frac{L^2}{4 \tan(\alpha)^2}}$$

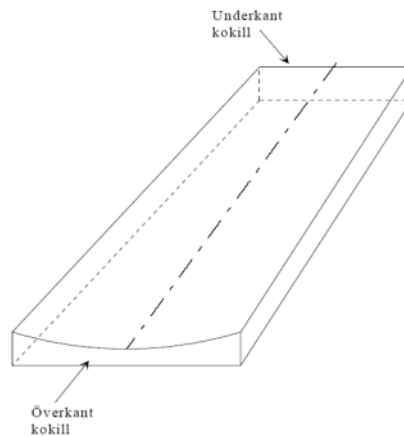


Figure 14. Mould with curvature on top and flat bottom.

The final result of the shrinkage, bending and taper calculations is shown below:

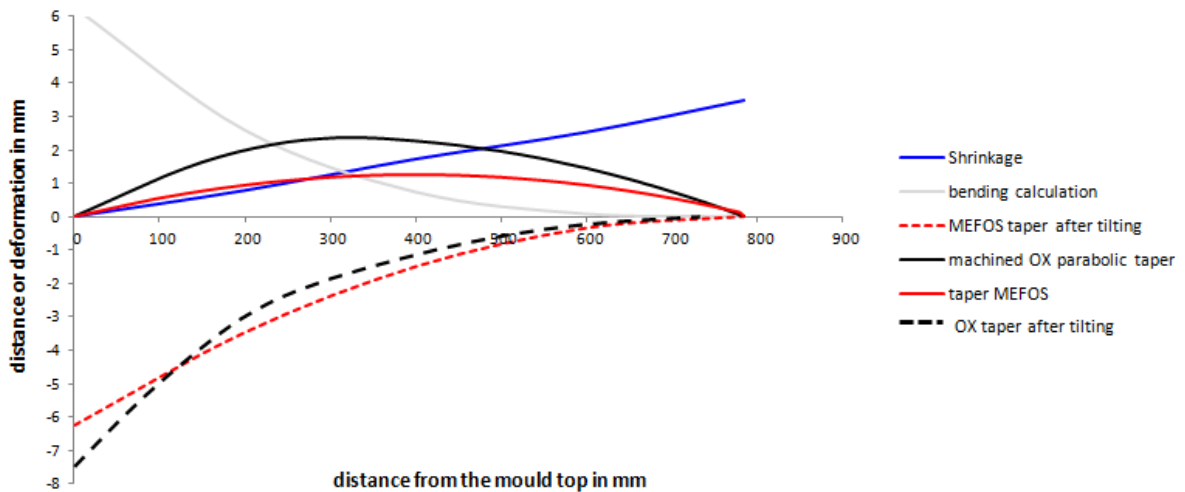


Figure 15. Shrinkage, bending and taper calculations.

Approximation of  $R'$  can be made to match the integral under the curve of the shrinkage found earlier (blue curve) compensated by the bending calculation (gray curve). Moreover, a direct comparison of the suggested taper (solid red curve) with a previously tested taper (solid black curve) can be made. Naturally, these curves were tilted in order to provide a smooth lower section and linking with the rest of the strand without discontinuities at the end of the

mould (dotted curves). This curvature was added to the design in the spreadsheet developed later.

**5.3.5. Separate face design concept**

Another important concept when designing the mould is that changes in one of the faces produces changes in the rest. For instance, the changes in the mould design for a slab narrow face are necessarily linked to the taper in the wide face. Therefore, if a new width for the narrow side is designed (from the perimeter concept) the taper in the wide face should be adjusted to compensate the shrinkage. It becomes obvious as well that it is not possible to have curved sides for the narrow face in a slab mould, since fitting of the wide face would not be possible.

However, the IMMODOCO concept creates an increased length of the narrow face which could be compensated by the taper in the wide face. Hence, the actual length of the narrow face is not dictated by the shrinkage of the narrow face but by the shrinkage of the wide face (Figure 16).

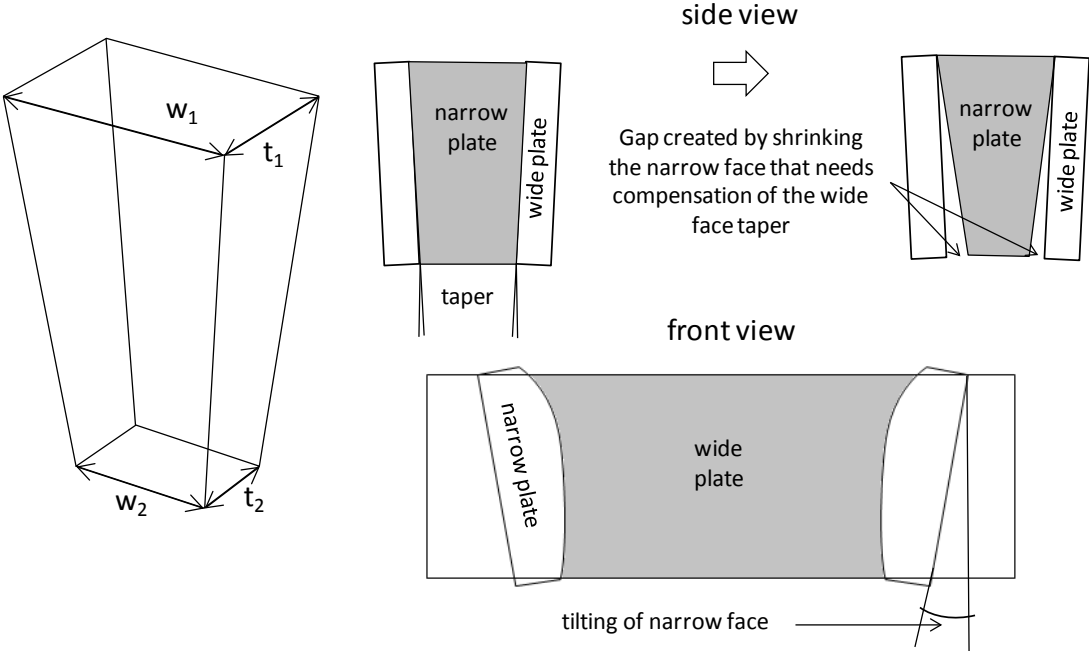


**Figure 16.** Effect of taper changes for wide and narrow faces.

The same concept applies to a bloom mould were changes in the side plates (east/west) must be matched by changing the width of the north and south sides. However, the problem is more complex when there is added curvature from the caster radius; this will be discussed in later sections. A natural consequence of separating the design is that the width of the narrow face could be calculated for half a face to match the necessary taper per side. So, from now onwards, all the calculations are considered for half the wide or narrow sides for all the designs. This is discussed next.

**5.3.6. Combining shrinkage predictions and dimensioning**

The final shrinkage for the strand is a combination of the shrinkage with the Perimeter model and the shrinkage across the thickness. The shrinkage is added to the final width of the product to calculate the required length from top to bottom that will match the desired width after shrinkage. For instance, if the desired size at the mould exit for a slab is 1680mm x 296mm. The final width for the wide face required is 1680/2= 840mm (following the half face

concept); so, the shrinkage (from the perimeter method) could be added to calculate the initial length that the strand (and mould) should have to produce the required size at the mould exit.

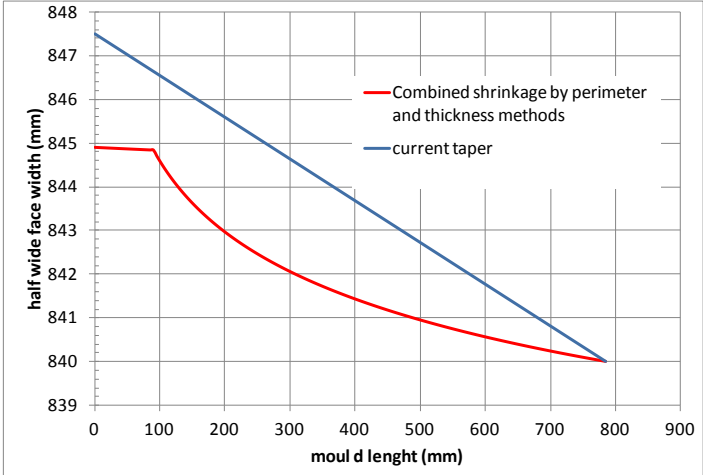


**Figure 17.** Predicted shrinkage and gap produced by current taper.

The figure shows evidently that the current taper is not ideal to follow the shrinkage of the strand if a final size of 840 mm is required. The change in curvature of the predicted strand length from 0-90 is the absence of steel due to the metal level (red line, normally at 90 mm below the mould edge). For instance, in SMT’s case, the final bloom side has to be 295 mm. The blue line describes the reduction in length according to the linear taper already built-in; while the red line shows the expected shrinkage by combining the perimeter and shell thickness methods. The gap between the 2 lines is the lack of contact of the strand with the mould which needs to be eliminated. This also shows the need for a non-linear taper since the shrinkage is non-linear:

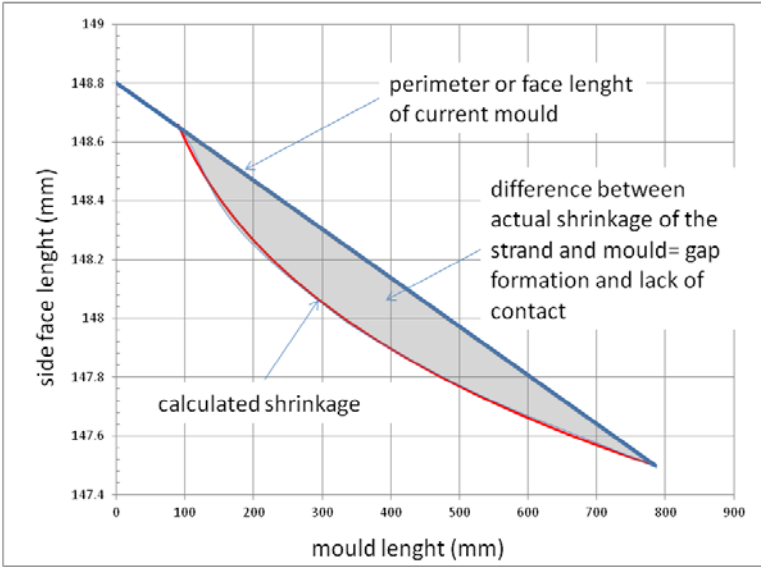


**Figure 18.** Predicted shrinkage and gap produced.

The IMMODOCO concept provides the required angle at the corner from which the actual curvature of the face can be calculated through a simple analogy with a circle. So the actual mould curvature is a result from a reference radius (Page 10, IM-2000-518). This allows calculation of the actual radius



**b) Perimeter method spreadsheet:** Including design and taper calculations for wide and narrow faces separately.

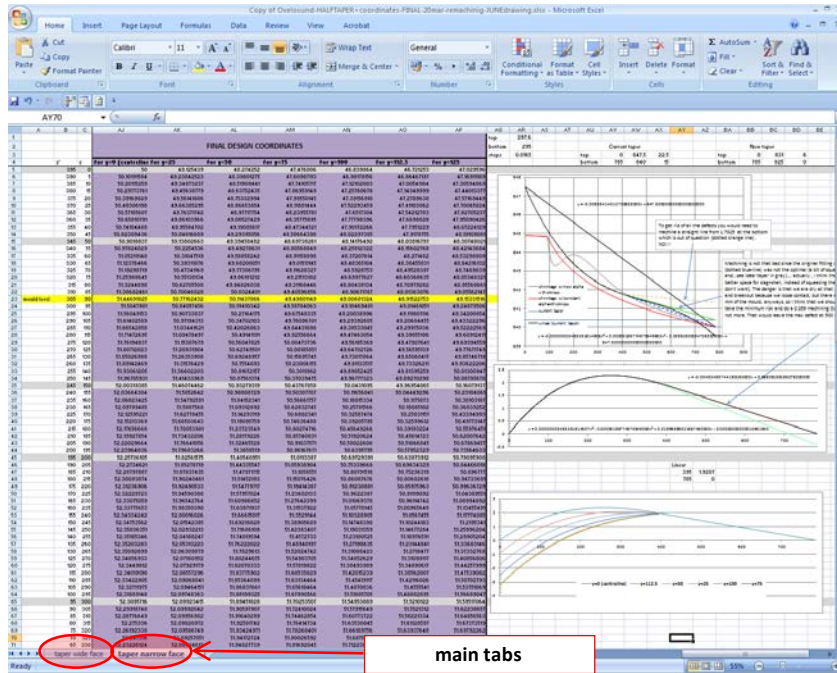


**Figure 21.** Perimeter method spreadsheet (screenshot).

The final dimensioning of the mould is defined in this spreadsheet by coordinates (not equations) in the previously described coordinate system ( $x$ =mould thickness,  $y$ =mould width and  $z$ = mould length). Coordinates in  $x$  are presented at different intervals:  $y$  at 12.5 and 25 mm spacing and  $z$  at 5 mm spacing. Mould level was defined at  $z=90$  mm (marked in yellow) from the mould top and the half mould is marked in green. Whenever coordinates do not appear, a straight line links the extreme coordinates.

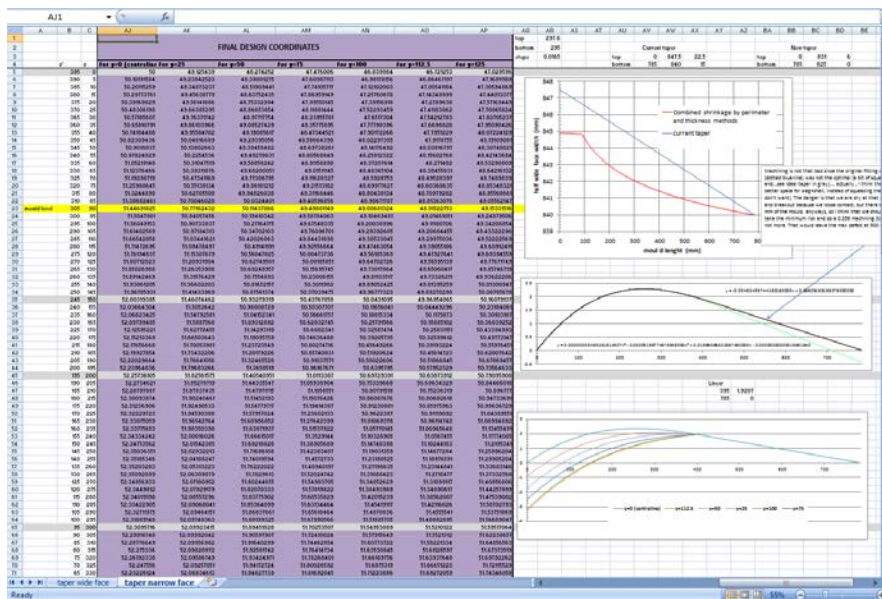


**Figure 22.** Final mould dimensioning (screenshot).

- c) **Tilting spreadsheet:** Including design and taper calculations for wide and narrow faces separately.

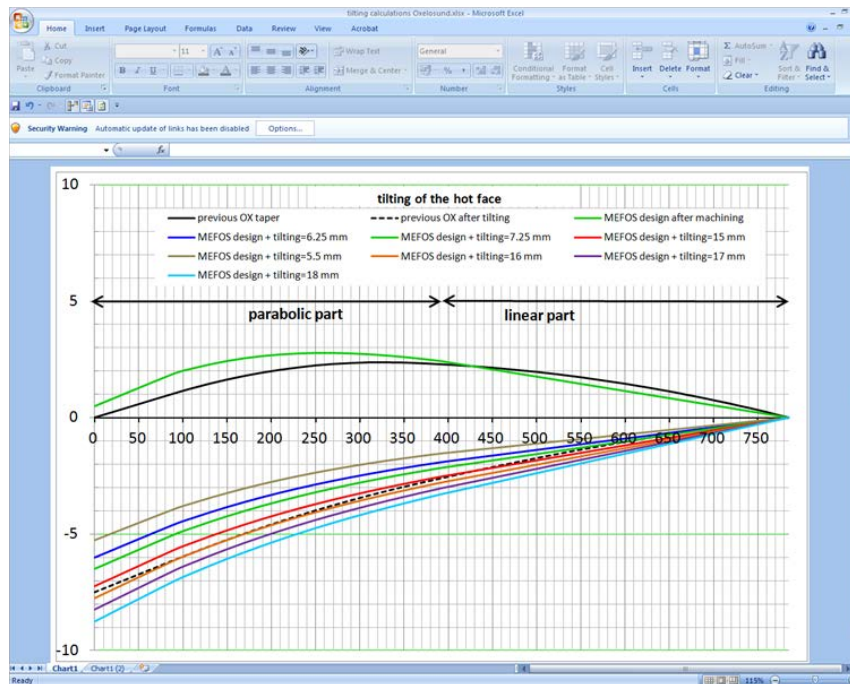


Figure 23. Tilting spreadsheet (screenshot).

## 5.5. Mould design for SSAB EMEA Oxelösund

A new design based in the previous experiences of the IMMODOCO concept plus the perimeter concept, parabolic taper and thickness shrinkage concepts was proposed to SSAB. Additionally, a series of guidelines were proposed including:

- Increasing the original IMMODOCO corner angle for the new design for thicker slabs
- Adding a non-linear taper to the narrow face
- The nonlinear part applies to the first 400 mm of the mould measured from the top and the rest of the mould length should have a linear taper.
- Testing of a convex part (nose) along the centreline for compensating shrinkage through bending (Brolund concept).

Taking these as reference, a model to describe the deformations of the strand based on the thermal expansion coefficient, previous knowledge and additional data from simulations and experiments was formulated. A specific set of spreadsheets was developed for SSAB's mould based on the combination of the perimeter and thickness methods as well as considering the actual dimensions of the mould (not disclosed in this document). Two thermal expansion coefficients were tested (one constant and another based on the volumetric change of density). The curvature was defined as the non-linear taper for the mould centreline and the mould sides.



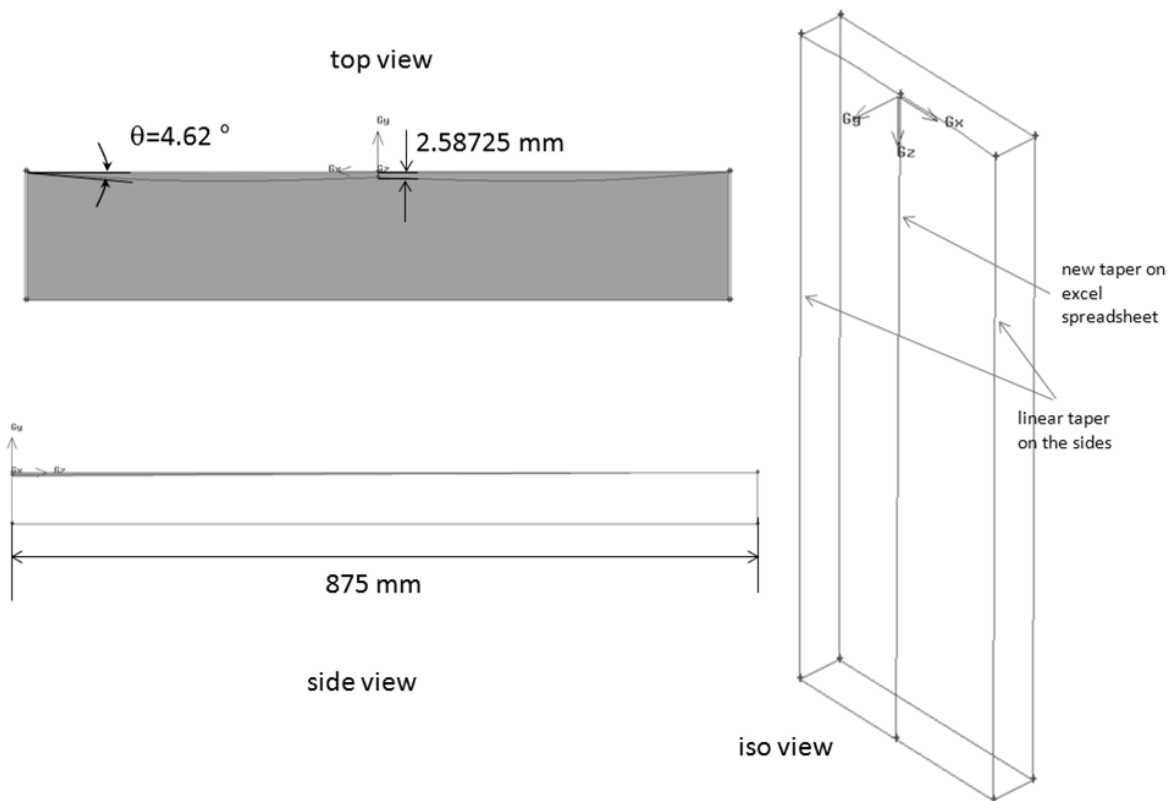


**Figure 25.** Views of mould design for SSAB Oxelösund, Mark I.

After discussions with SSAB, it was decided to increase  $\theta = 5.4^\circ$  to produce a concavity of 7 mm at the narrow face centreline. This was considered as the 2<sup>nd</sup> design iteration (Mark II).

OX NARROW FACE –CONCAVE

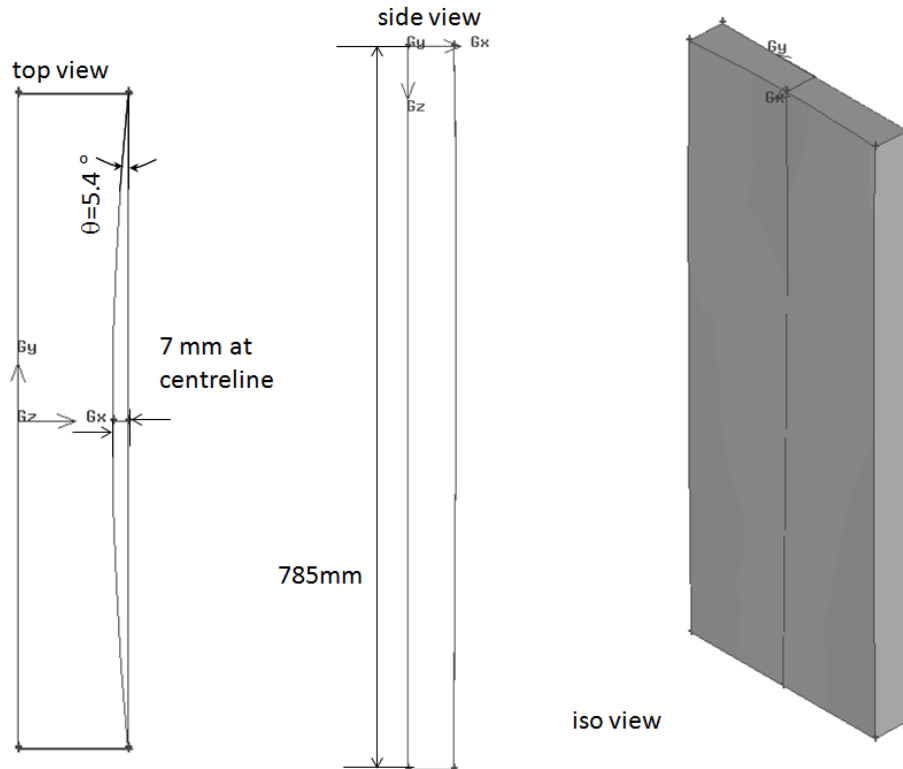


**Figure 26.** Views of mould design for SSAB Oxelösund, Mark II.

The final design was produced by adding a convex part along the narrow face centreline:

OX NARROW FACE – HALFTAPER CONVEX+CONCAVE

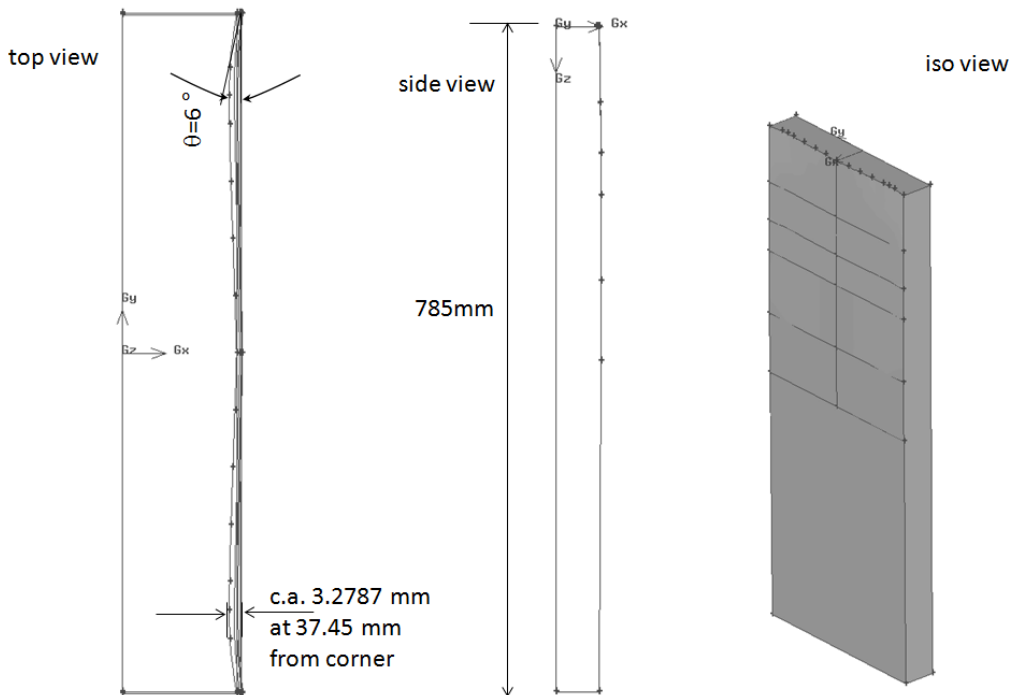
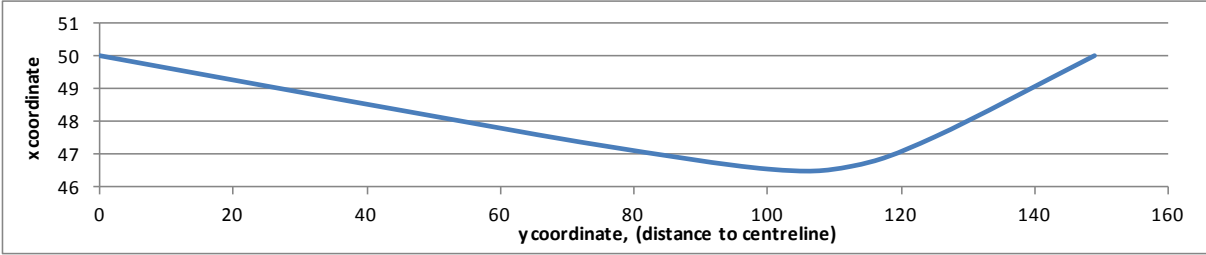


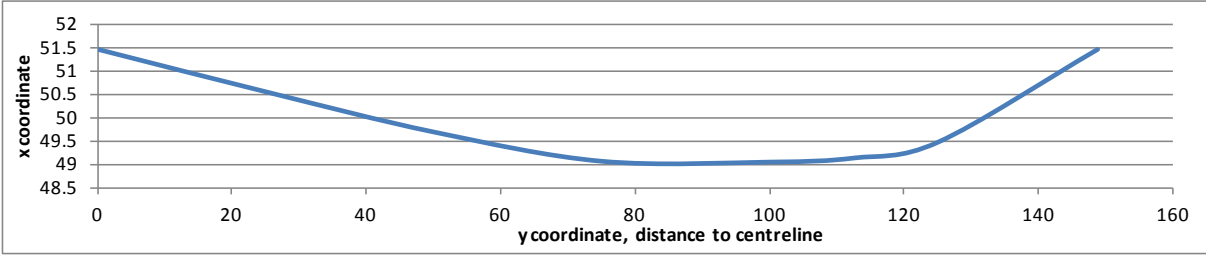
**Figure 27.** Views of mould design for SSAB Oxelösund, Mark III.

**Coordinates summary:**

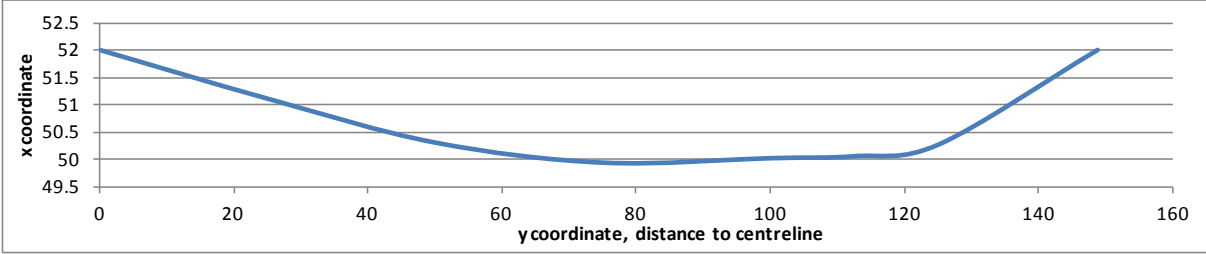
$z=0$  (mould top)



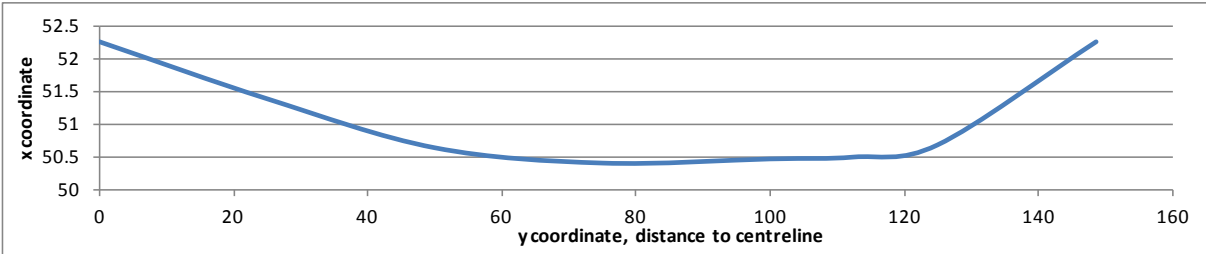
$z=90$



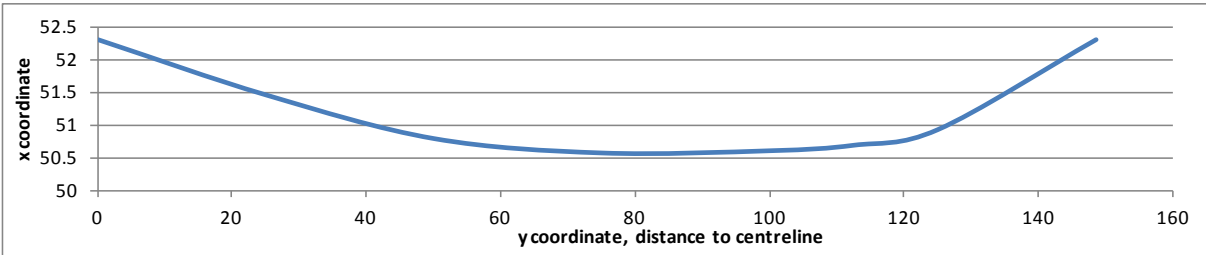
$z=150$



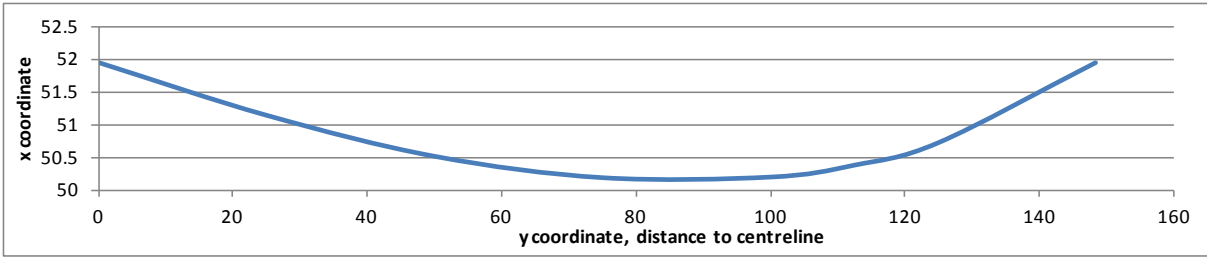
$z=200$



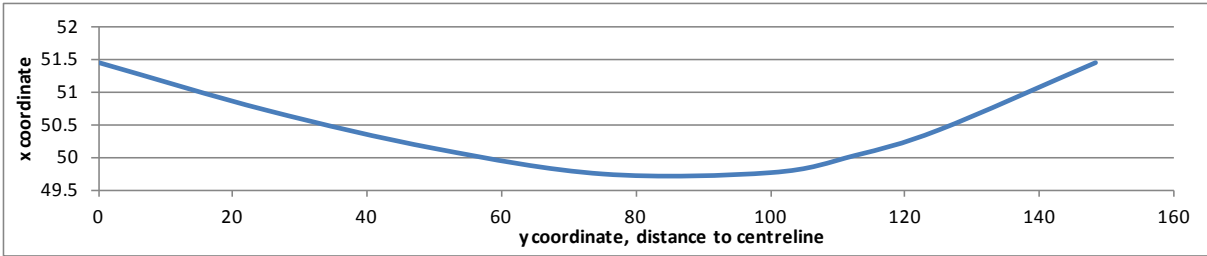
$z=300$



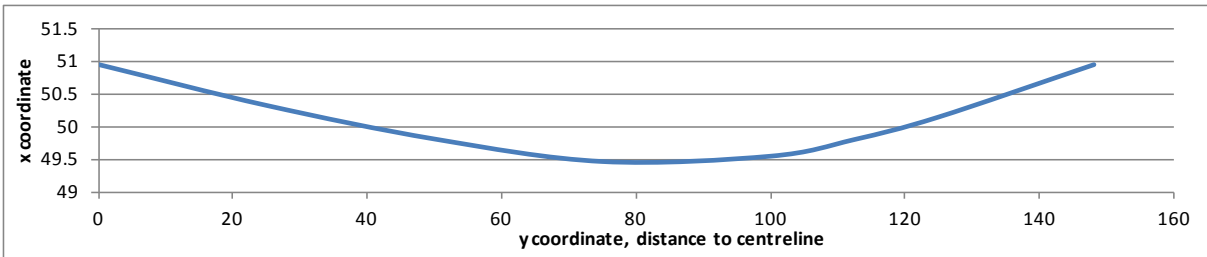
$z=400$



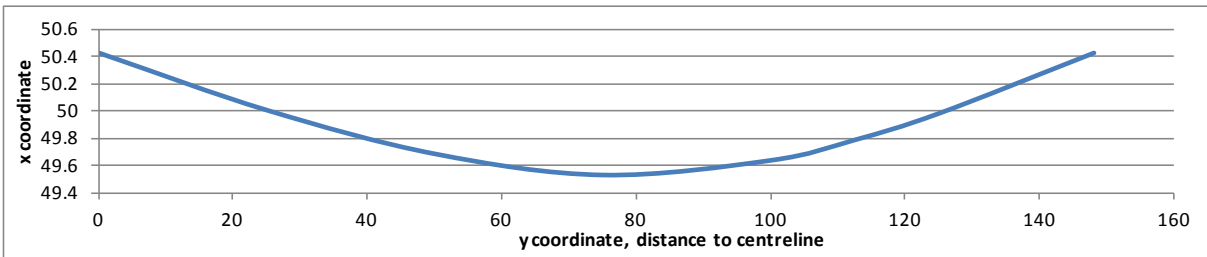
$z=500$



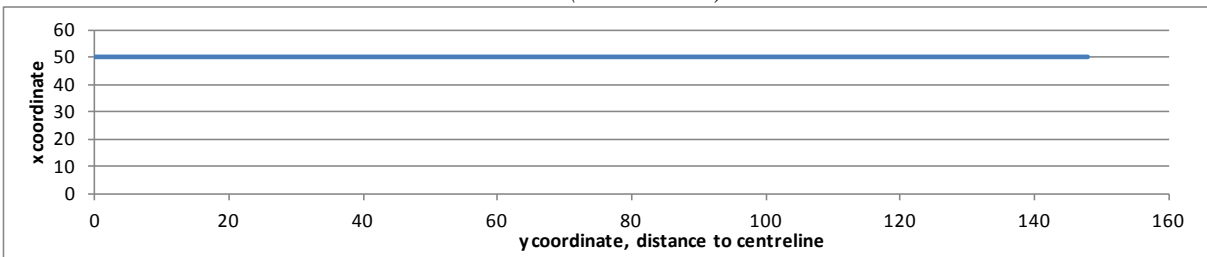
$z=600$

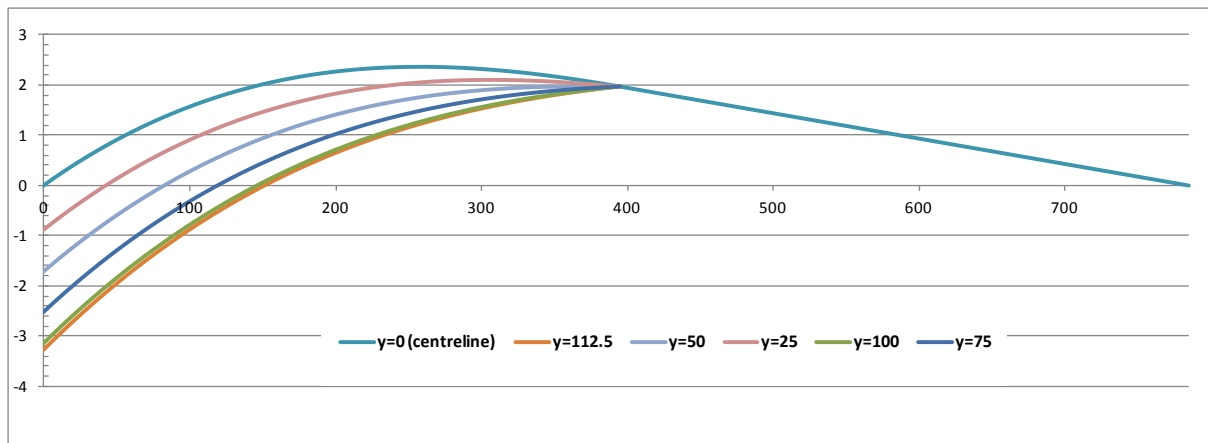


$z=700$



$z=785$  (mould exit)





*x coordinate at different sections along the mould length*

### **5.5.1. Modifications to design due to machining**

The suggested coordinates were modelled with a 3D geometry modeller known as GAMBIT. Unfortunately, this activity was unbudgeted and not foreseen. Therefore, it took longer than expected and several iterations had to be made to translate the actual design to a format that could be read by a CNC machine for manufacture. These design iterations included translation to a 3D model format with extension .igs, .parasolid, .unv, etc. None of these formats proved useful until a .stp or STEP file was used for exporting the solid model. The company in charge of the manufacture (KWD) was finally able to read such a file, but the actual shape was altered due to translation from one format to the other (common problem when exchanging CAD files). Unfortunately, this incorrect shape was used for the first machining producing small defects on the copper plate surface. These had to be corrected to produce a smooth surface for the final design. However, these also produced changes to the original calculated taper which now was accentuated (Figure 28). The final design had to be adjusted by machining the surface defects by cutting the end of the mould on a deeper linear taper. The same procedure was carried out to smoothen the convex part at the mould centreline (nose).

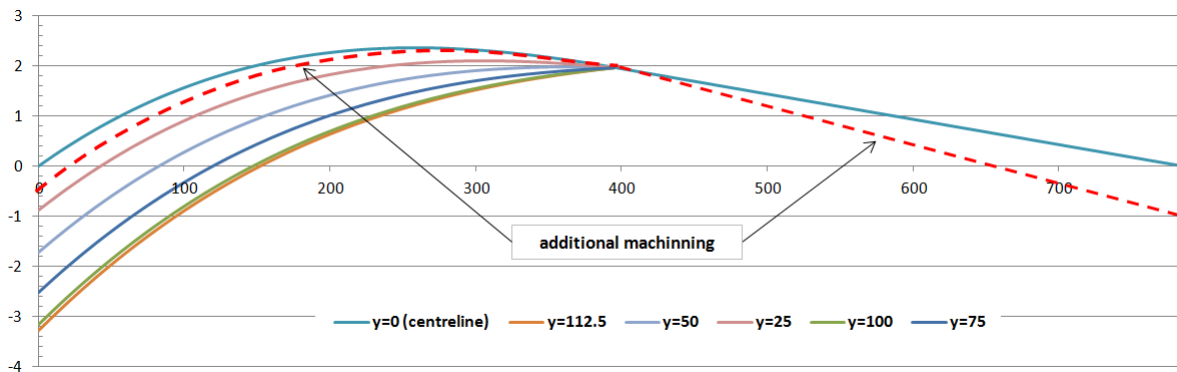
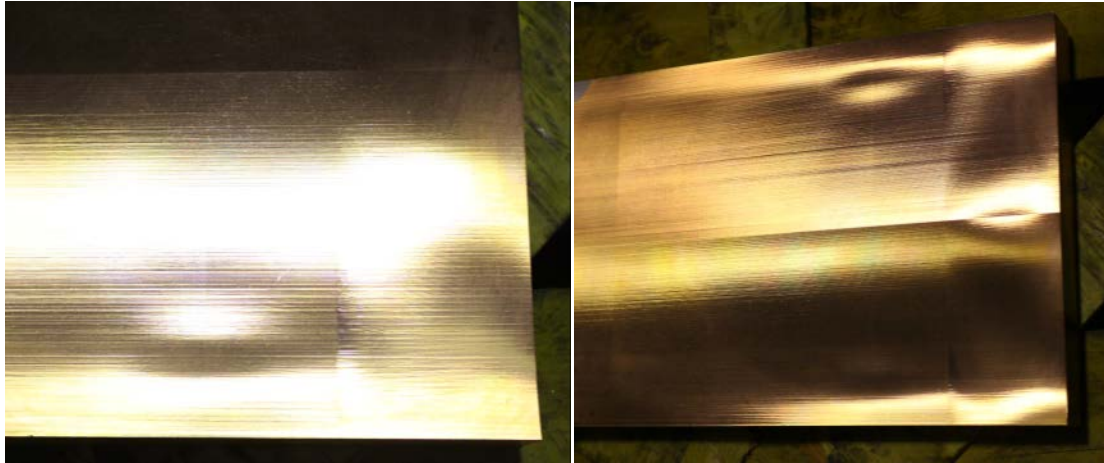
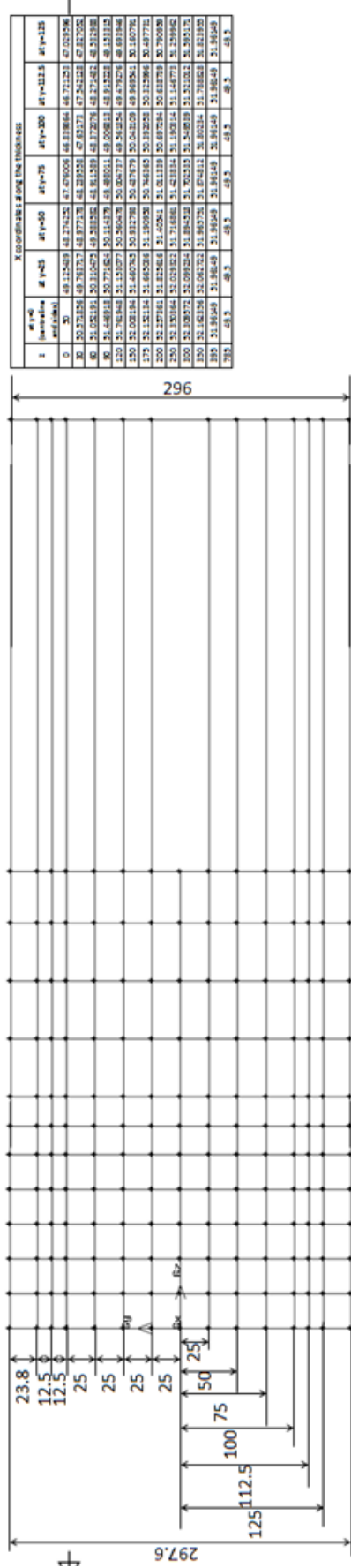
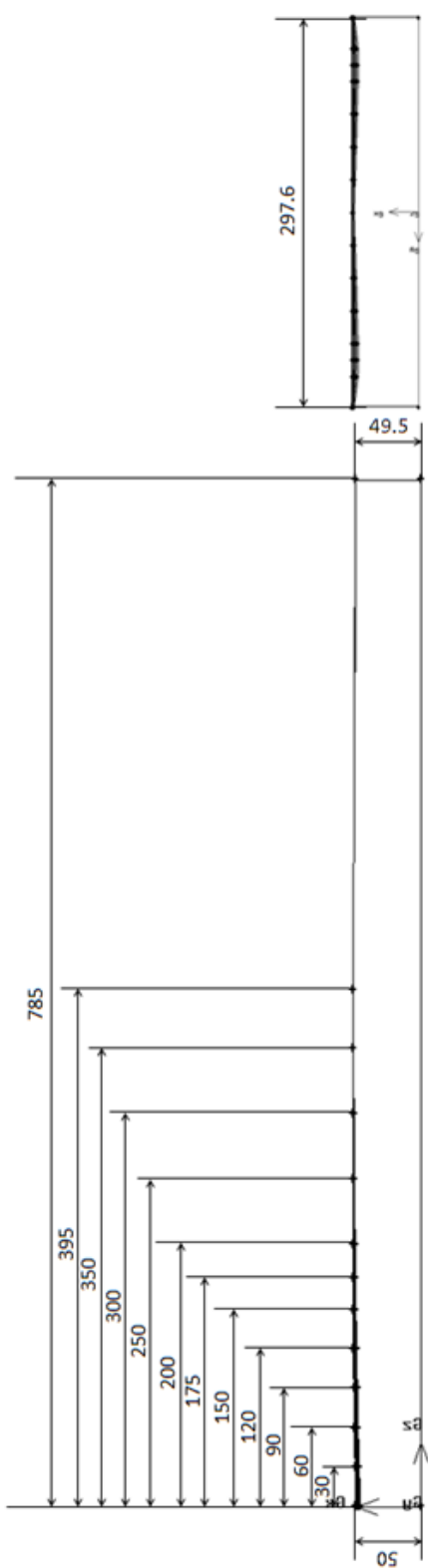


**Figure 28.** Irregularities during machining of mould design for SSAB Oxelösund, Mark III and corrective machining at the mould end (0.5 mm), corner and “gull-wing” sections. Please note that red line applies for further machining at the nose body from 0-400 mm and the straight line from 400-785 applies to all the width.

The final mould coordinates delivered to SSAB as reference take into account these changes. The final model produced was also translated to an engineering drawing as additional documentation.



Z	W	X	Y	Z	W	X	Y	Z	W	X	Y
0	20	48.11249	48.27425	47.29006	48.31864	48.71121	47.21298				
10	20	48.31864	48.71121	48.29006	48.31864	48.71121	47.21298				
20	20	48.31864	48.71121	48.29006	48.31864	48.71121	47.21298				
30	20	48.31864	48.71121	48.29006	48.31864	48.71121	47.21298				
40	20	48.31864	48.71121	48.29006	48.31864	48.71121	47.21298				
50	20	48.31864	48.71121	48.29006	48.31864	48.71121	47.21298				
60	20	48.31864	48.71121	48.29006	48.31864	48.71121	47.21298				
70	20	48.31864	48.71121	48.29006	48.31864	48.71121	47.21298				
80	20	48.31864	48.71121	48.29006	48.31864	48.71121	47.21298				
90	20	48.31864	48.71121	48.29006	48.31864	48.71121	47.21298				
100	20	48.31864	48.71121	48.29006	48.31864	48.71121	47.21298				
110	20	48.31864	48.71121	48.29006	48.31864	48.71121	47.21298				
120	20	48.31864	48.71121	48.29006	48.31864	48.71121	47.21298				
130	20	48.31864	48.71121	48.29006	48.31864	48.71121	47.21298				
140	20	48.31864	48.71121	48.29006	48.31864	48.71121	47.21298				
150	20	48.31864	48.71121	48.29006	48.31864	48.71121	47.21298				
160	20	48.31864	48.71121	48.29006	48.31864	48.71121	47.21298				
170	20	48.31864	48.71121	48.29006	48.31864	48.71121	47.21298				
180	20	48.31864	48.71121	48.29006	48.31864	48.71121	47.21298				
190	20	48.31864	48.71121	48.29006	48.31864	48.71121	47.21298				
200	20	48.31864	48.71121	48.29006	48.31864	48.71121	47.21298				
210	20	48.31864	48.71121	48.29006	48.31864	48.71121	47.21298				
220	20	48.31864	48.71121	48.29006	48.31864	48.71121	47.21298				
230	20	48.31864	48.71121	48.29006	48.31864	48.71121	47.21298				
240	20	48.31864	48.71121	48.29006	48.31864	48.71121	47.21298				
250	20	48.31864	48.71121	48.29006	48.31864	48.71121	47.21298				
260	20	48.31864	48.71121	48.29006	48.31864	48.71121	47.21298				
270	20	48.31864	48.71121	48.29006	48.31864	48.71121	47.21298				
280	20	48.31864	48.71121	48.29006	48.31864	48.71121	47.21298				
290	20	48.31864	48.71121	48.29006	48.31864	48.71121	47.21298				
300	20	48.31864	48.71121	48.29006	48.31864	48.71121	47.21298				
310	20	48.31864	48.71121	48.29006	48.31864	48.71121	47.21298				
320	20	48.31864	48.71121	48.29006	48.31864	48.71121	47.21298				
330	20	48.31864	48.71121	48.29006	48.31864	48.71121	47.21298				
340	20	48.31864	48.71121	48.29006	48.31864	48.71121	47.21298				
350	20	48.31864	48.71121	48.29006	48.31864	48.71121	47.21298				
360	20	48.31864	48.71121	48.29006	48.31864	48.71121	47.21298				
370	20	48.31864	48.71121	48.29006	48.31864	48.71121	47.21298				
380	20	48.31864	48.71121	48.29006	48.31864	48.71121	47.21298				
390	20	48.31864	48.71121	48.29006	48.31864	48.71121	47.21298				
400	20	48.31864	48.71121	48.29006	48.31864	48.71121	47.21298				
410	20	48.31864	48.71121	48.29006	48.31864	48.71121	47.21298				
420	20	48.31864	48.71121	48.29006	48.31864	48.71121	47.21298				
430	20	48.31864	48.71121	48.29006	48.31864	48.71121	47.21298				
440	20	48.31864	48.71121	48.29006	48.31864	48.71121	47.21298				
450	20	48.31864	48.71121	48.29006	48.31864	48.71121	47.21298				
460	20	48.31864	48.71121	48.29006	48.31864	48.71121	47.21298				
470	20	48.31864	48.71121	48.29006	48.31864	48.71121	47.21298				
480	20	48.31864	48.71121	48.29006	48.31864	48.71121	47.21298				
490	20	48.31864	48.71121	48.29006	48.31864	48.71121	47.21298				
500	20	48.31864	48.71121	48.29006	48.31864	48.71121	47.21298				

FILE NAME	Mould design SS.AB	PROJ NO	JK-CAD-20june2013	SHEET	SCALE
SIZE	mm				1:1
ISSUED	1/16/2013				
CHECK	Tomas Seilgren				
APPR.					
ISSUED	20 June 2013				
REV	1				
CONTINUED	JK 24-055				

## 5.6. Mould design for SMT

A new design based on the previous experiences of the IMMODCO concept plus the perimeter and thickness shrinkage concepts was proposed to SMT with the following ingredients:

- Adjustment of the corner angle in accordance with the previous IMMODCO concept.
- Change of reference design radius.
- Installation of thermocouples in corner positions
- Proposal of a parabolic design for the wide (fixed / loose plates) of the mould.

### 5.6.1. Description of the SMT blooms machine equipped with a plate mould

Sandvik Materials Technology offers a wide range of highly engineered products based on an integrated production platform and extensive R&D as well as premium standard products. Examples of products are steam generator and umbilical tubing, strip for flapper valves and razor blades, wire for surgical applications and springs, bars and billets for implant applications and forgings. Rock drill steel is another important product. Heating-related applications and thermal processing are also within the product portfolio.

The continuous casting machine was put into operation in 1981 with the main aim to cast blooms for extrusion billets and rock drill steels. A summary of the basic data are listed in Table 1.

**Table 1.** Basic data for the CC-machine

<b>Concast S-type</b> 3 strand curved machine installed 1981. Radius: 12 m	<b>Strand size:</b> Blooms 365x265, 265x265 mm Billets: 150x150 mm
<b>Casting speed:</b> Blooms: 0.6 to 1.2 m/min Billets: 1.8 to 2.5 m/min	<b>Mould level control:</b> Blooms: Eddy current Billets: Radioactive Co60
<b>Withdrawal unit:</b> 3 pinch and unbending rollers located at 17.7 m, 14.8 m, and 22 m from meniscus	<b>Stirrer:</b> SEMS, 18 Hz 0.4-1.2 m below mould and FEMS, 1000 Gauss, 14.1 m from meniscus
<b>Subentry nozzle:</b> Blooms: 4 port nozzle Billets: Straight	<b>Mould:</b> Blooms: Convex type plate Billets: Convex tube

The bloom machine is of a bent type and has a radius of 12 m. Unbending is done in 2 steps at the withdrawal unit, first to 18 m and then to straight. A sketch of the machine is presented in Figure 29. The radius 12 m is indicated and is located at the fixed wide side of the strand. The figure also indicate that the curvature extend to the top of the mould.

In Figure 30 a detailed sketch of the mould is presented. The mould is made of Cu-plates and the bloom size is 365x265 mm. The fixed wide side is marked out as well as the radius, R12000 mm. The opposite side, the loose side, has a curvature of R11735 mm. The corners are chamfered with a length of  $\sqrt{2} \cdot 7.4 \text{ mm} = 10.5 \text{ mm}$ . The mould has a linear taper of 1%/m.

The parallel sides are of convex type. Figure 31 shows a sketch of a parallel side. The curvature is described by a radius,  $R_c$ . By that the corner angle between the parallel side and the fixed / loose side will be  $90^\circ + \alpha$ . The angle  $\alpha$  is indicated in the figure. The parallel side is straight at the bottom and convex at the top.

Due to that the machine reference line of  $R= 12 \text{ mm}$  coincide with the inner wall fixed wide side, a problem arises when adjusting the mould to the cooling segment. This is indicated in Figure 32 which shows a sketch of the side view of the mould and the supporting rollers below. The tapered mould has to be adjusted in a certain way and the figure shows the original recommendations from the machine supplier. The problem here is that the gap between the strand shell and the fixed / loose plates will not be equal. An uneven heat transfer between strand shell and mould wall can develop which can be harmful and lead to the development of surface cracks.

<p><b>Figure 29. Sketch of SMT blooms CC machine</b></p>	<p><b>Figure 30. Plate mould. Size 365x265 mm. Taper 1%/m.</b></p>
<p><b>Figure 31. Sketch of parallel plate with convex radius.</b></p>	<p><b>Figure 32. Adjustment between strand and mould.</b></p>

**Figure 29- 32. Description of SMT:s bloom caster with plate mould, bloom size 365x265 mm.**

The taper of 1 %/m holds for both the fixed/loose sides (365 mm) and for the parallel sides (265 mm). Figure 33 shows how the conicity in mm decreases from top to bottom of the mould. Figure 34 indicates how the angle  $\alpha$  decreases from the top of the mould. As can be seen the shape of the curve is irregular and SMT wishes to adjust the angle to coincide with the distribution indicated by measurements conducted by Swerea KIMAB in earlier work.

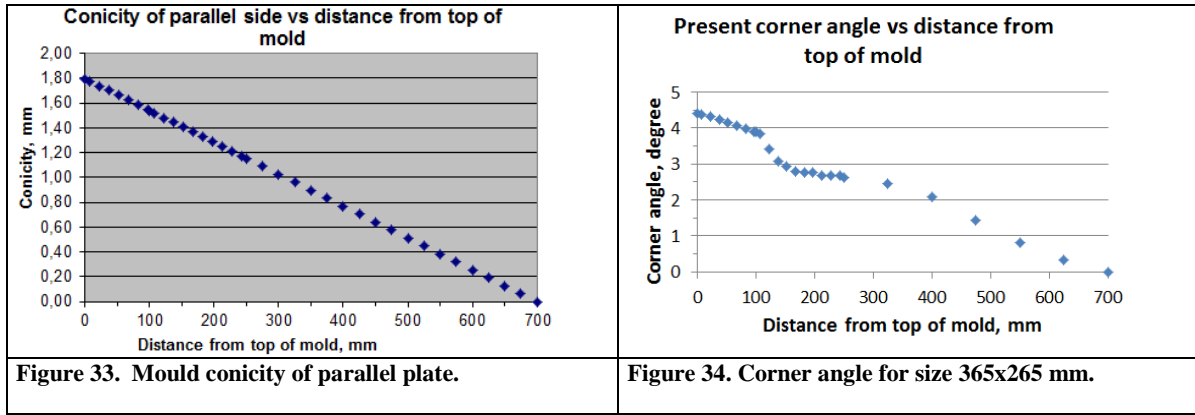


**Figure 33-34.** Outline of present SMT parallel mould plate conicity and corner angle  $\alpha$  from top to the bottom of the mould. Mould length is 700 mm.

### 5.6.2. New design of parallel plates to obtain an improved corner angel distribution

The convex shape of the parallel side is calculated by aid of the equation of a circle, see definitions in Figure 35. The equation can be written as:

$$y^2 + (z-z_0)^2 = R_c^2 \quad (1)$$

or

$$z = z_0 + \sqrt{(R_c^2 - y^2)} \quad (2)$$

Where  $R_c$  is the radius of the circle and  $z_0$  is a constant that can be evaluated at a point in the coordinate system  $(y,z)$  where  $(y=L/2, z=0)$ .  $L$  is the width of the parallel side at a certain height,  $h$ , below the top of the mould. This gives:

$$z_0 = -\sqrt{(R_c^2 - (L/2)^2)} \quad (3)$$

At the point  $(y=L/2, z=0)$  the following equation holds:

$$\tan(\alpha) = dz / dy \quad (4)$$

Inserting eq x in eq x gives the radius  $R_c$  as function of the  $L$  and  $\alpha$ :

$$R_c = (L/2) \cdot \sqrt{(1-\tan^2(\alpha))} / \tan(\alpha) \quad (5)$$

Here  $z$  is equal to  $\Delta z$  in Figure 35 and describe the depth of the curvature.

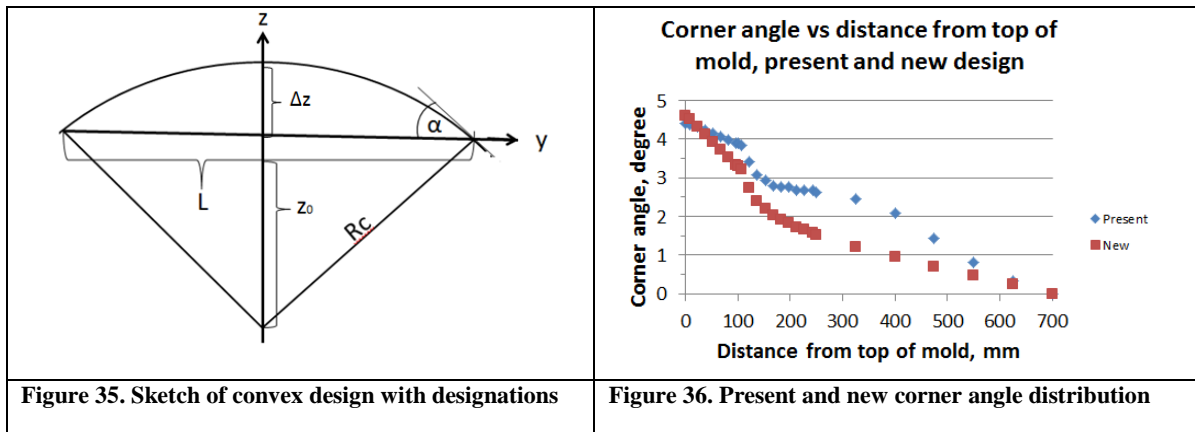


**Figure 35-36.** Sketch of the shape of the convex design with designations and the new corner angle distribution.

The variation of the width of the parallel plate,  $L(h)$ , with height of the mould is the same as in Figure 33. The variation of the angle  $\alpha(h)$  is the same as the curve presented in Figure 36.

The new design of the parallel side is presented in Figure 37 and 38. As can be seen the shape of the angle distribution is more in accordance with Figure 1 in this report.

One should observe that in Figure 37 the curves for  $h=400$  mm is shifted in the  $y$ -direction due to the curvature of the strand.

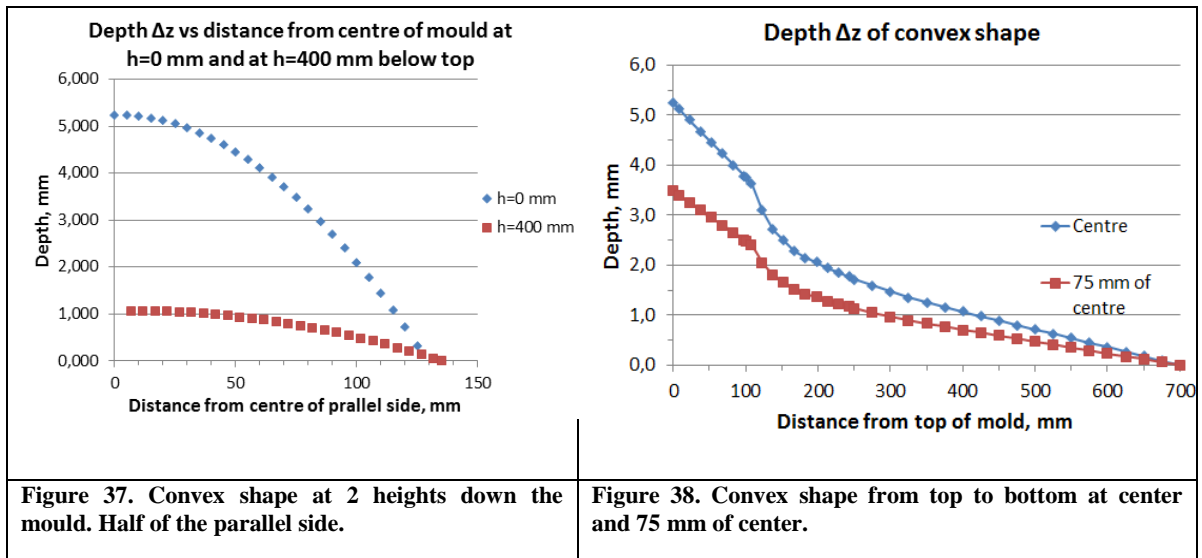


**Figure 37-38.** Design of the new parallel sides.

### 5.6.3. Change of reference design radius

Due to the asymmetry, having the machine reference line at  $R=12$  m when designing the mould taper, it was decided to move the reference radius to a position at half of the width of the parallel side,  $L_0/2$ , where  $L_0$  correspond to the width of the plate at the bottom of the mould (at  $h=700$  mm). This implies that all 4 plates have to be machined with different radii. The curvature of a parallel side is composed of both the taper,  $C=0.01$  and of the curvature. The conicity,  $\Delta L(h)$  [mm] as function of mould length,  $h$ , from the top can be described by the equation:

$$\Delta L (h) = L_0 \cdot C \cdot (700-h) \quad , \text{ [mm]} \quad (6)$$

The reference radius,  $R_{\text{ref}}$ , can be calculated as:

$$R_{\text{ref}} = 12000 \text{ mm} - 7,4 \text{ mm} - L_0/2 \quad , \text{ [mm]} \quad (7)$$

The reference radius is horizontal at a distance of 400 mm below the top of the mould. To be able to describe the curvature of the parallel plates at the fix and loose side the profile was approximated by 2 radiuses  $R_f$  and  $R_l$ .

The equation for each radius has 3 unknown constants which can be solved by the equation systems below and with reference to Figure 39:

$$\left. \begin{aligned} (y_1 - y_0)^2 + (h_1 - h_0)^2 &= R^2 \\ (y_2 - y_0)^2 + (h_2 - h_0)^2 &= R^2 \\ (y_3 - y_0)^2 + (h_3 - h_0)^2 &= R^2 \end{aligned} \right\} \quad (8)$$

Where the constants are calculated by aid of eq. (9)

$$\left. \begin{aligned} h_0 &= (a_2 \cdot b_1 - a_1 \cdot b_2) / (c_1 \cdot b_2 - c_2 \cdot b_1) \\ y_0 &= (a_1 + h_0 \cdot c_1) / b_1 \\ R &= \sqrt{(y_1^2 - 2 \cdot y_1 \cdot y_0 + y_0^2 + h_1^2 - 2 \cdot h_0 \cdot h_1 + h_0^2)} \end{aligned} \right\} \quad (9)$$

and

$$\left. \begin{aligned} a_1 &= y_2^2 - y_1^2 + h_2^2 - h_1^2 \\ a_2 &= y_3^2 - y_2^2 + h_3^2 - h_2^2 \\ b_1 &= 2 \cdot (y_2 - y_1) \\ b_2 &= 2 \cdot (y_3 - y_2) \\ c_1 &= 2 \cdot (h_1 - h_2) \\ c_2 &= 2 \cdot (h_2 - h_3) \end{aligned} \right\} \quad (10)$$

The results of the calculations are presented in Figure 39 and 40.

As the profiles of the parallel sides were changed, also the fixed and loose sides had to be remachined.

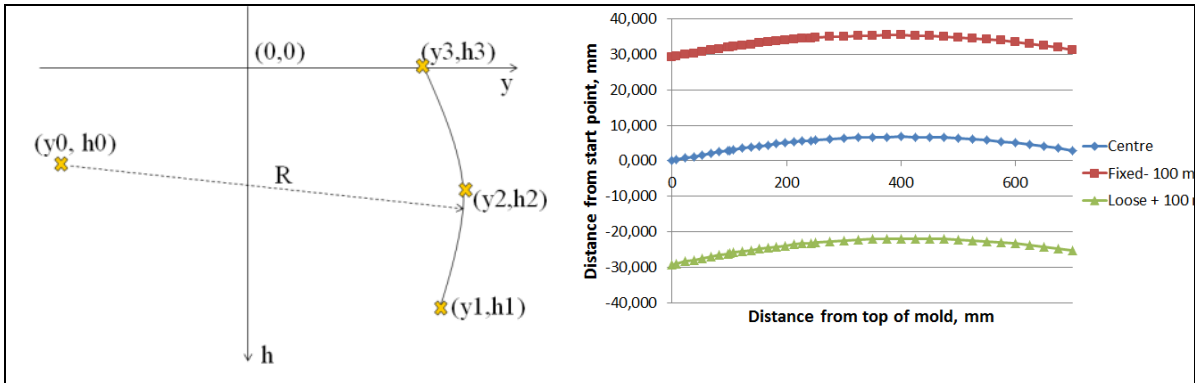


**Figure 39. Coordinate system for the parallel plate fix and loose side radius,  $R_f$  and  $R_l$**

**Figure 40. Profile of parallel plate at center, fixed and loose side**

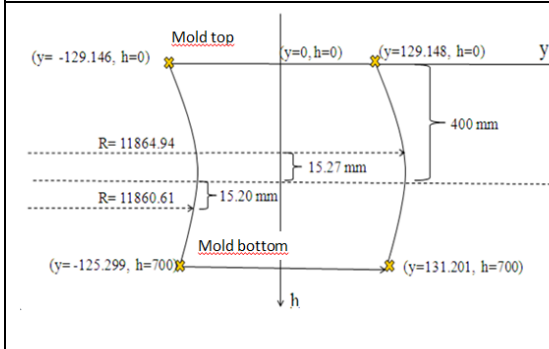


**Figure 41. Fixed and loose radius,  $R_f=11864,94$  and  $R_l=11860,61$**

**Figure 39-41. New curvature of the 4 plates after changing the reference design radius.**

The results of the calculations are presented in Figure 40 and 41.

As the profiles of the parallel sides were changed the fixed and loose wide sides also had to be remachined.

#### 5.6.4. Parabolic design of the fixed and loose wide side

A parabolic taper shall compensate for the shrinkage of the shell. The temperature evolution of the shell in the mould is therefore important to understand. The shell shrinkage is proportional to the temperature drop and the thermal expansion coefficient  $\alpha_{exp}$ .

Swerea MEFOS has provided SMT with an equation (11) describing the temperature drop,  $\Delta T$ , in the shell:

$$\Delta T = 1255,9 - 191,7 \cdot \ln(h) \quad (11)$$

Where h is the distance from top of the mould.

This equation can be compared with a simple analytical solution of the shell surface temperature.

$$T_{surf} = (T_L - T_m) / (1 + H \cdot h / k) + T_m \quad (12)$$

Here  $T_{surf}$ =Shell surface temperature,  $T_L$ =Liquidus temperature=1480 C,  $T_m$ =Mould temperature= 200 C,  $H$ = heat transfer coefficient [ W/m<sup>2</sup>K],  $k$ =Shell heat conductivity=28 [J/m sec C]

Equation (11) and equation (12) is plotted in Figure 42. As can be seen Swerea MEFOS eq. (11) agree very well with the curve with  $H= 900$  W/m<sup>2</sup>K. A deviation can be seen close to the meniscus at 100 mm from the top of the mould.

The equation (11) was chosen to estimate a new parabolic shape. Figure 43 shows two curves, the read with a linear taper of 1%/m and the green curve with a parabolic taper. The total normalized taper,  $L / L_0$ , between 100-700 mm is the same for the two curves. However the parabolic curve is steeper close to the meniscus and flattens out near the mould exit.

It is proposed that at the distance between  $h=0$ -100 mm the curves coincide.

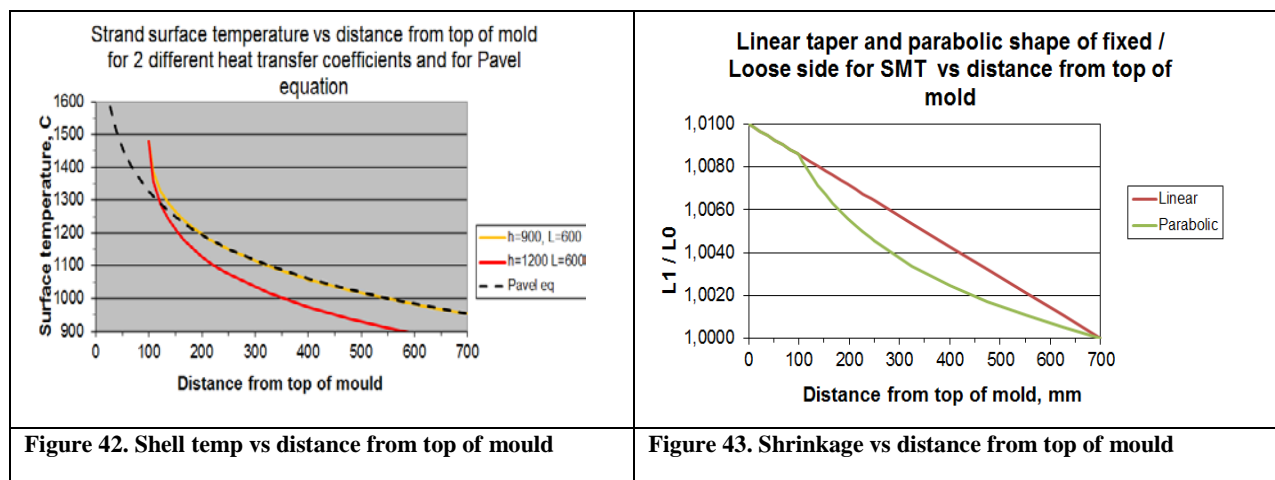


**Figure 42- 43.** Shell temperature and normalized shrinkage vs distance from top of the mould for SMT.

### 5.6.5. Machining of the mould

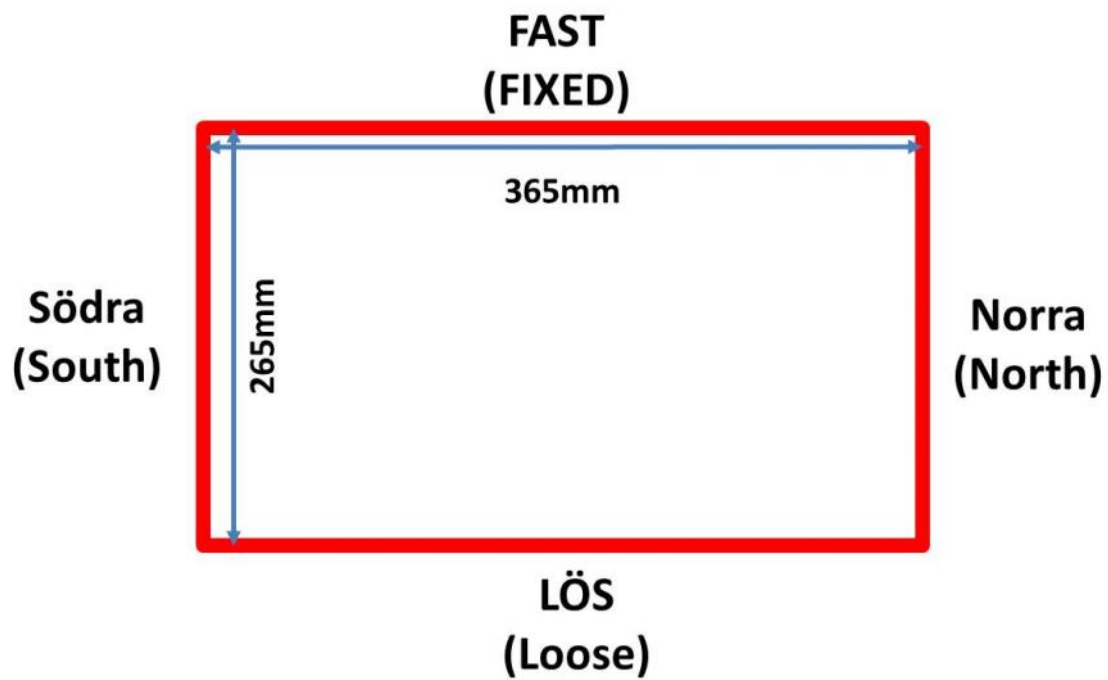
The NC-equipment to machine the copper plates could either be programmed with coordinates or with a fixed coordinate + a radius for machining in one direction. It was decided that the convexity should be programmed by a mesh of data points, (h,y,z). The mesh had a grid of 53x38 data points. The curvature was calculated by giving a radius and starting point.

To be able to succeed with this project a close cooperation was established with SMT's subcontractor who did the machining.

## 6. EXPERIMENTS AND EVALUATION OF OPTIMAL MOULD FOR SANDVIK MATERIALS TECHNOLOGY

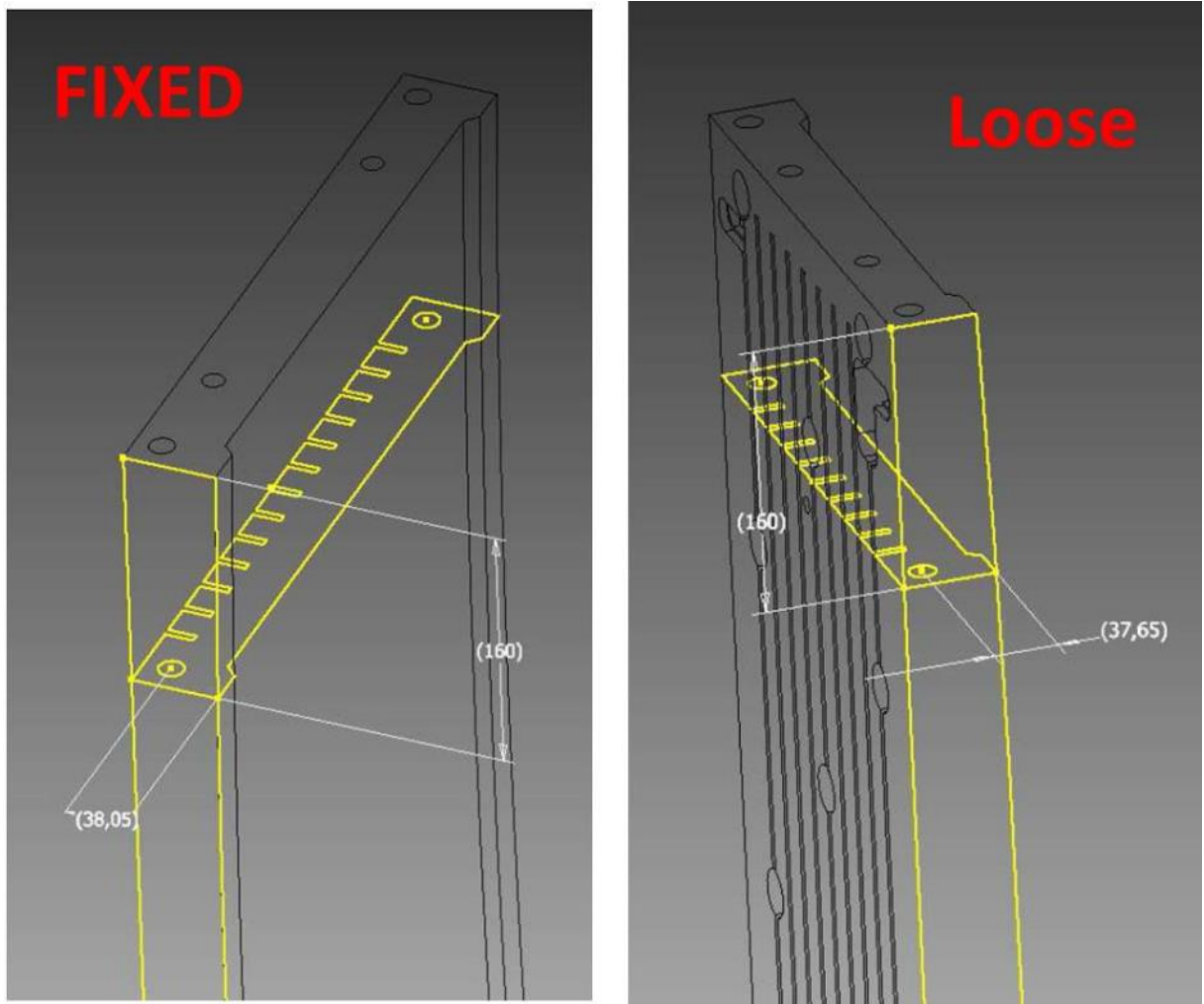
### 6.1. Instrumentation of the design mould

The design mould was instrumented with 4 type K thermocouples. The instrumentation concerns the four corners of the bloom mould 365mm×265mm. Figure 44 shows a cross section of the mould and the definition of positions used in the report.



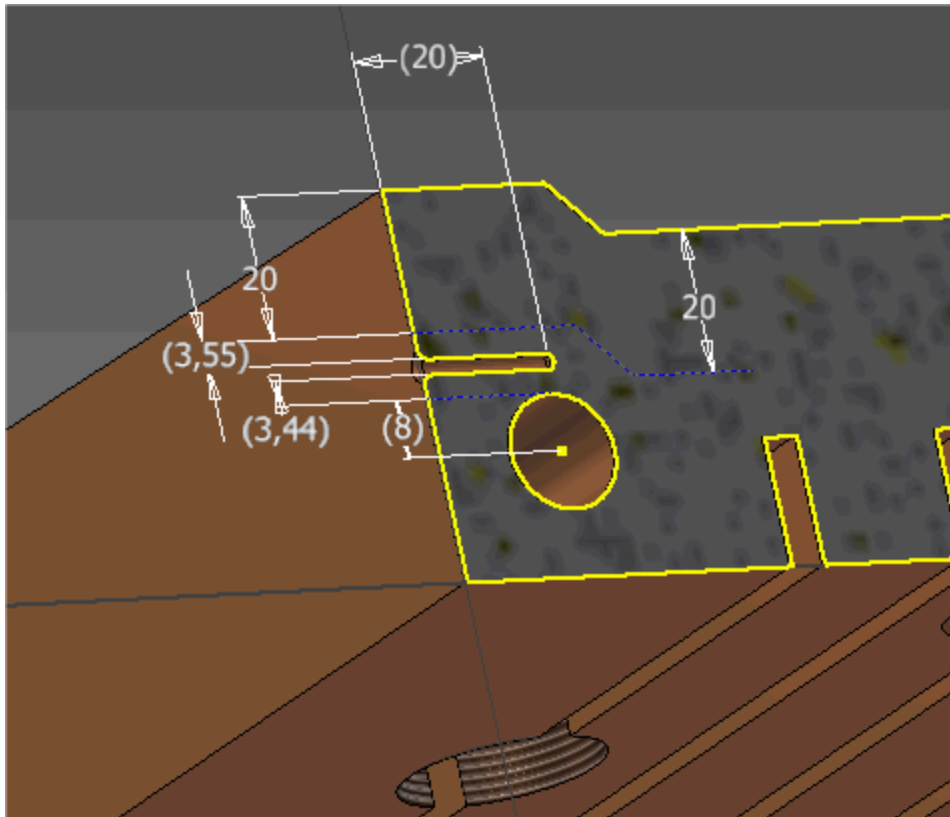
**Figure 44.** *Position for the instrumentation of the design mould*

The drillings were performed in both the fixed and loose wide plates. More specifically, two holes in each plate. The drilling was made 160 mm from the upper edges of the plates as shown in Figure 45.



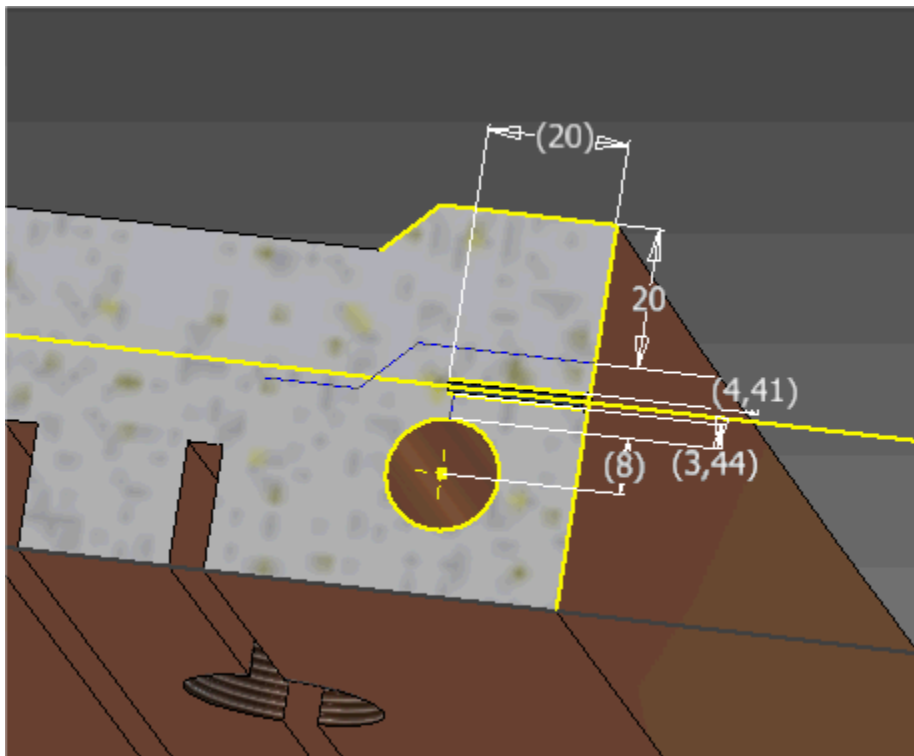
**Figure 45.** Fixed and loose wide side of the mould

Figure 46 and 47 shows the position of drilling for thermocouples in the loose wide plate. The diameter of the hole diameter is 2.2 mm and its length 20 mm.



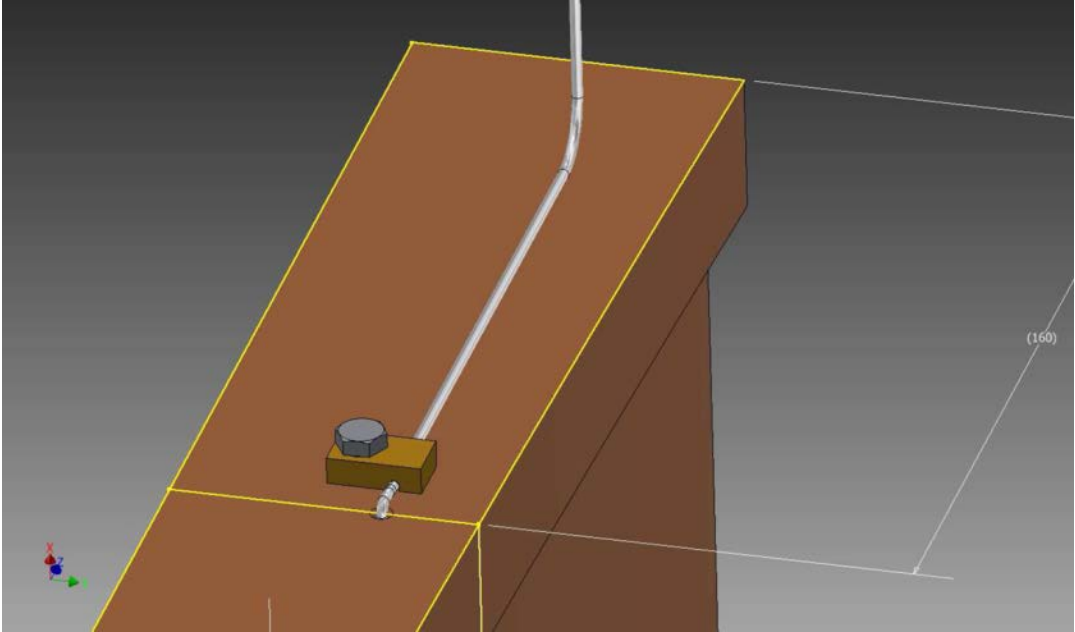
**Figure 46.** Position of hole for thermocouple on the loose side.

Figure shows the position of drilling for thermocouples in fixed plate. The hole diameter is 2.2 mm and 20 mm long inside.



**Figure 47.** Position of hole for thermocouple installation on the loose side.

To fix all four thermocouples at the intended places a fixture arrangement was designed by SMT which is shown schematically in Figure 48-49



**Figure 48.** Fixture arrangement designed by SMT.

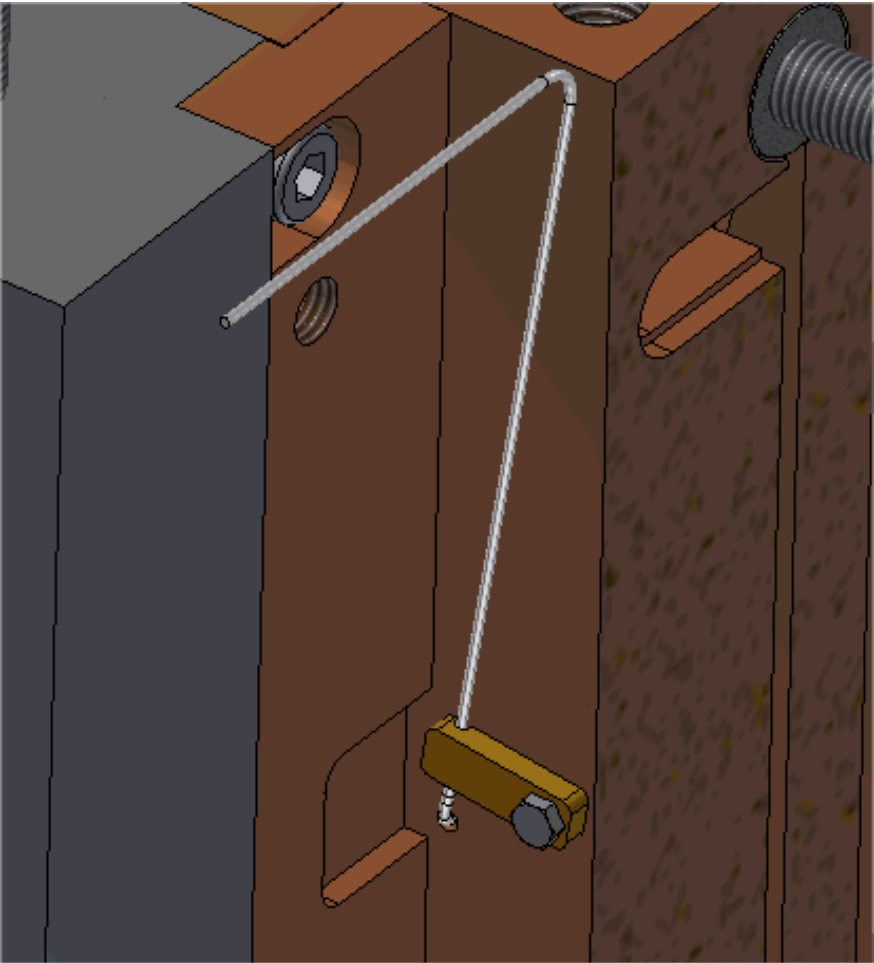


**Figure 49.** Fixture arrangement after mould assembling.

During the experiments at SMT, the temperature of the thermocouples was measured using a data logger. Four temperatures were registered at a sampling rate of one per second. The thermocouples had been calibrated by SMT's calibration laboratory before the trials.

## 6.2. Thermocouples

### 6.2.1. Numbering of thermocouples

The numbering of the thermocouples is shown in Table 2.

**Table 2.** Numbering of thermocouples at the southwest positions

positions	Distance from the top of the mould/mm	Depth from the copper surface/mm	Designation
<b>Fixed-North</b>	160	20	Fast-norr
<b>Fixed-South</b>	160	20	Fast-söder
<b>Loose-North</b>	160	20	Lös-norr
<b>Loose-South</b>	160	20	Lös-söder

Figure 50 shows the T.C. installation in the mould.



**Figure 50.** T.C. installation in the mould.

Totally 30 heats were followed up and recorded including three different steel grades: carbon steel, stainless steel and stainless steel with a high Ni-content. (Six single heats and twelve sequences). The following results are a section from 8 of the followed heats.

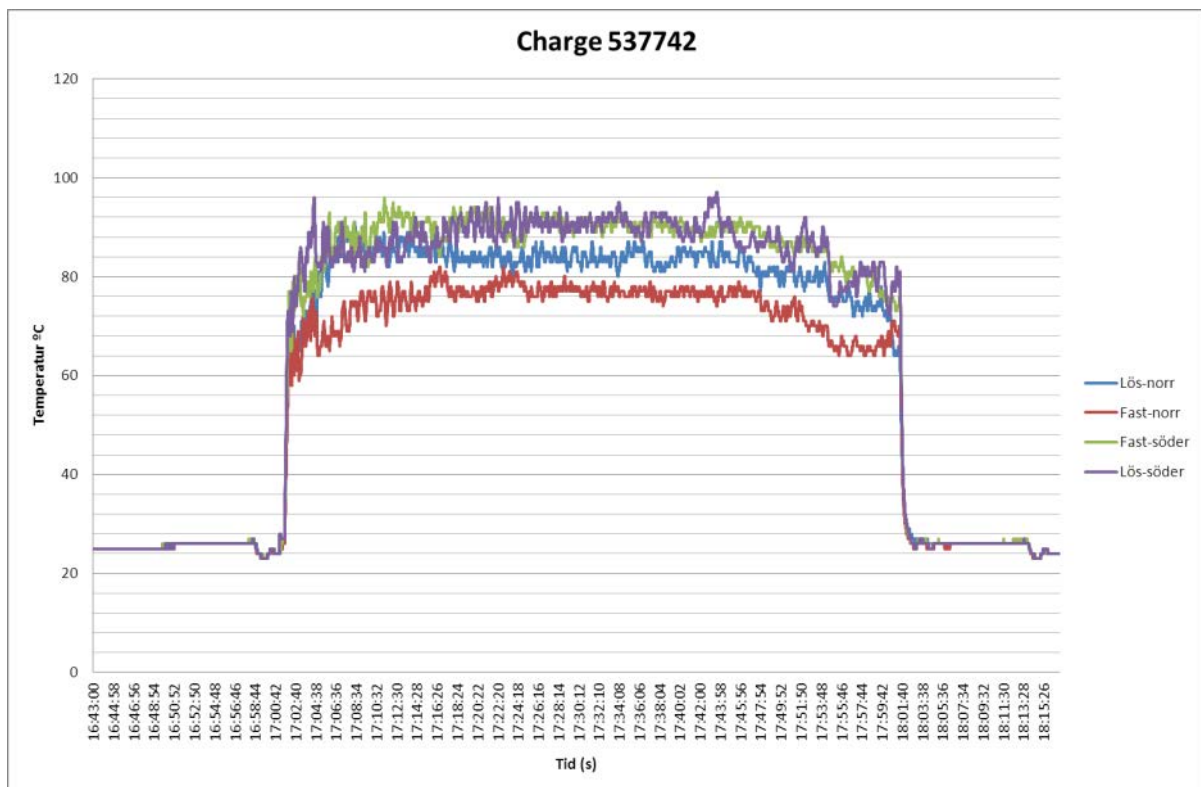
### 6.3. Results SMT

Table 3 shows the investigated heats and their temperatures registrations. The cast blooms were visually examined and corner cracks noted if any. In the last column number of blooms with corner cracks is listed.

**Table 3.** Investigated heats

Heat number	Group	Blooms with cracks
537742	stainless steel	1
537740	stainless steel	1
537741	stainless steel	0
537738	stainless steel	0
537739	stainless steel	0
53767	carbon steel	0
53766	carbon steel	0
537731	stainless steel high Ni	0

#### 6.3.1. Heat Number 537742 (single, stainless steel).



**Figure 51.** Heat Number 537742 (single, stainless steel).

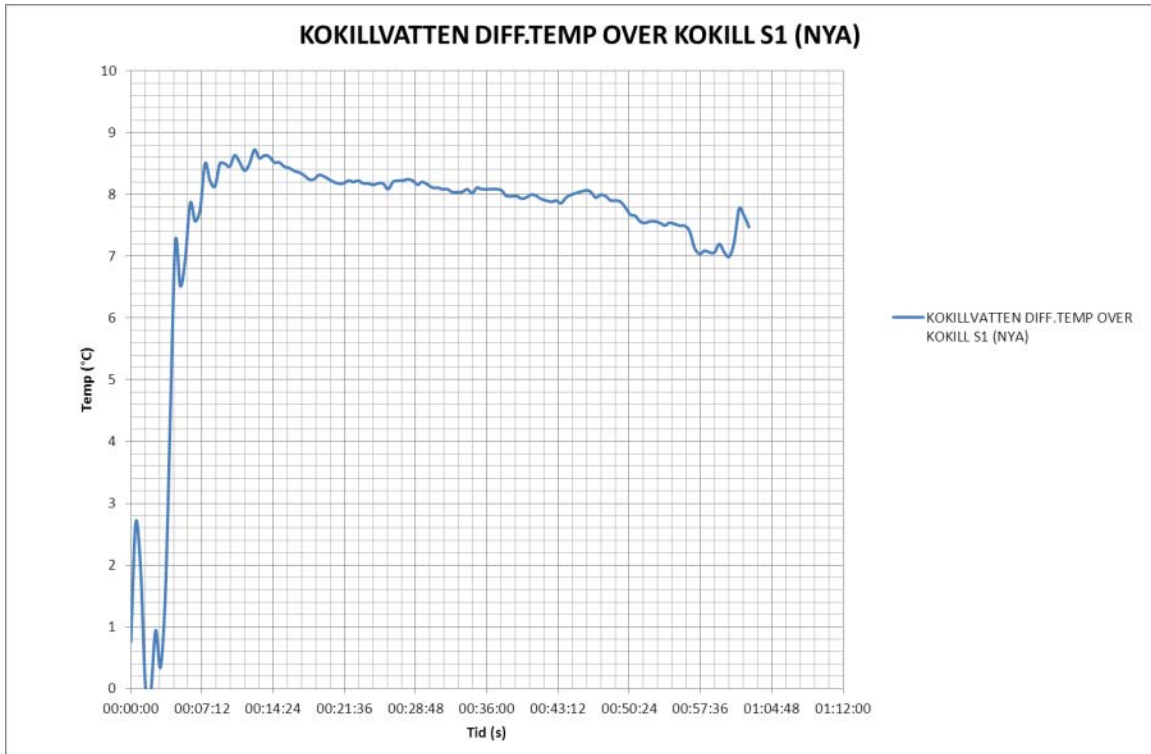


**Figure 52.**  $\Delta T$  of mould water.

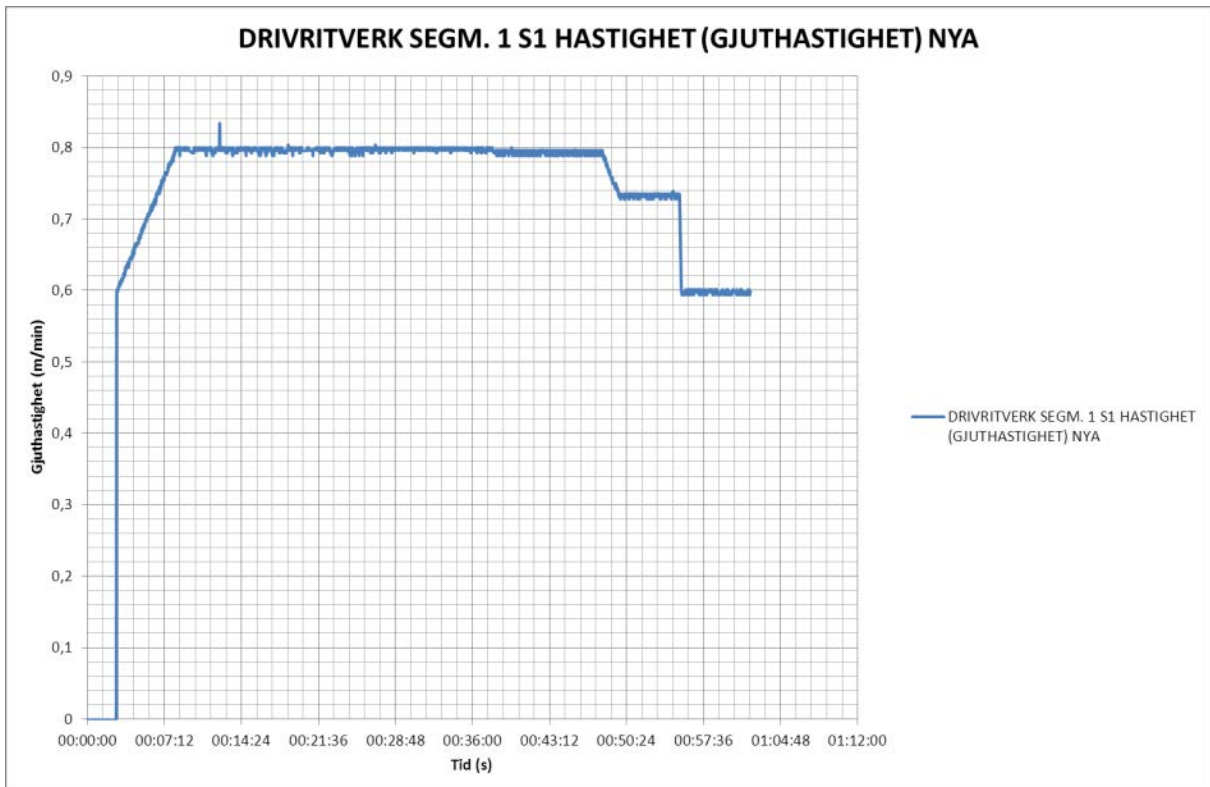


**Figure 53.** Casting speed  $V_c$ .

### 6.3.2. Heat Number 537740 and 537741 (sequence, stainless steel)

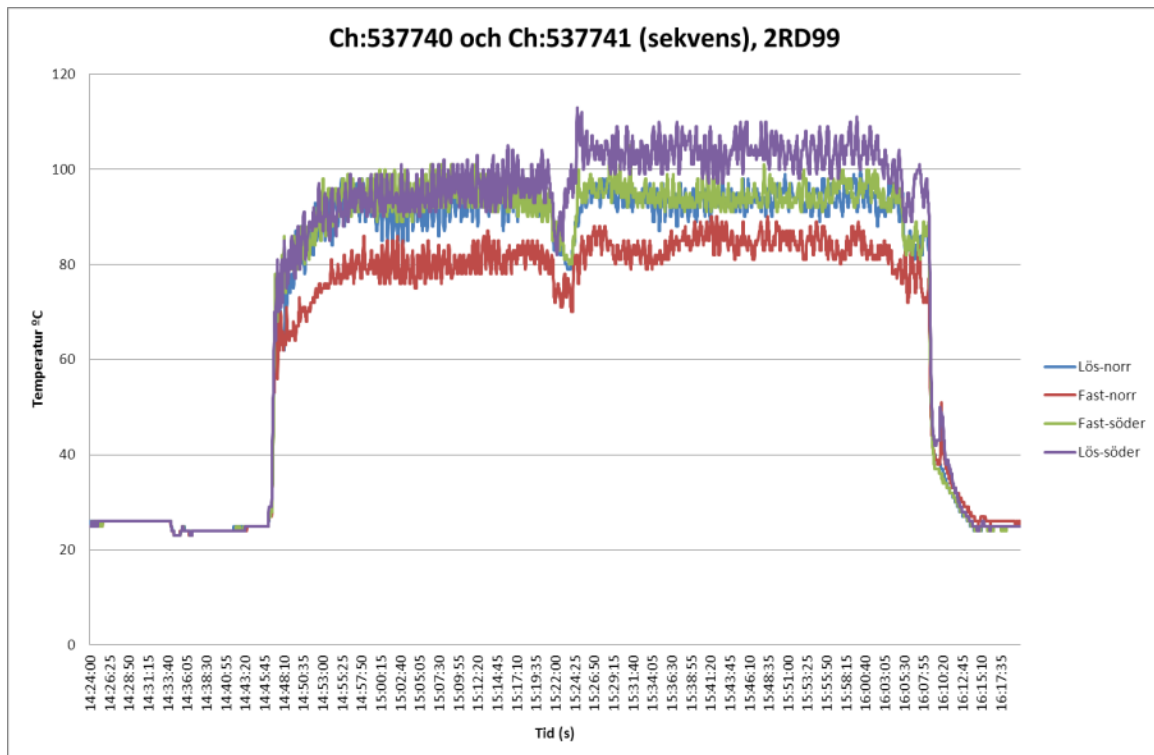


Figure 54. Heat Number 537740 and 537741 (sequence, stainless steel).

### 6.3.3. Heat Number 537766 and 53767 (sequence, carbon steel)

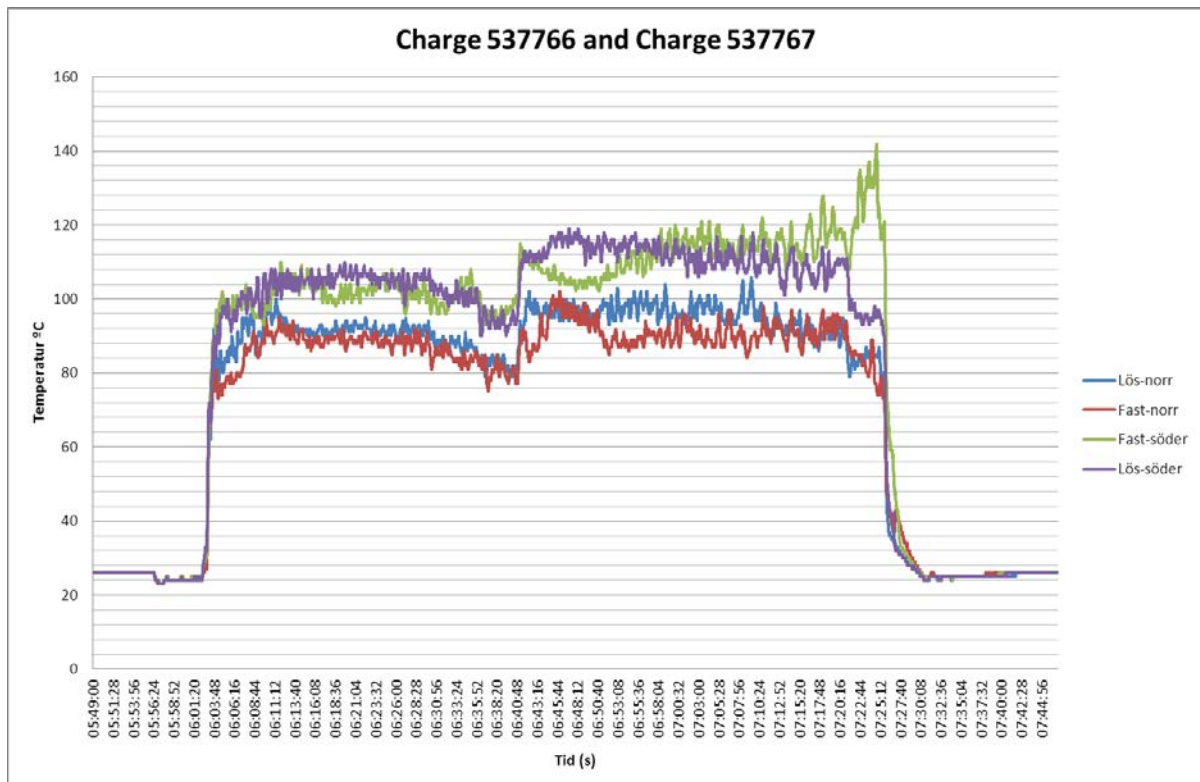
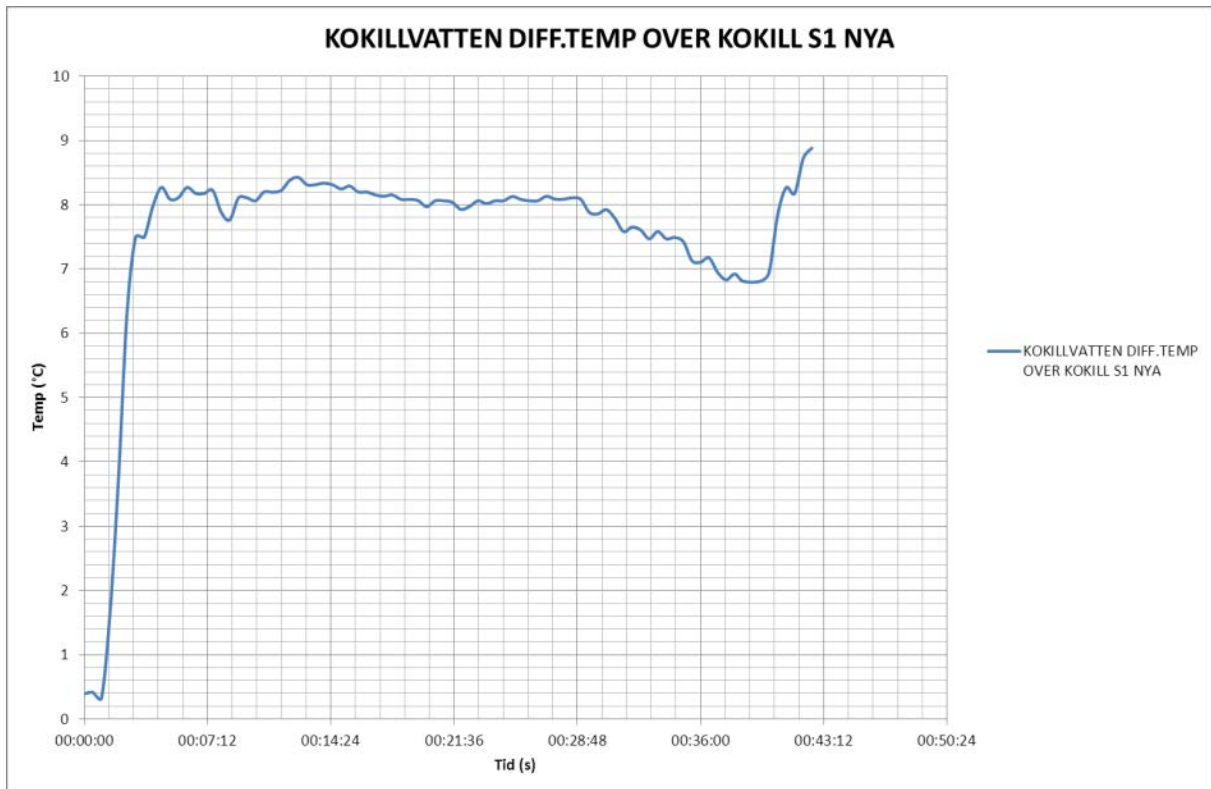
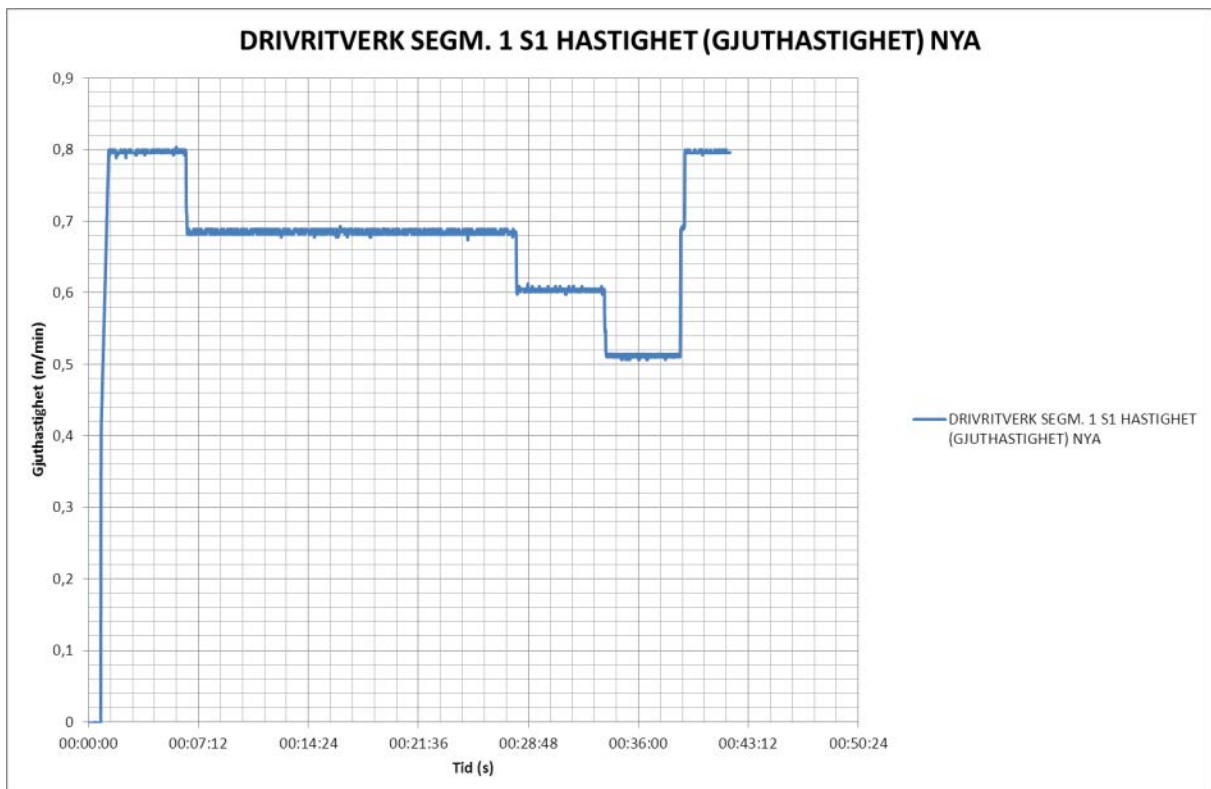


Figure 55. Heat Number 537766 and 53767 (sequence, carbon steel).



**Figure 56.**  $\Delta T$  of mould water.



**Figure 57.** Casting speed  $V_c$ .

### 6.3.4. Heat Number 537731 (single, stainless steel high Ni)

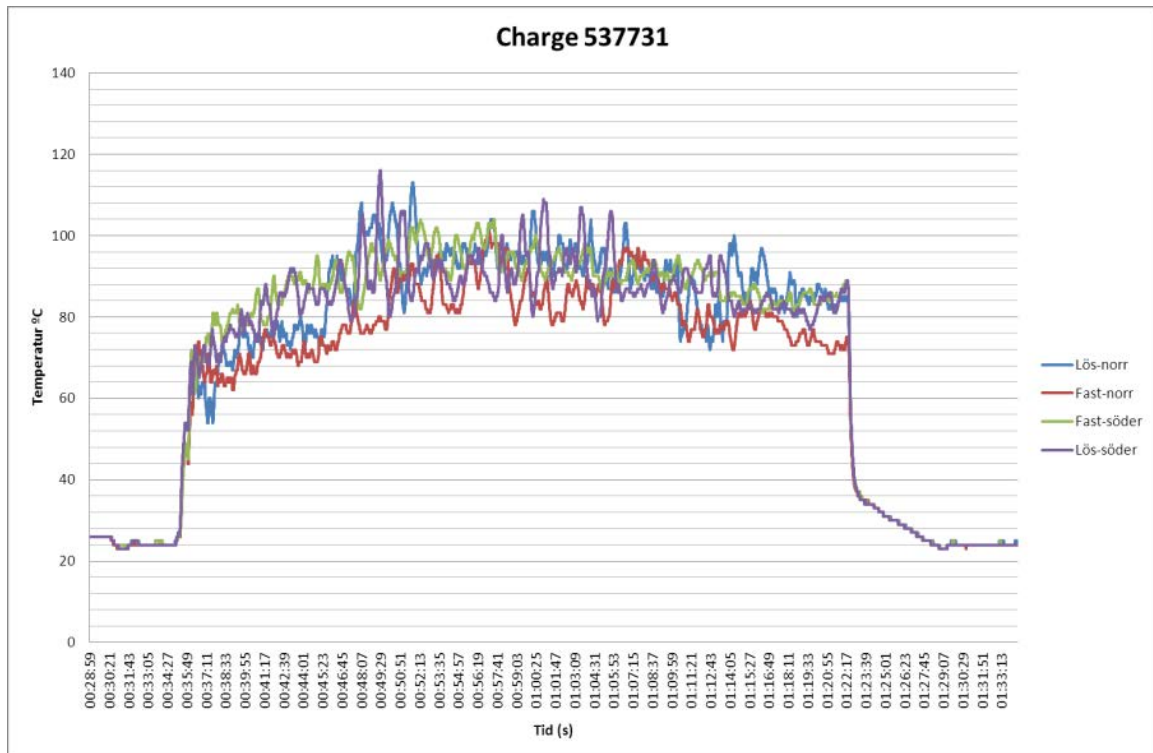


Figure 58. Heat Number 537731 (single, stainless steel high Ni).

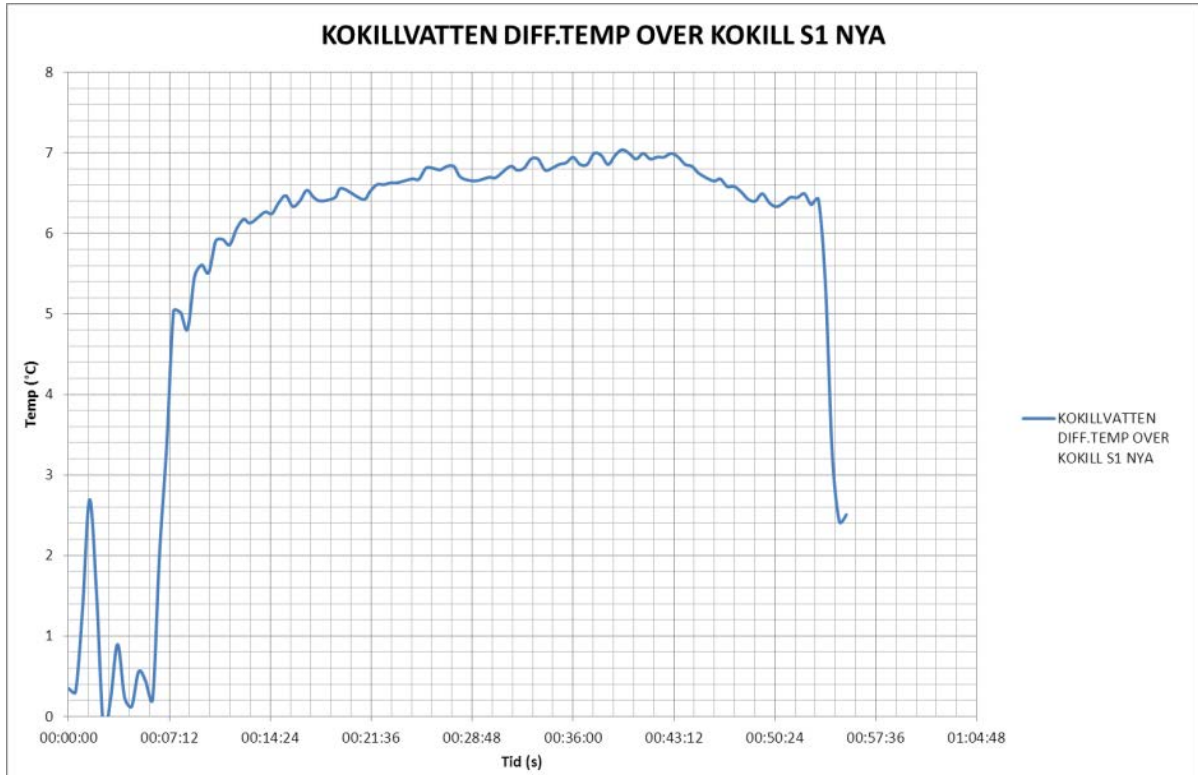


Figure 59.  $\Delta T$  of mould water.

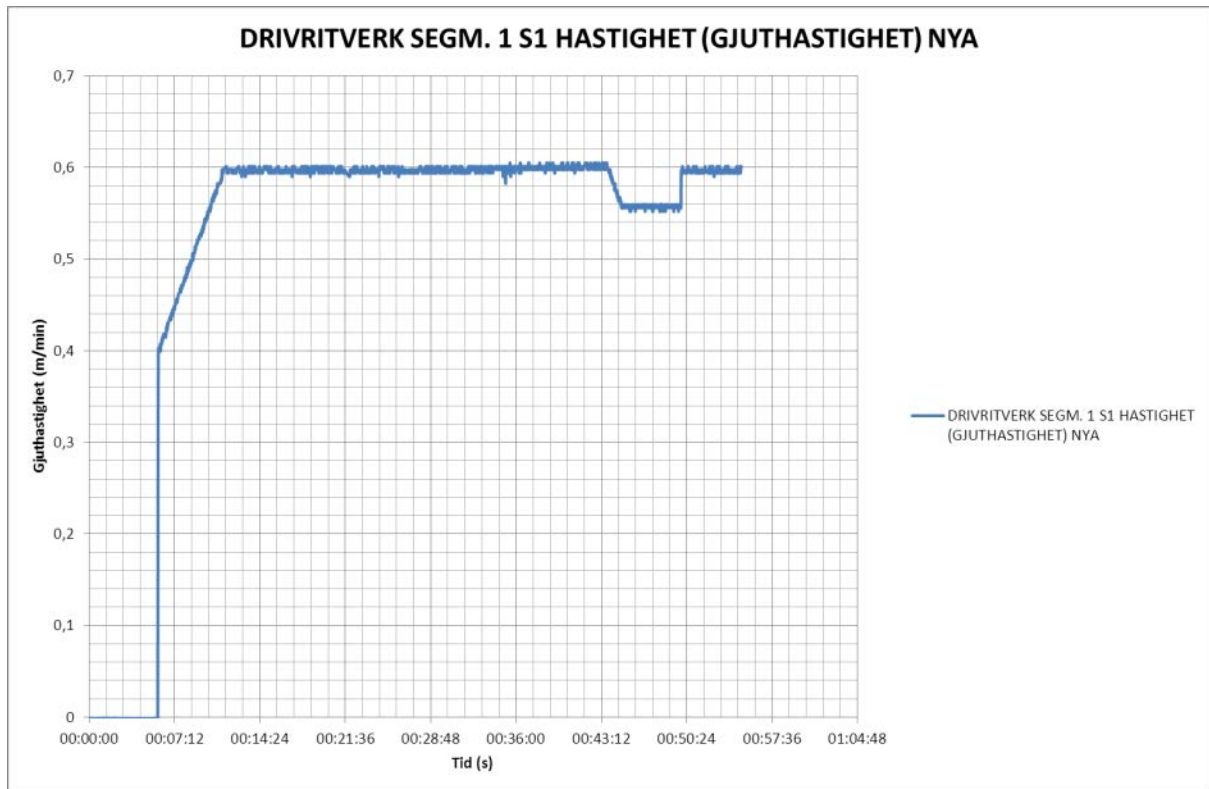


Figure 60. Casting speed  $V_c$ .

### 6.3.5. Heat Number 537738 and 537739 (sequence, stainless steel)

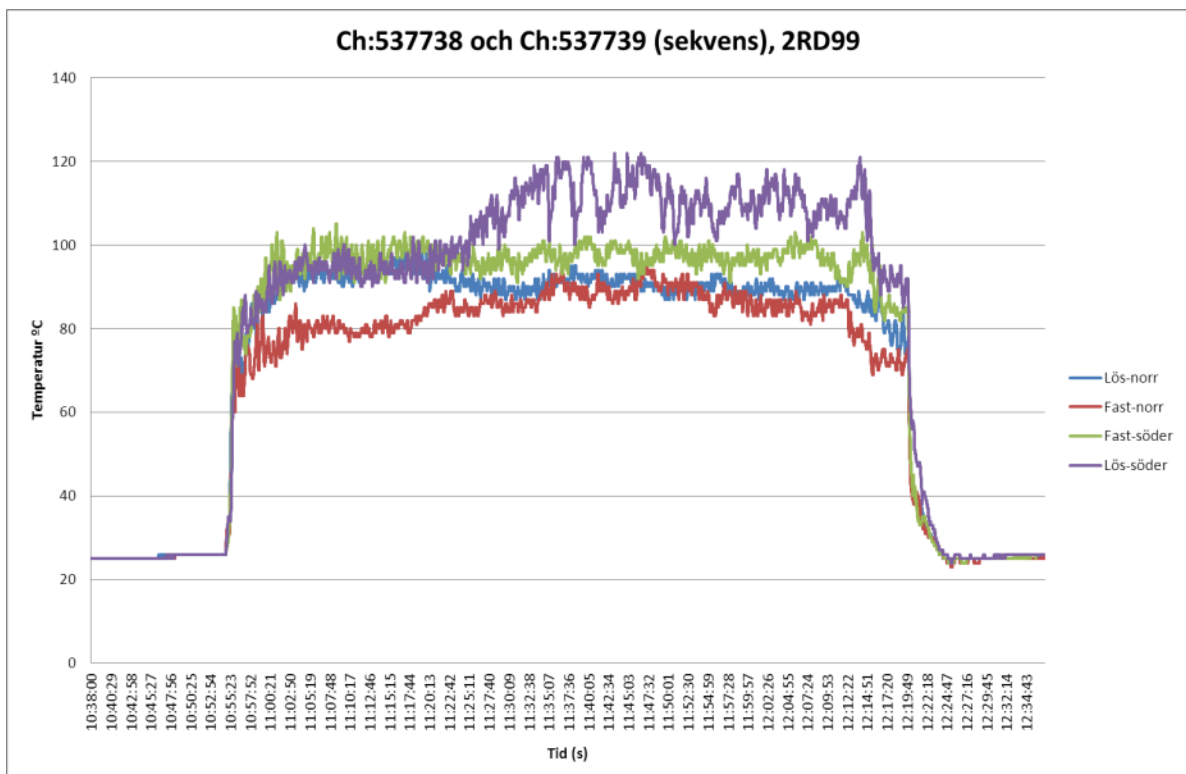


Figure 61. Heat Number 537738 and 537739 (sequence, stainless steel).

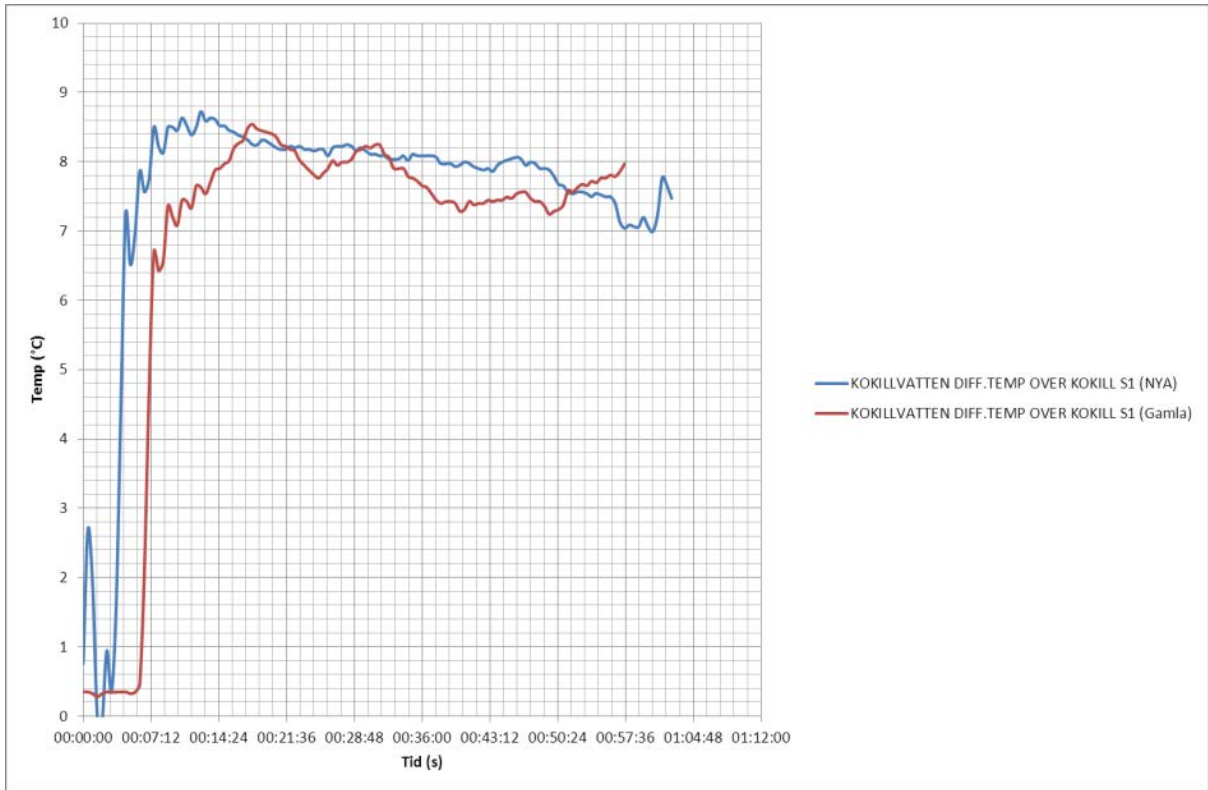


Figure 62.  $\Delta T$  of mould water.

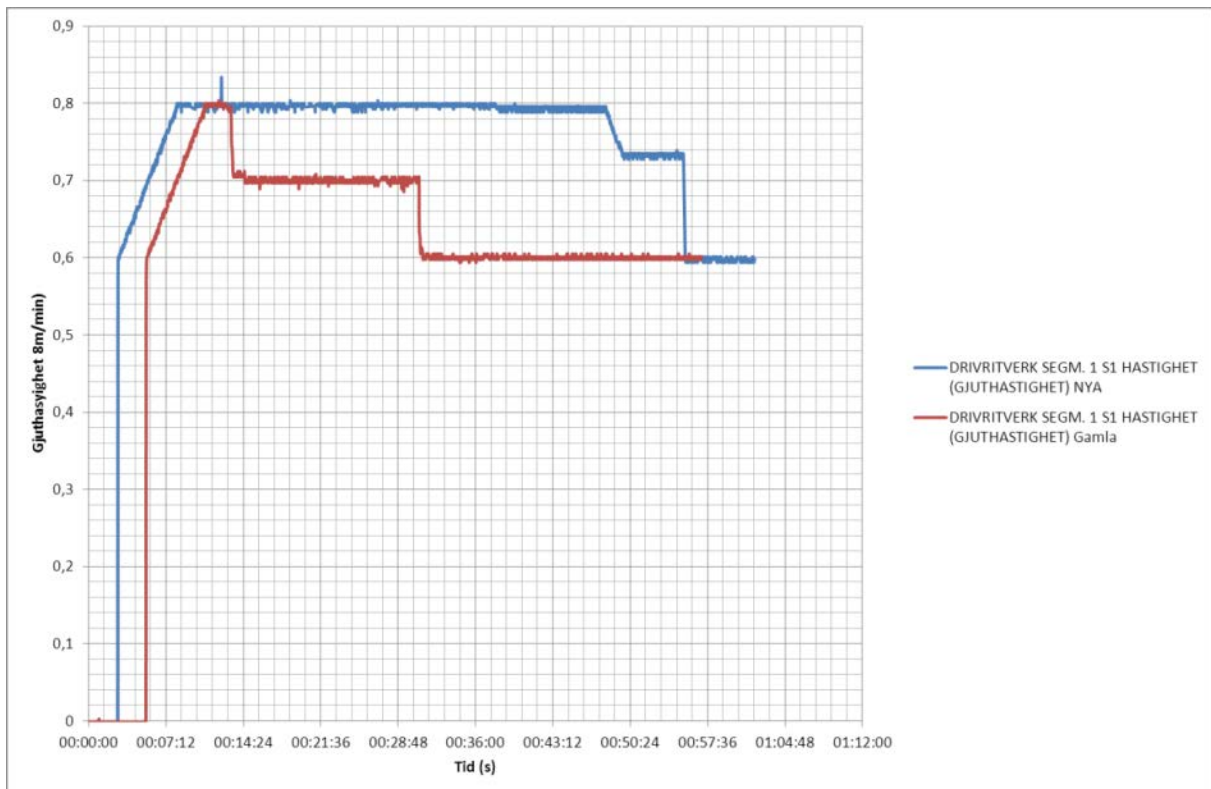


Figure 63. Casting speed  $V_c$ .

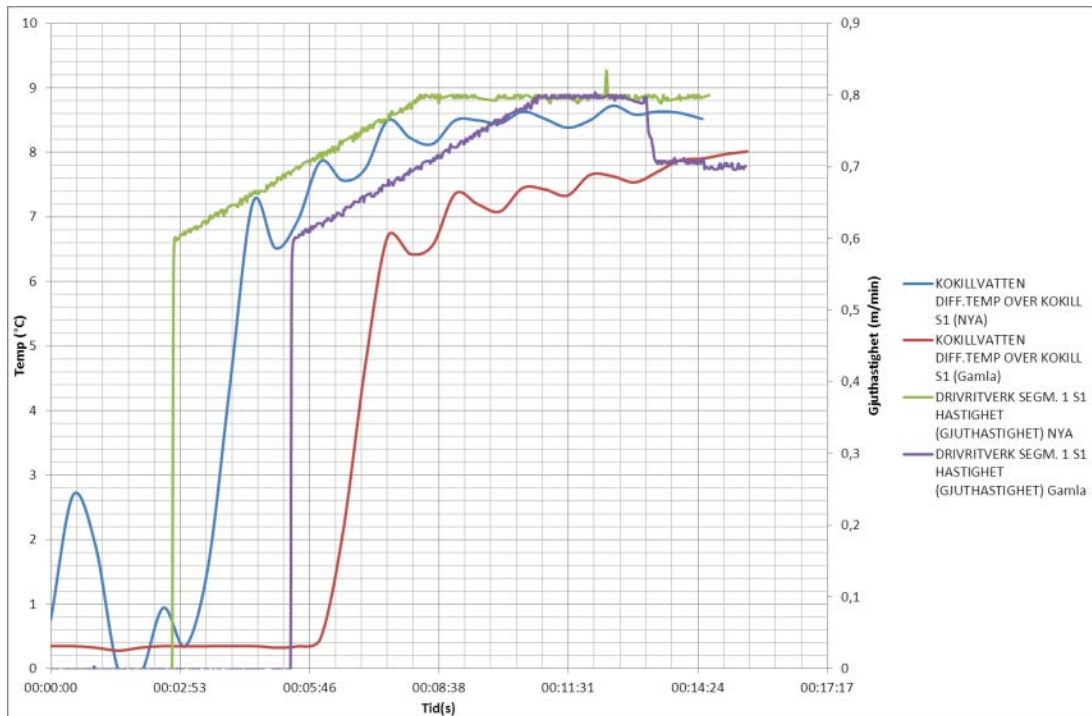


Figure 64.  $\Delta T$  and casting speed.

Table 4. Tundish temperatures.

Heat	Temperature in tundish
537176	1490
537742	1505

### 6.3.6. Heat Number 537766 (carbon steel, new design) and Heat Number 537944 (carbon steel, old design)

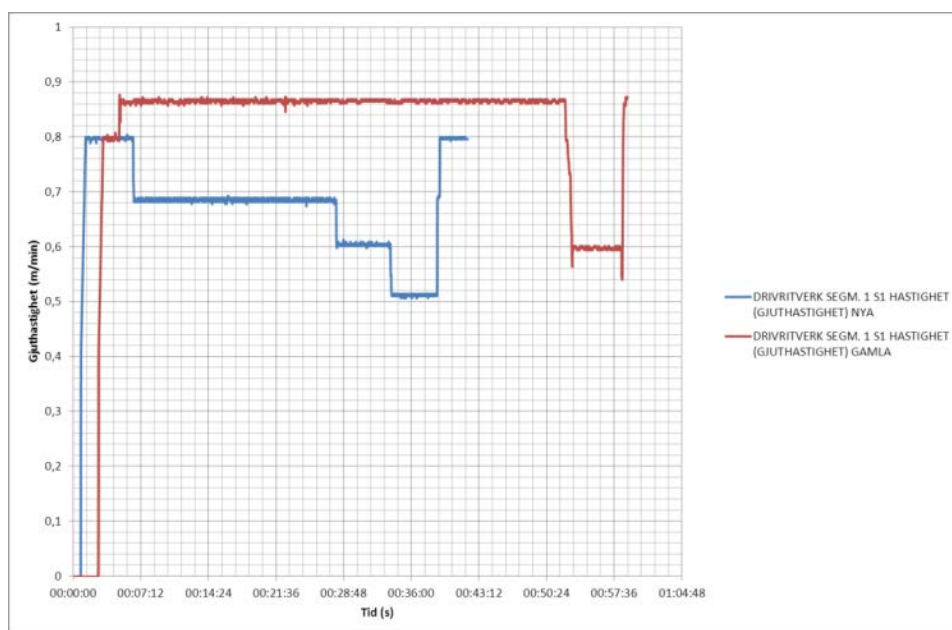


Figure 65. Casting speed.

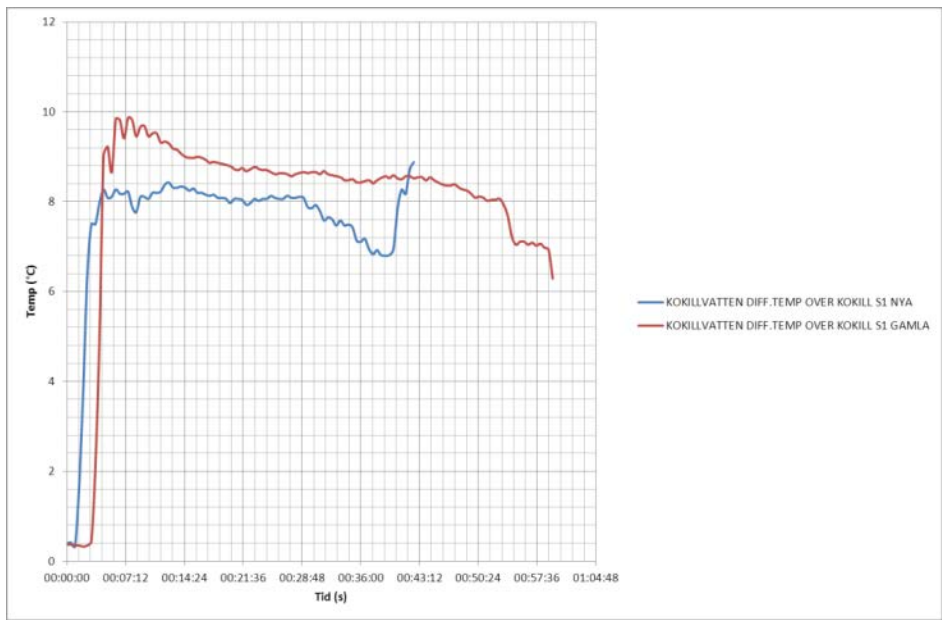


Figure 66.  $\Delta T$  of mould water.

Table 5. Tundish temperatures.

Heat	Temperature in tundish
537766	1544
537944	1538

6.3.7. Heat Number 537731 (stainless steel high Ni, new design) and Heat Number 537399 (stainless steel high Ni, old design)

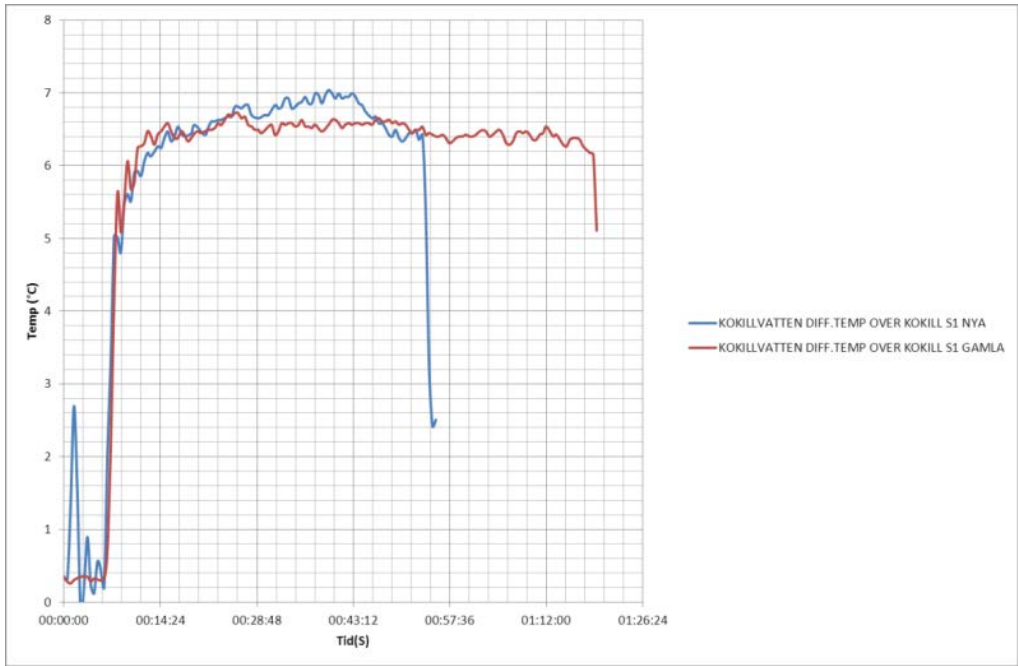


Figure 67.  $\Delta T$  of mould water.

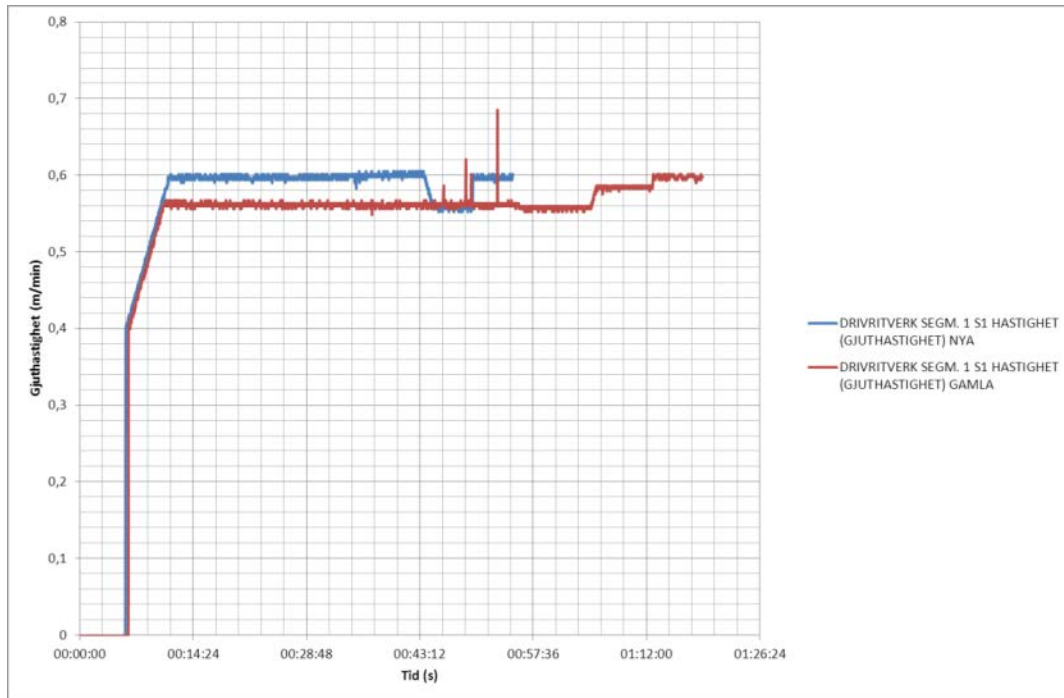


Figure 68. Casting speed.

Table 6. Tundish temperatures.

Heat	Temperature in tundish
537731	1448
537399	1446

## 6.4. Conclusions and future work for SMT

- The visual inspection of the cast blooms still shows some corner cracks for the duplex stainless steel. The ratio of corner cracks for the first 4 blooms, in total 4 blooms x 5 heats = 20 blooms, gives a value of 2 bloom with cracks/20 blooms = 0.1 or 10%. This figure should be compared with the average figure of 14.3%, a marginal improvement.
- It is very important to have a close co-operation with the SMT subcontractor performing the machining of the copper moulds otherwise misunderstanding can easily develop.
- The new design of the thermocouple attachment worked out very well. The cost for the preparation was low.
- The temperature varies between the different corners and with the casting speed.
- In future the proposed parabolic design should be tested at the SMT bloom caster.

## 7. EXPERIMENTS AND EVALUATION OF OPTIMAL MOULD FOR SSAB EMEA OXELÖSUND

### 7.1. Instrumentation of the design mould

The design mould has been instrumented by 18 type K thermocouples. The instrumentation concerns the narrow side which is orientated to west in the steel plant. The thermocouples placed in the mid of the narrow side are called “centreline”. The thermocouples placed 39 mm from the corners are called “southwest” and “northwest”, respectively. The wide fixed side is orientated to the south, and the loose side to the north. Figure 69 shows the drawings for the drilling of holes for the thermocouples.

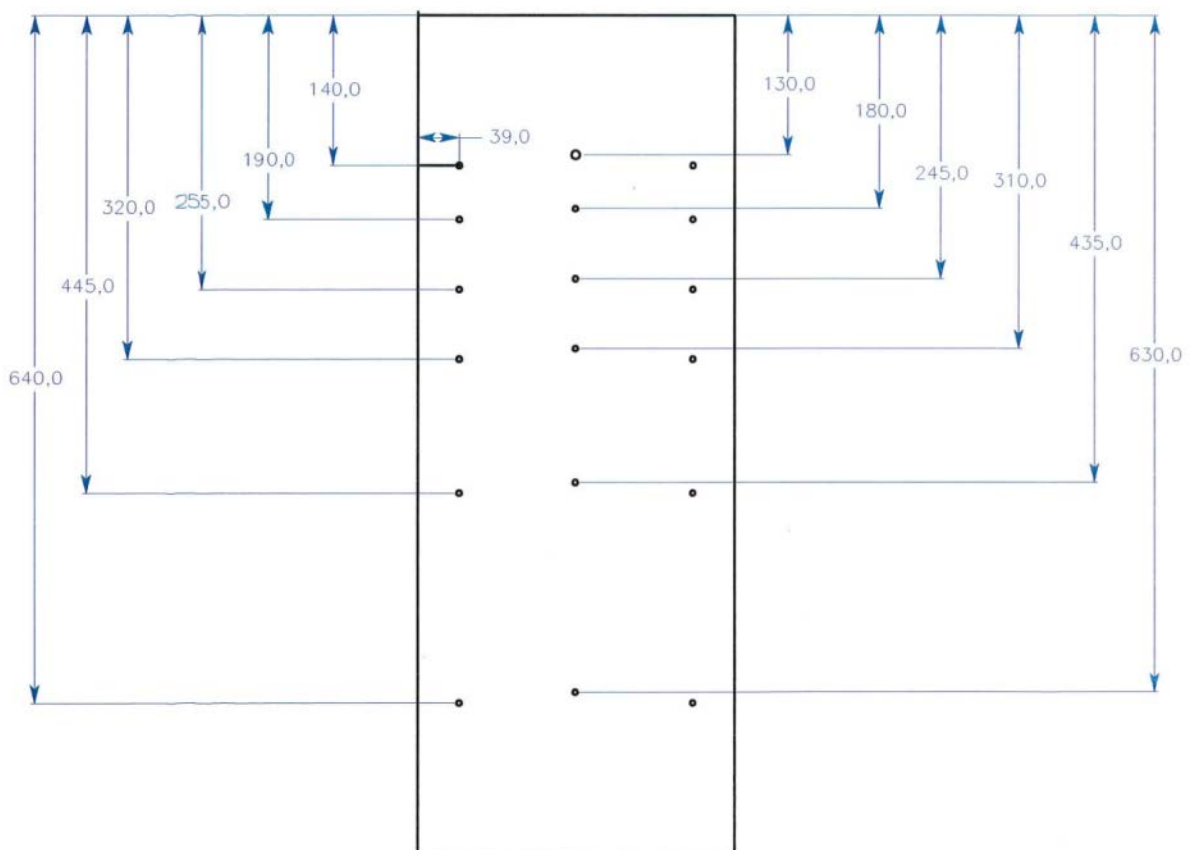


Figure 69. The positions for the drilling of the thermocouples.

## **7.2. Logger, calibration and inaccuracy**

### **7.2.1. Logger**

At the experiments at SSAB in Oxelösund the temperature of the thermocouples was measured by using an SCXI logger from National Instruments. The system consists of SCXI-1000 chassis. The SCXI-1000 is a rugged, low-noise chassis that can hold up to four SCXI modules (cards). For the analog inputs a NI SCXI-1125 was used, which consists of eight programmable isolation amplifiers. In order to measure 18 thermocouples 3 modules SCXI-1125 were used. For connecting signals, from the thermocouples, 3 general-purpose terminal blocks SCXI-1320 were used. For data acquisition and control a NI SCXI-1600, USB module was used. NI SCXI-1600 is a full-featured 16-bit USB DAQ and control module for SCXI analog input, analog output, digital I/O, and switching modules.

### **7.2.2. Calibration of type K thermocouples with SCXI logger**

The purchased thermocouples from the company Pentronic has a test certificate according to EN10204 3.1b regarding temperature. The thermocouples are supplied with 8 digits ID-numbers for traceability. This test certificate is given in Appendix 1, but the whole system needs to be calibrated channel to channel with the specific compensating cables, connector which be used for each thermocouple. The compensation cables (connectors) and logger channels are marked (labelled) for each ID number of thermocouples.

The main source of the errors for temperature measurements is due the logger system. The SCXI-1125 contains calibration hardware to null out error sources. With programmable offset calibration, software-programmable analog switches ground the inputs of each of the instrumentation amplifiers for offset error calibration. An on-board EEPROM stores the calibration constants for each channel for each input range in a user-defined area. NI-DAQ driver software transparently uses the calibration constants to correct for gain and offset errors.

The type K thermocouples with SCXI logger are calibrated by comparison with a reference thermocouple of type S which was placed in two vertical furnaces, one at 250°C and one at 413°C. The emfs generated by the thermocouples are measured by SCXI logger and Martel TC100 Beta TC-100 Precision Thermocouple Calibrator. Martel TC100 Beta TC-100 Precision Thermocouple Calibrator was also used to generate 0°C output signal to the SCXI logger. All of the type K thermocouples, with their unique compensating cables, were connected to the SCXI-1320 terminal block, which has reference temperature sensors (cool junction sensors).

The type S thermocouple is directly connected to a Martel TC100 Beta TC-100 Precision Thermocouple Calibrator. The calibration data of each channel of SCXI-1125 with terminal block SCXI-1320 for the thermocouples, which has been carried, is given in Appendix 1.

### **7.2.3. Temperature error using the SCXI-1125 with SCXI-1600 device (inaccuracy)**

Using a K - type thermocouple with a required temperature range 0°C to 450°C, the corresponding voltage range is -1.002 mV to 18.516 mV. A gain of 250 gives an overall voltage range  $\pm 20$  mV and that gives the maximum temperature resolution for this temperature range (voltage range is -1.002 mV to 18.516 mV). RTI means that it refers to

input – i.e. calculate a specification relative to the input. The total inaccuracy is calculated and shown in Table 7.

**Table 7.** Calculation of the total inaccuracy.

Quantity	Inaccuracy	Inaccuracy in voltage	Maximum Inaccuracy in T at 450°C	According to the ISO Guide to the Expression of Uncertainty in Measurement” T at 450°C
Offset error (gain=250)	± 3mV/gain RTI	±12×10 <sup>-6</sup> V		
Gain error (range 20 mV)	± 0.03%	±6.0×10 <sup>-6</sup> V		
Noise	±0.1mV/gain RTI	±0.4×10 <sup>-6</sup> V		
Total inaccuracy in the voltage signal	±18.4×10 <sup>-6</sup> V	±18.4×10 <sup>-6</sup> V		
Conversion factor from voltage to temperature (of Type K thermocouple) ΔU/ΔT=41.1×10 <sup>-6</sup> V/°C	±18.4×10 <sup>-6</sup> V	±18.4×10 <sup>-6</sup> V	±0.45 °C	
A 16-bit NI DAQ device system error	0.153×10 <sup>-6</sup> V		±0.004 °C	
Cool junction sensor			±1.6 °C	
Inaccuracy in the measurement device SCXI-1125 and the NI DAQ together			± 2.05 °C	
Thermocouple, Type K			± 1.6 °C	
<b>Total inaccuracy in T</b>			<b>± 3.65 °C</b>	<b>± 3.09 °C</b>

## 7.3. Results from the temperature measurements

### 7.3.1. Numbering of thermocouples

The numbering of the thermocouples is shown in Table 8, 9 and 10.

**Table 8.** Numbering of thermocouples at the southwest positions.

Southwest positions	Distance from the top of the mould/mm	Depth from the copper surface/mm	Channel (logger)
<b>1</b>	140	15,6	K-card-1-ch-8
<b>2</b>	190	16,34	K-card-1-ch-6
<b>3</b>	255	17,04	K-card-1-ch-1
<b>4</b>	320	17,4	K-card-1-ch-10
<b>5</b>	445	17,35	K-card-1-ch-4 ny
<b>6</b>	640	15,95	K-card-1-ch-0

**Table 9.** Numbering of thermocouples at the centreline positions.

Centerline	Distance from the top of the mould/mm	Depth from the copper surface/mm	Channel (logger)
<b>7</b>	130	17,27	K-card-1-ch-9
<b>8</b>	180	18,84	K-card-1-ch-7
<b>9</b>	245	17,92	K-card-1-ch-2
<b>10</b>	310	17,94	K-card-1-ch-14
<b>11</b>	445	17,63	K-card-1-ch-5
<b>12</b>	630	16,39	K-card-1-ch-3

**Table 10.** Numbering of thermocouples at the northwest positions.

Northwest positions	Distance from the top of the mould/mm	Depth from the copper surface/mm	Channel (logger)
<b>13</b>	140	15,37	K-card-1-ch-17
<b>14</b>	190	16,12	K-card-1-ch-15
<b>15</b>	255	16,82	K-card-1-ch-13
<b>16</b>	320	17,2	K-card-1-ch-12
<b>17</b>	445	17,14	K-card-1-ch-11
<b>18</b>	640	15,84	K-card-1-ch-16

### 7.3.2. Sequence Number 25733 (single)

- Heat 75787, Peritectic steel grade, Tsort 846, 0.156% C.
- Tilting 7.6 mm.
- Steel level 80 mm from the top of the mould.
- 2013-07-02 Time 18:38 (Start of casting) to 19:48 (End of casting).

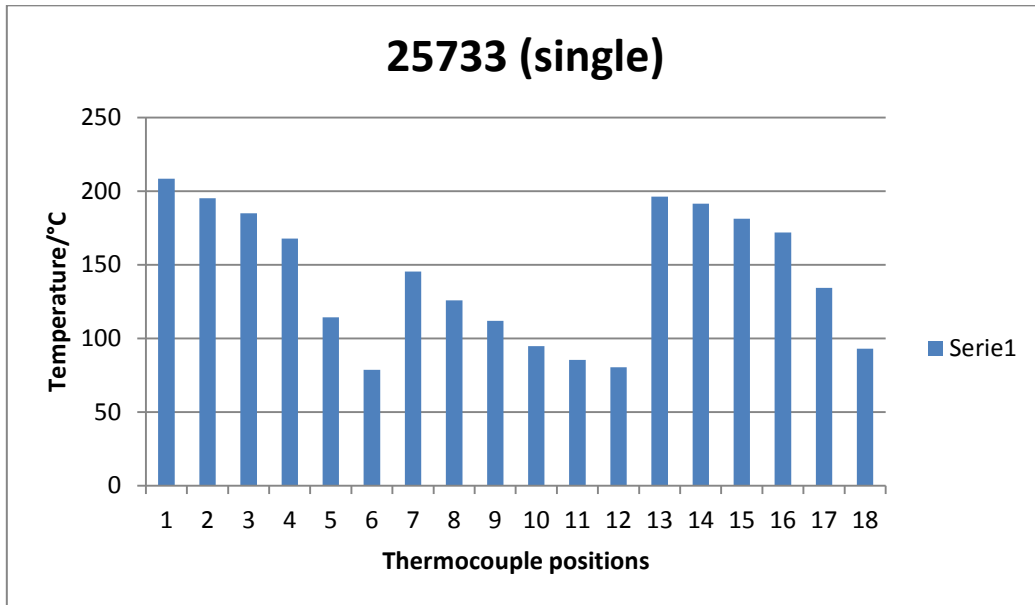


Figure 70. Average values of the measurement of the temperature at thermocouple positions.

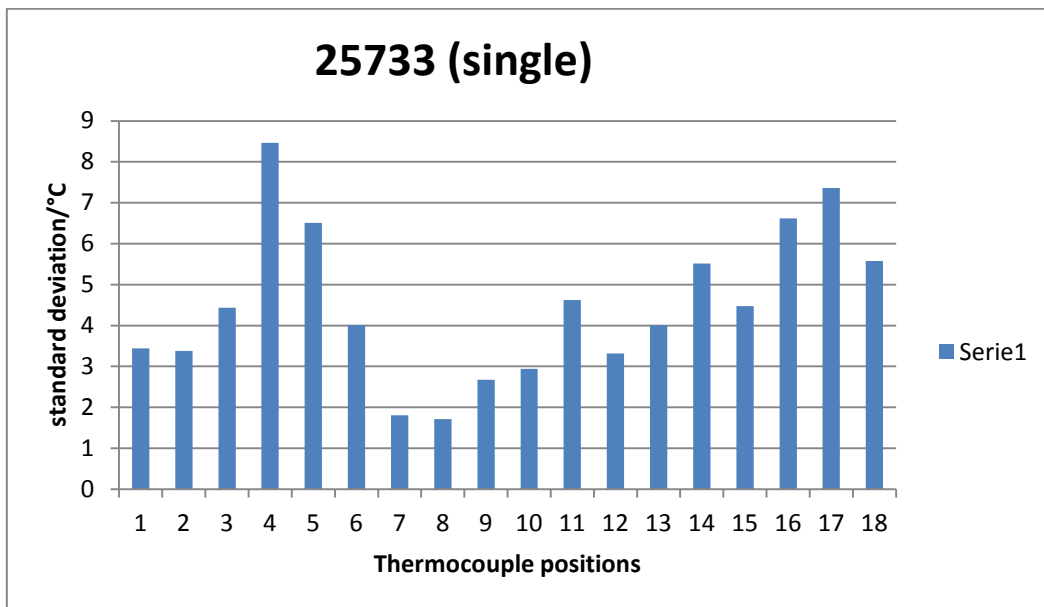
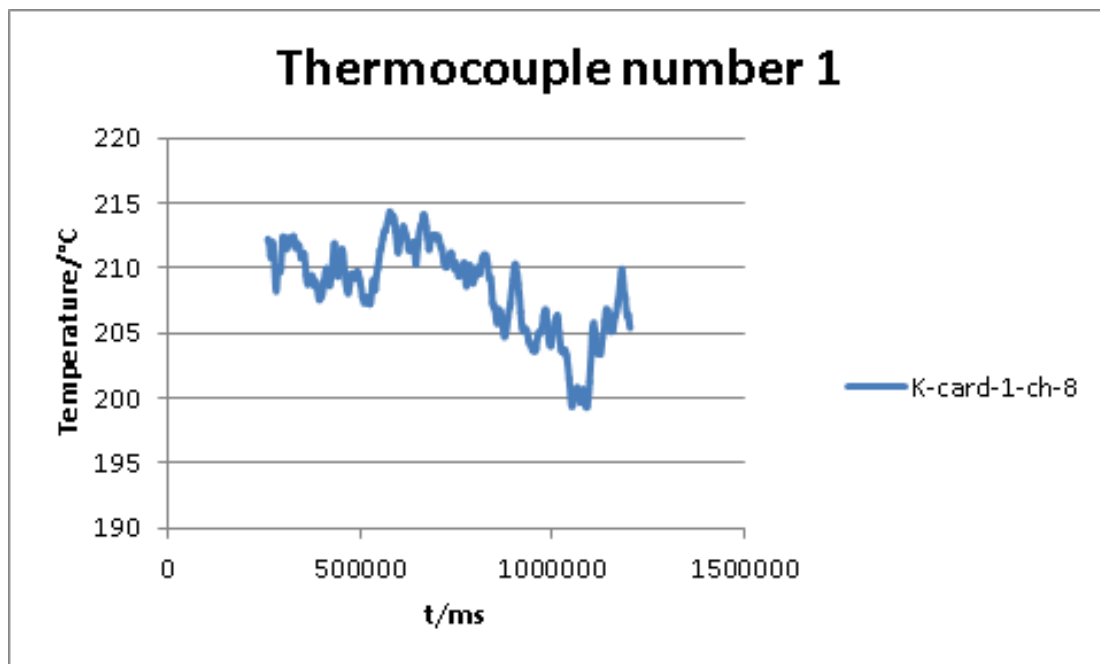
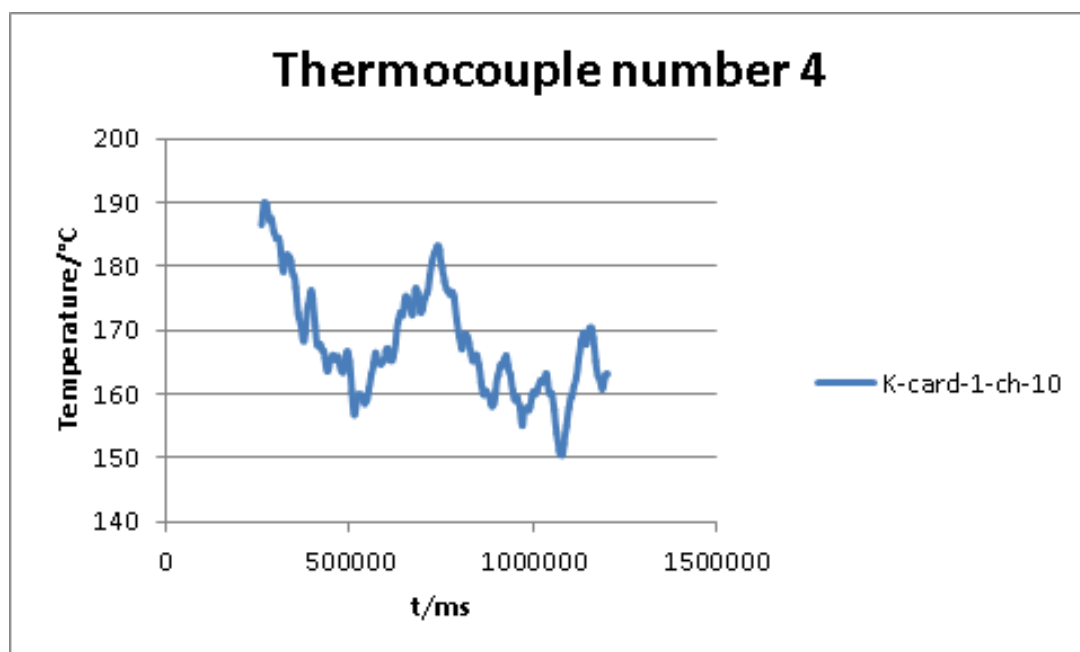


Figure 71. Standard deviation of the measurement of the temperature at thermocouple positions.



**Figure 72.** Measurement of thermocouple number 1.



**Figure 73.** Measurement of thermocouple number 4.

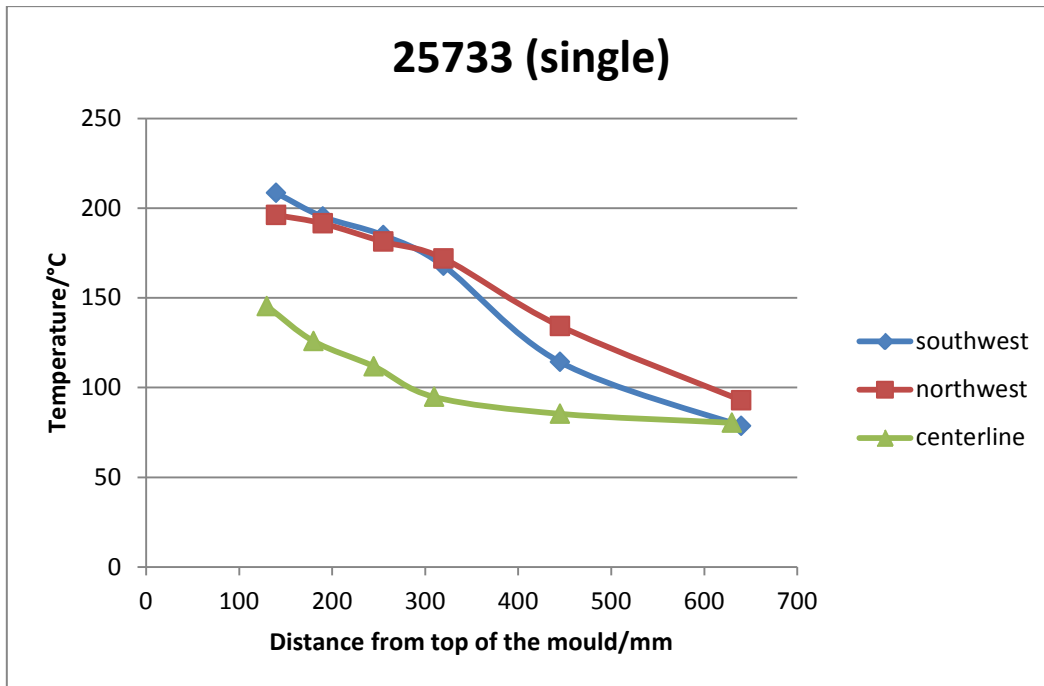


**Figure 74.** Average temperature in the mould as function of distance from the top of the mould.

- Average value for all thermocouples is 142.24 °C.
- The average of the standard deviation of all thermocouples is 4.49 °C.

### 7.3.3. Sequence Number 25735

- Heat 75789, Peritectic steel grade, Tsort 541, 0.191% C.
- Heat 75790, Peritectic steel grade, Tsort 541, 0.195% C.
- Tilting 7.6 mm
- Steel level 80 mm from the top of the mould.
- 2013-07-02 Time 22:13 (Start of casting) to 00:21 (End of casting).
- (Active length of mould 705 mm)
- (Coefficient for the estimation of shell thickness 25.3)

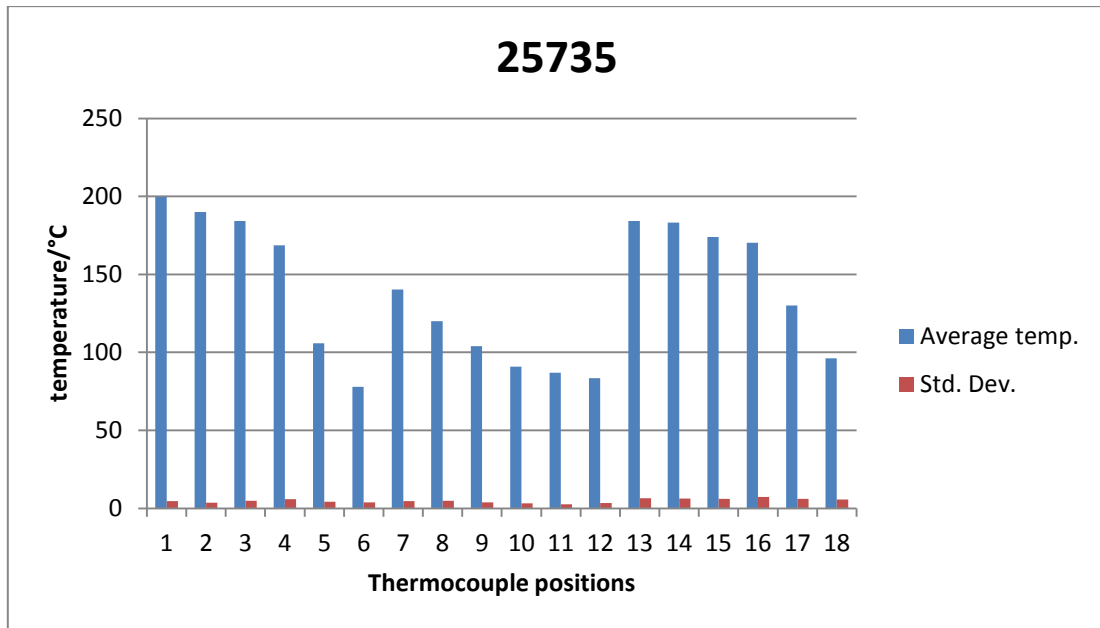


**Figure 75.** Average of the measured values of temperature by the thermocouples for each position and the corresponding standard deviation.

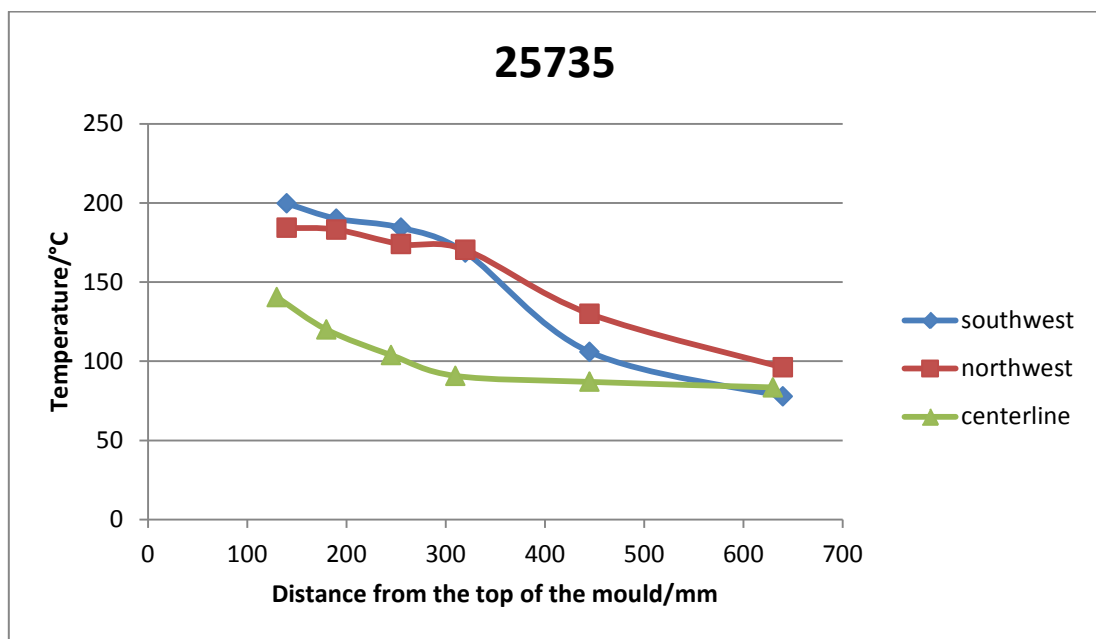


**Figure 76.** Average temperature in the mould as function of distance from top of the mould.

- Average value for all thermocouples is 138.32°C.
- The average of the standard deviation of all thermocouples is 4.88°C.

Figure 77 shows an etched near narrow side transverse slab sample 25735-6 and Figure 78 shows a zoomed photo.



**Figure 77.** Full size picture of the etched east near narrow side transverse slab sample (arrow points to lower-fixed south side).

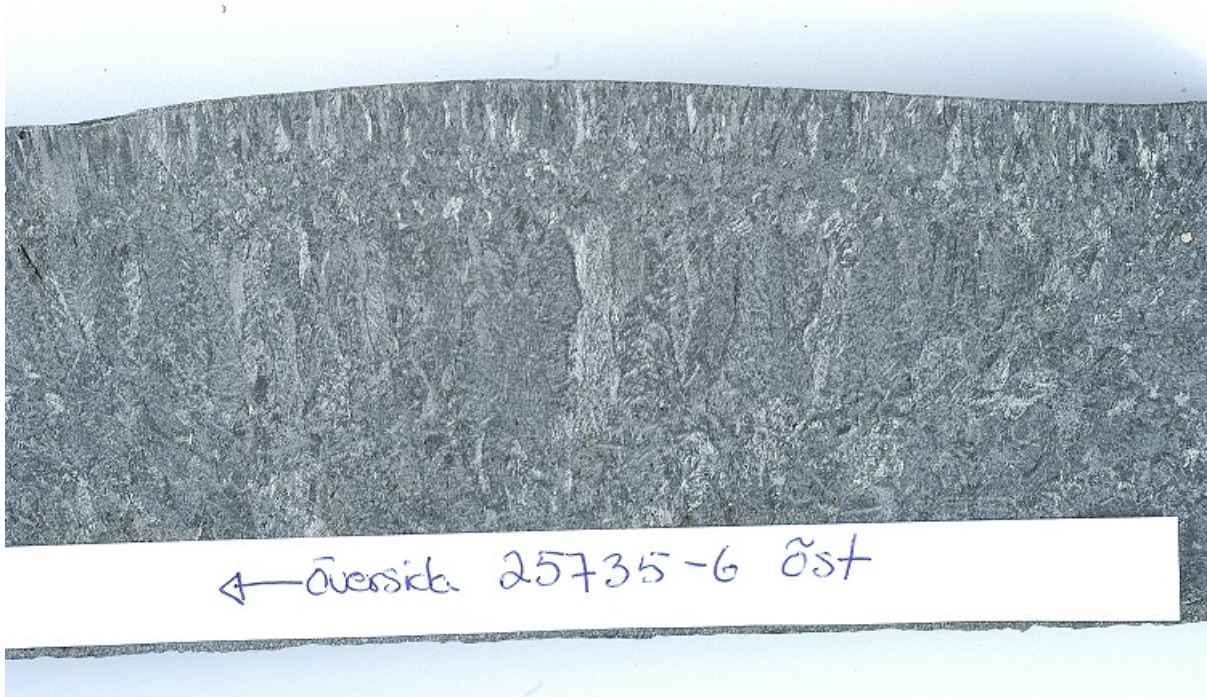


**Figure 78.** Zoomed picture of the etched east near narrow side transverse slab sample (arrow points to lower/fixed/south side).

#### 7.3.4. Sequence number 25737

- Heat 75791, Peritectic steel grade, Tsort 541, 0.206% C.
- Heat 75794, Peritectic steel grade, Tsort 541, 0.196% C.
- Tilting 7.6 mm
- Steel level 80 mm from the top of the mould
- 2013-07-03 Time 03:45 (Start of casting) to 06:00 (End of casting)

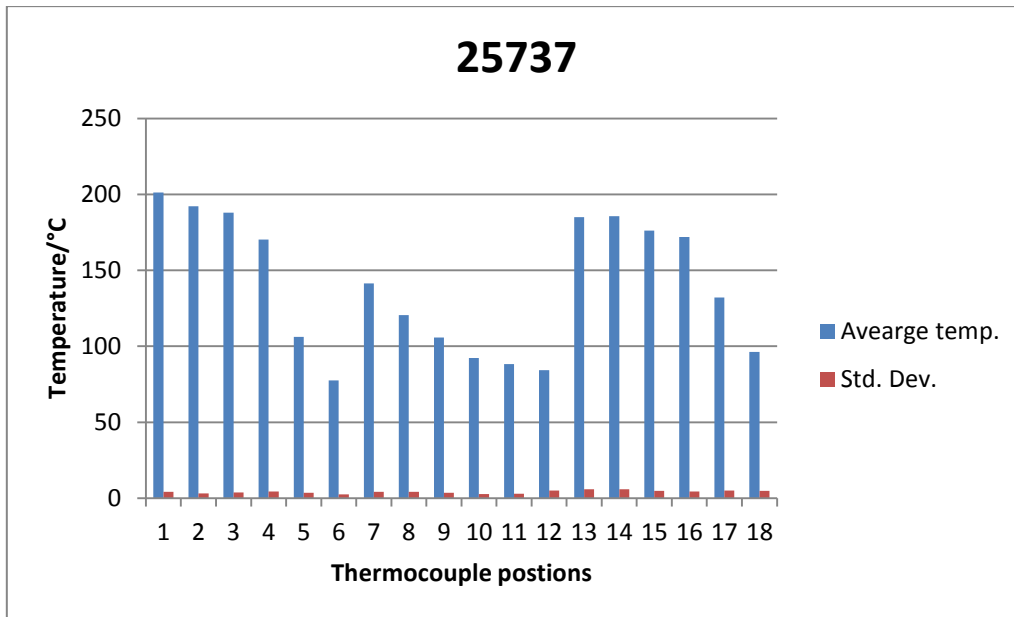


**Figure 79.** Average temperature and standard deviation for thermocouple positions.

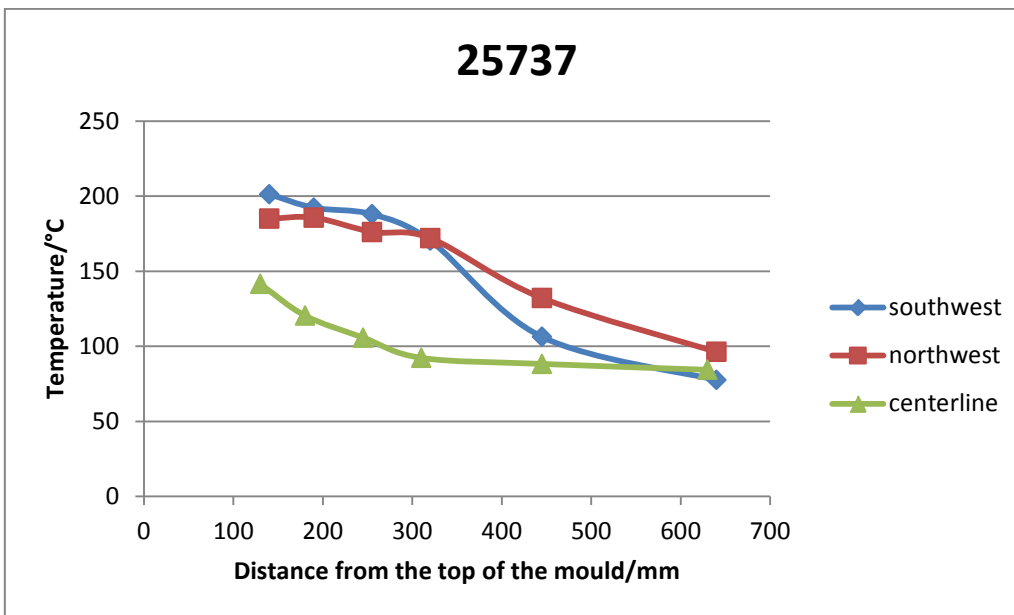


**Figure 80.** Average temperature in the mould as function of distance from top of the mould.

- Average value for all thermocouples is 139.76°C.
- The average of the standard deviation of all thermocouples is 4.19 °C.

### 7.3.5. Sequence number 25740

- Heat 75800, Peritectic steel grade, Tsort 846, 0.160% C.
- Tilting 7.6 mm (1h and 12 min).
- Steel level 90 mm from the top of the mould.
- 2013-07-03 Time 17:10 (Start of casting) to 18:18 (End of casting).

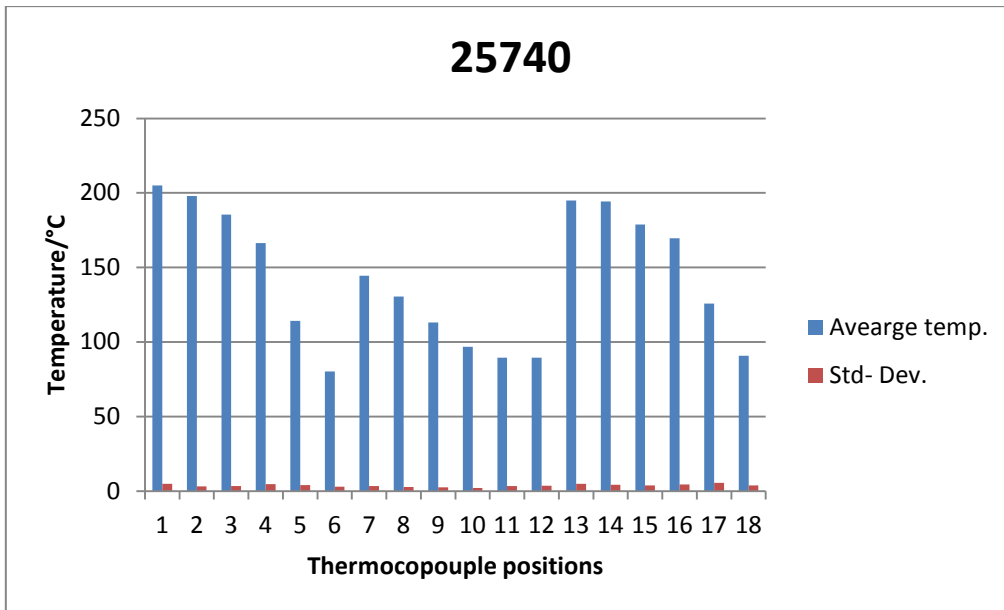


**Figure 81.** Average temperature and standard deviation at different thermocouple positions.

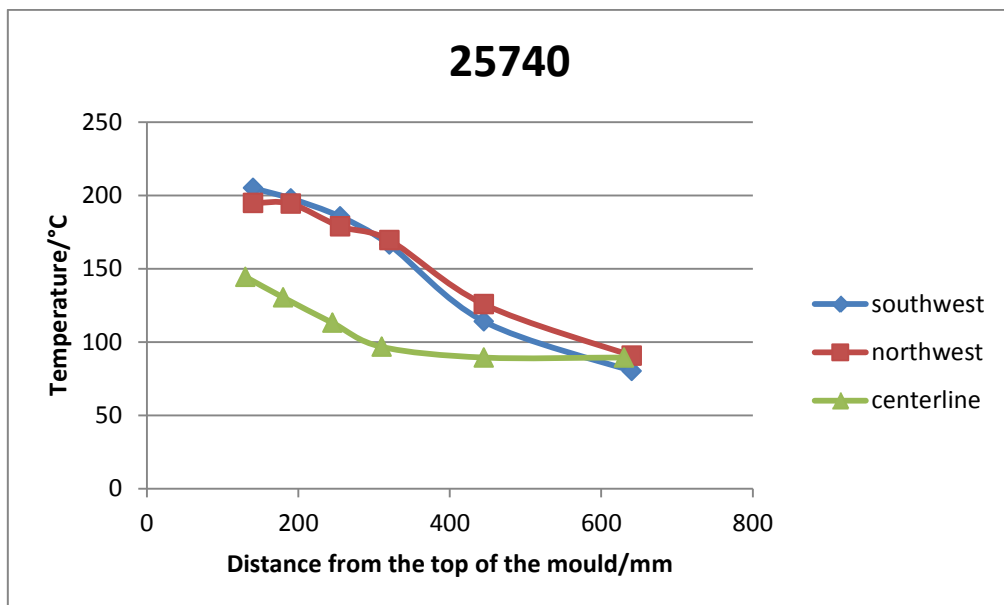


**Figure 82.** Average temperature versus distance from the top of the mould.

- Average value for all thermocouples is 142.61 °C.
- The average of the standard deviation of all thermocouples is 3.69°C

### 7.3.6. Tilting trials sequence number 25740

- Heat 757801, Peritectic steel grade, Tsort 846, 0.155% C.
- Tilting 8.0 mm (20 min) => 7.6 mm (20 min) => 7.3 mm (20 min).
- Steel level 90 mm from the top of the mould.
- 2013-07-03 Time 18:18:00. (Start of casting, sequence 2) to 19:37.

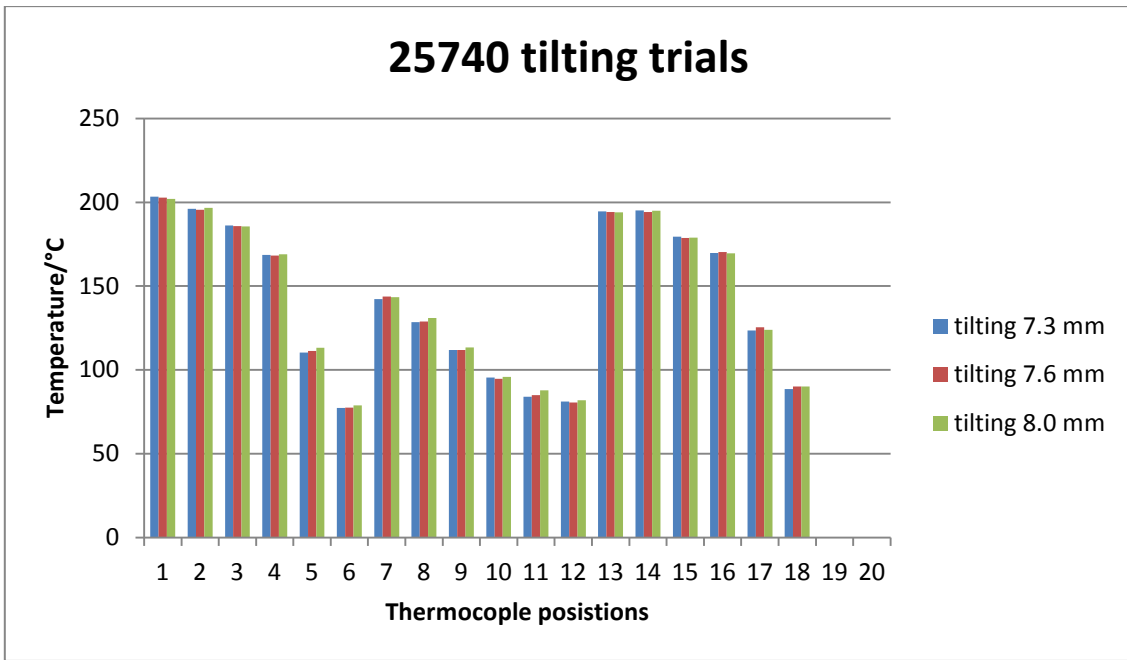


**Figure 83.** Average temperature versus distance from the top of the mould.

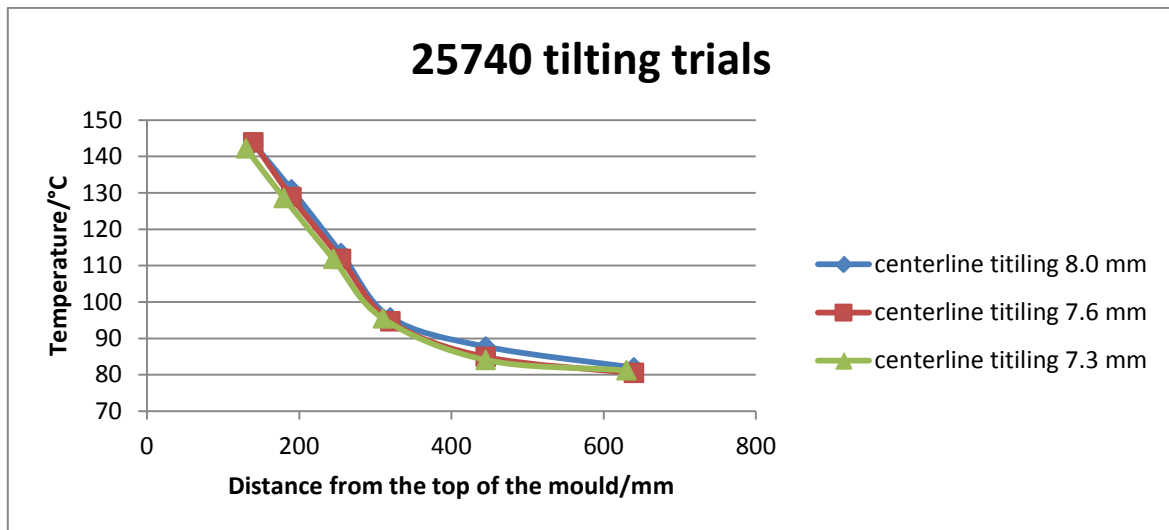


**Figure 84.** Average temperature of centreline for tilting trials versus distance from top of the mould.

**Tilting 8.0 mm**

- Average value for all thermocouples is 141.66°C.
- The average of the standard deviation of all thermocouples is 2.57°C
- Gives the highest temperatures and best contact for almost all thermocouple positions and also show the lowest standard deviation.

**Tilting 7.6 mm**

- Average value for all thermocouples is 141.02°C.
- The average of the standard deviation of all thermocouples is 2.75 °C

**Tilting 7.3 mm**

Average value for all thermocouples is 140.90°C.  
 The average of the standard deviation of all thermocouples is 2.80°C.

### 7.3.7. Sequence number 25742

- Heat 75804, Peritectic steel grade, Tsort 539, 0.30% C.
- Heat 75805, Peritectic steel grade, Tsort 539, 0.301% C.
- Tilting 7.6 mm.
- Steel level 90 mm from the top of the mould.
- 2013-07-03 Time 22:33 (Start of casting) to 00:44 (End of casting).

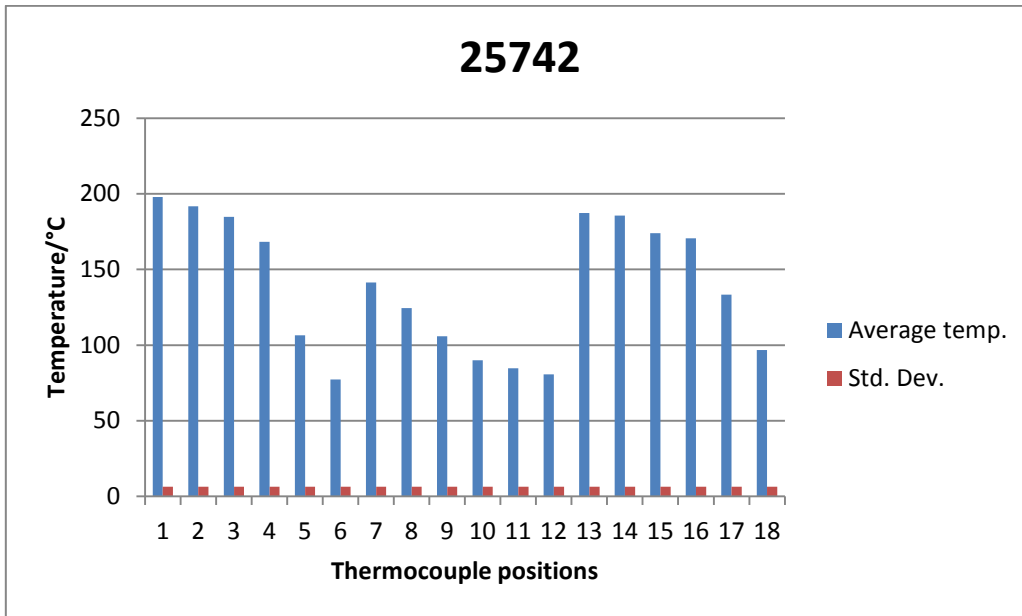


Figure 85. Average temperature at different thermocouple positions.

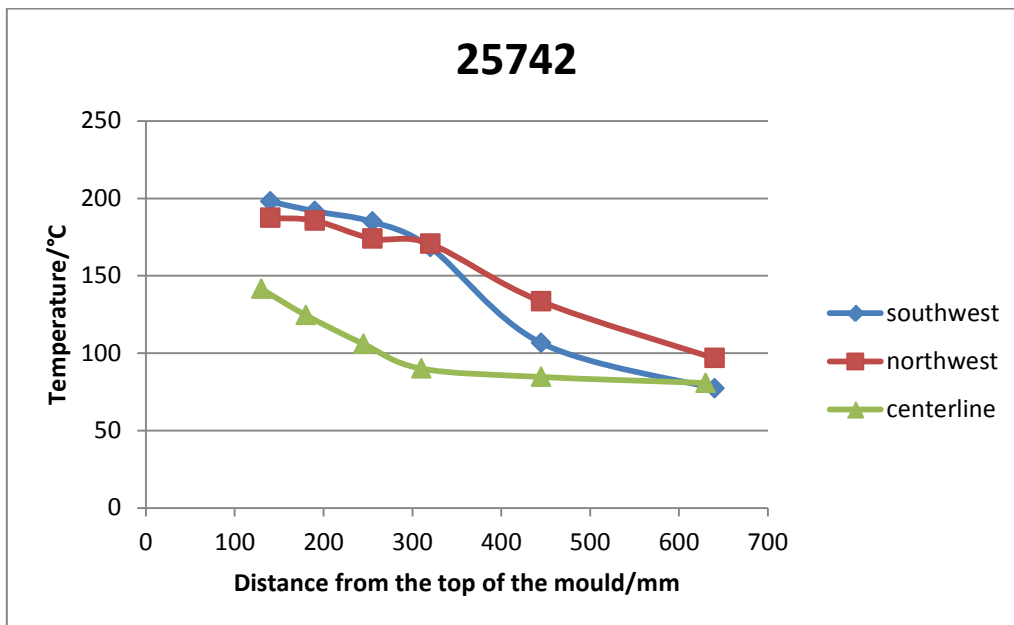


Figure 86. Average temperature versus distance from the top of the mould.

- Average value for all thermocouples is 138.99 °C.
- The average of the standard deviation of all thermocouples is 6.41 °C.

### 7.3.8. Sequence number 25745 (single)

- Heat 75810, Peritectic steel grade, T<sub>sort</sub> 865, 0.15% C.
- Tilting 7.6 mm.
- Steel level 90 mm from the top of the mould.
- 2013-07-03 Time 06:32 (Start of casting) to 07:46 (End of casting).

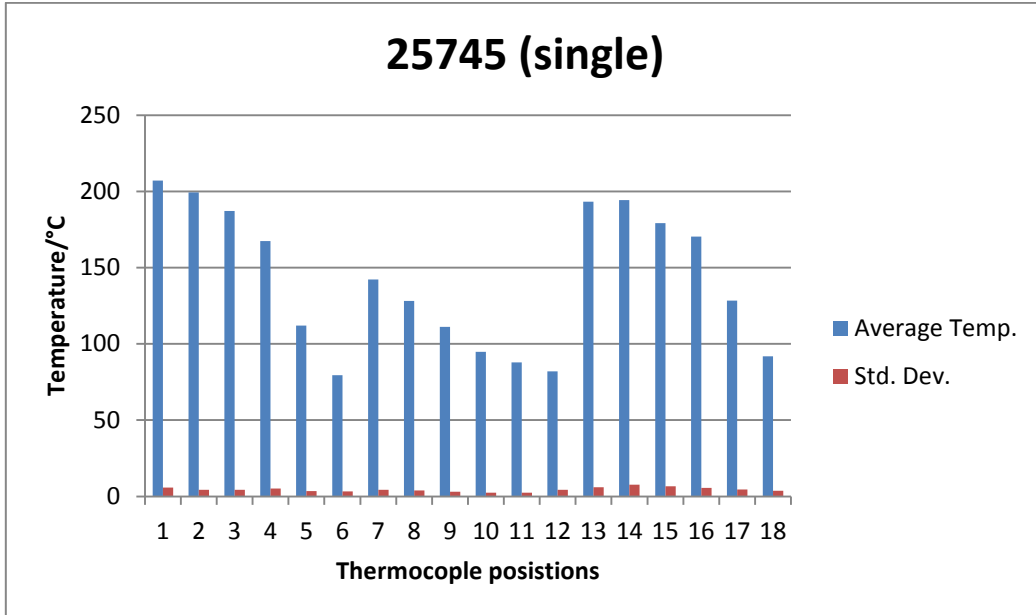


Figure 87. Average temperature at different thermocouple positions.

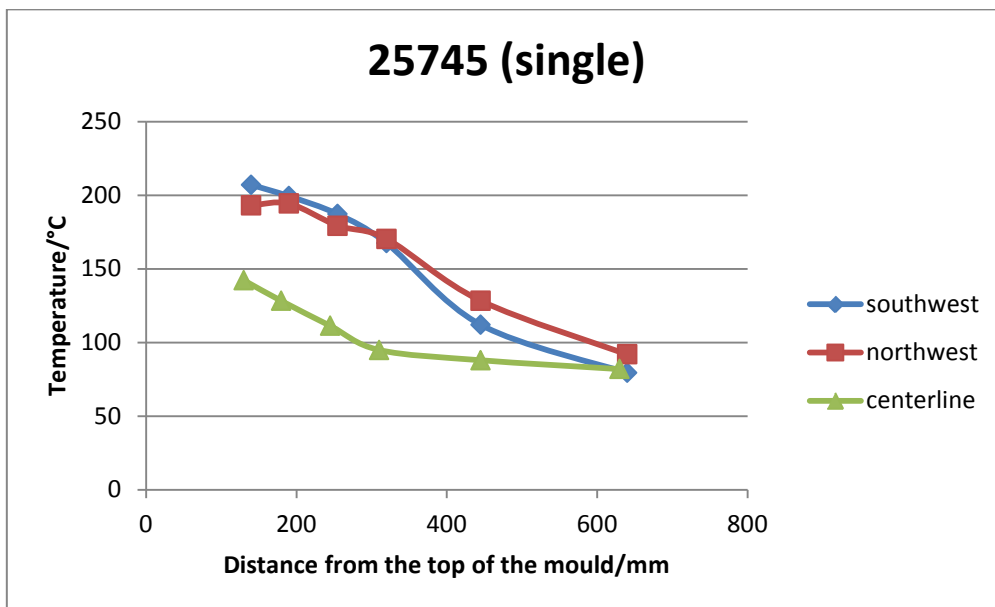


Figure 88. Average temperature versus distance from the top of the mould.

- Average value for all thermocouples is 142.01°C.
- The average of the standard deviation of all thermocouples is 4.51°C

### 7.3.9. Sequence number 25747

- Heat 75813, Peritectic steel grade, Tsort 548, 0.265% C.
- Heat 75814, Peritectic steel grade, Tsort 548, 0.26% C.
- Tilting 7.6 mm.
- Steel level 90 mm from the top of the mould.
- 2013-07-04 Time 11:16 (start of casting) to 13:26 (end of casting).

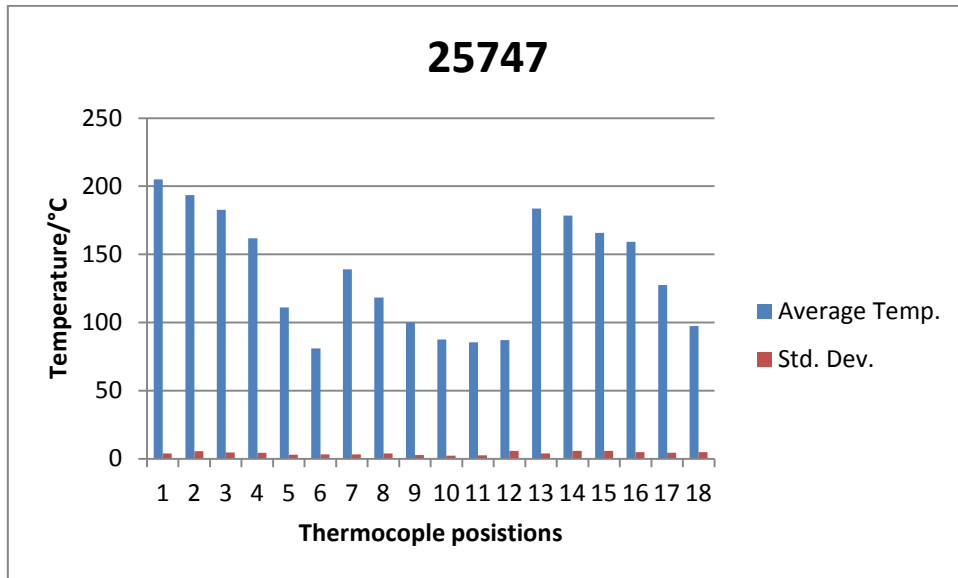


Figure 89. Average temperature at different thermocouple positions.

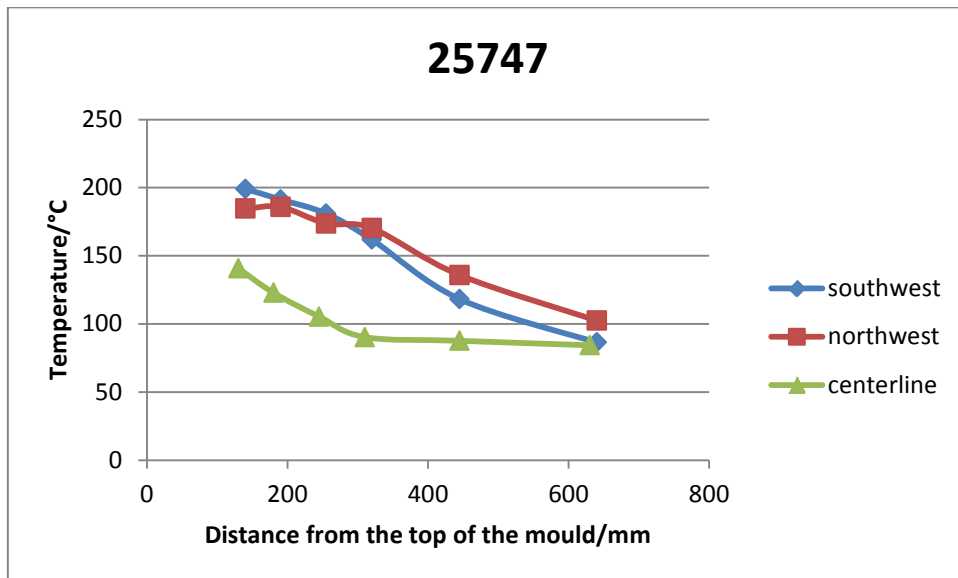


Figure 90. Average temperature versus distance from the top of the mould.

- Average value for all thermocouples is 140.10 °C.
- The average of the standard deviation of all thermocouples is 4.66 °C

### 7.3.10. Sequence number 25749

- Heat 75817, Peritectic steel grade, Tsort 734, 0.120 % C.
- Heat 75818, Peritectic steel grade, Tsort 734, 0.120 % C.
- Tilting 8.2 mm.
- Steel level 90 mm from the top of the mould.
- 2013-07-04 Time 20:52 (Start of casting) to 22:09 (End of casting).

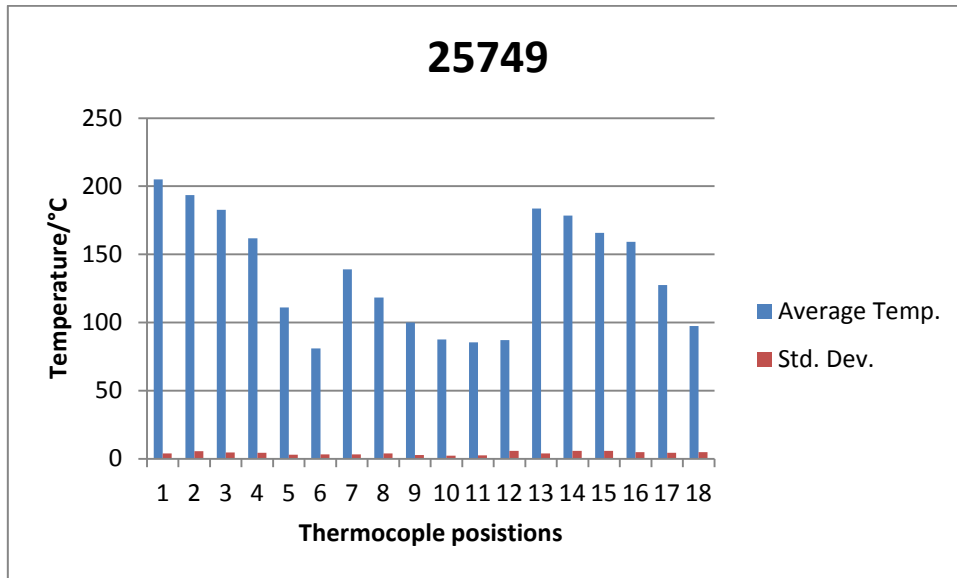


Figure 91. Average temperature at different thermocouple positions.

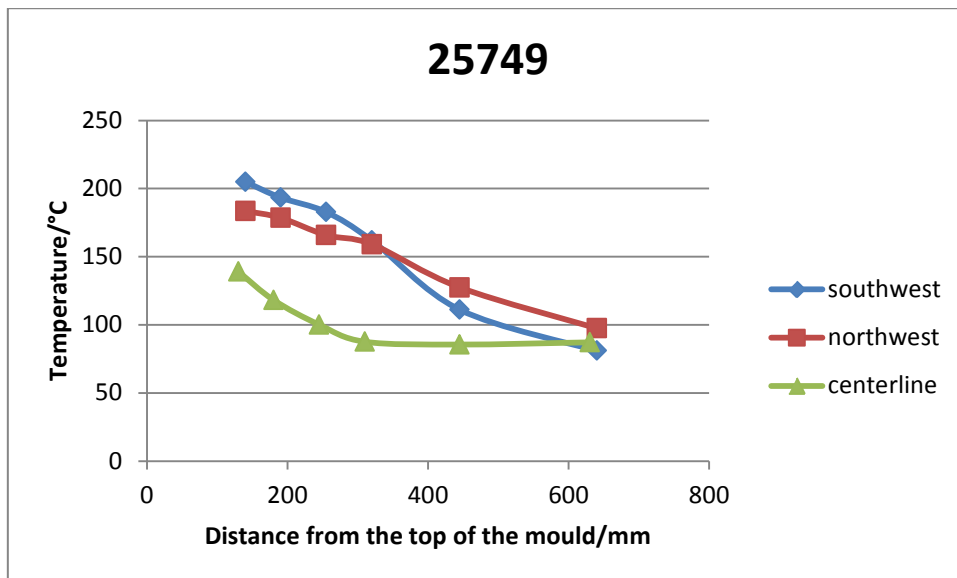
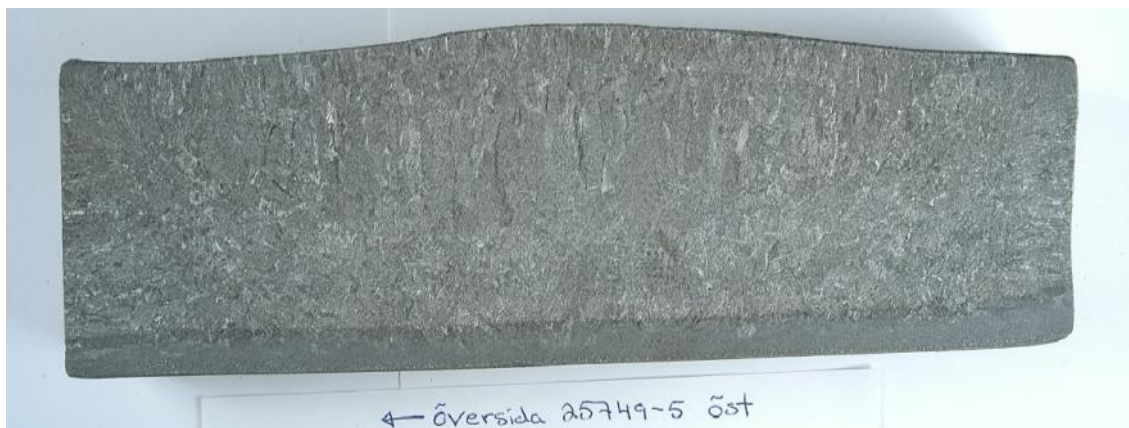


Figure 92. Average temperature versus distance from the top of the mould.

- Average value for all thermocouples is 136.94 °C.
- The average of the standard deviation of all thermocouples is 4.10 °C.

A photo of an etched near narrow side transverse slab sample and zoomed photo is shown in Figure 93 and Figure 94 respectively.



**Figure 93.** Photo of etched east narrow side transverse slab sample (arrow points at upper-loose/north side).

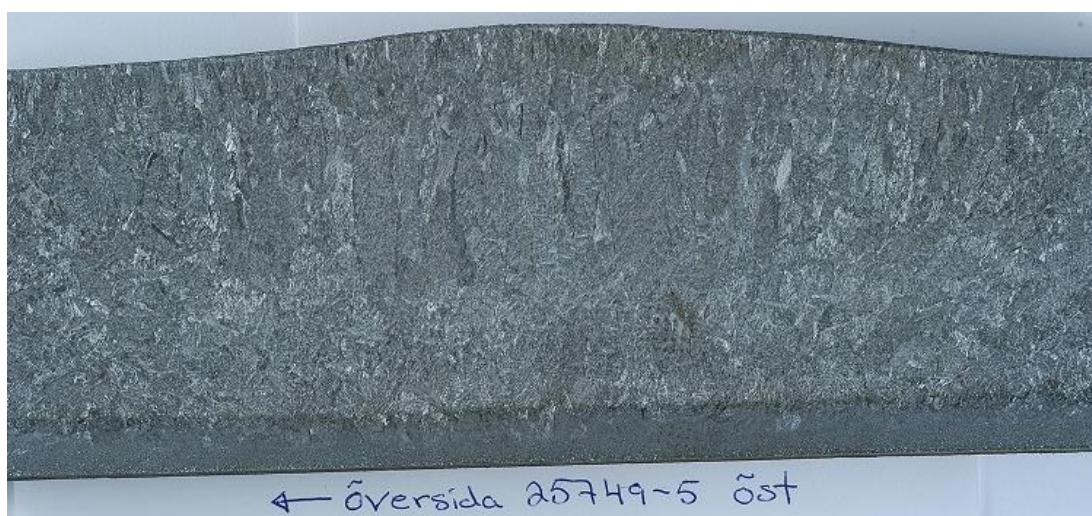


**Figure 94.** A zoomed photo of etching east narrow side transverse slab sample (arrow points at upper-loose/north side).

### **7.3.11. Sequence number 24751 and 25753**

Additional experiments have been carried out for sequence number 24751 and 25753. However, the logger was disconnected. No measurements of temperature in the mould are available for sequence number 24751 and 25753.

## **7.4. Summary of measurements of temperature in the mould**

For sequence number 25722 to 25739 the steel level is 80 mm from the top of the mould, and for sequences number 25740 to 25749 the steel level is 90 mm from the top of the mould. The tilting 7.6 mm has been used in nearly all sequences. The tilting experiments in the sequence number 25740 give, however, some effects on the average temperature of the thermocouples (highest temperatures with highest tilt 8.0 mm). In the sequence number 25749 a tilting of 8.2 mm has been used. This is exhibiting the lowest average temperature of thermocouples (due to being the most peritectic steel grade of all with the largest shrinking) but does not influence the average of the standard deviation. The average temperature for all thermocouples for all experiments is shown in Figure 95. The corresponding average of the standard deviation for all thermocouples for all experiments is shown in Figure 96.

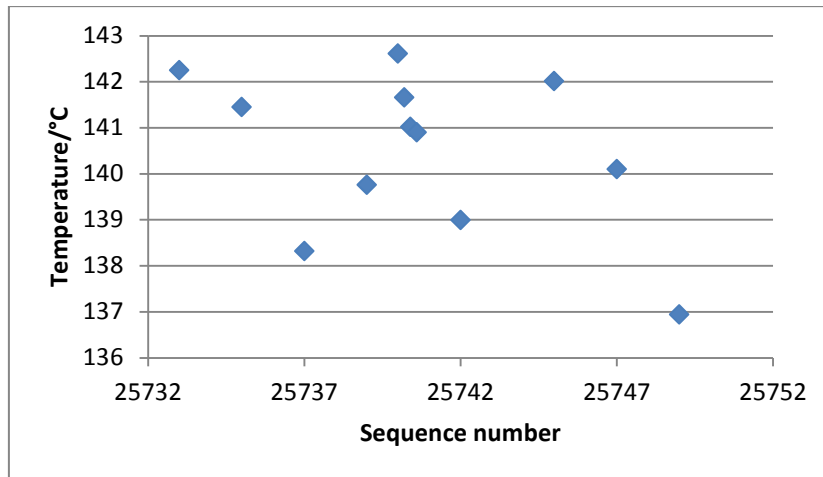


**Figure 95.** Average temperature for thermocouples versus sequence number.

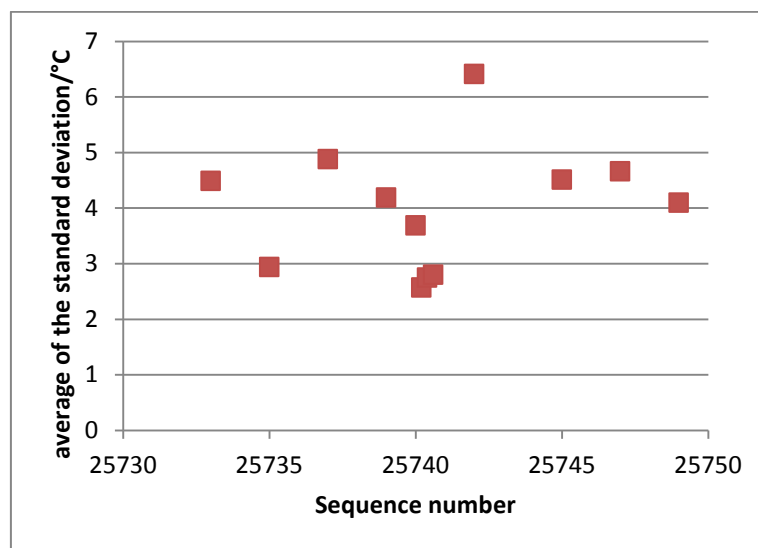


**Figure 96.** Average of the standard deviation versus sequence number.

Figure 72-92 show that the temperature of the south west corner is lower than the northwest corner from about 300 mm from the meniscus to the end of the mould. That is an influence from the bending operation taking place. At upper part of the mould south west and south east show minor deviation.

Figure 97 shows a summary of the temperatures along the centreline in the mould. The tilting experiment in the second part of the sequence 25740 shows the highest temperature in the upper part of the mould at a tilt of 8,0 mm.

The worst case of thermal contact of the upper parts of the mould was sequence 25749. This is due to grade 734 being the most peritectic steel and most prone to shrinking of all grades investigated.

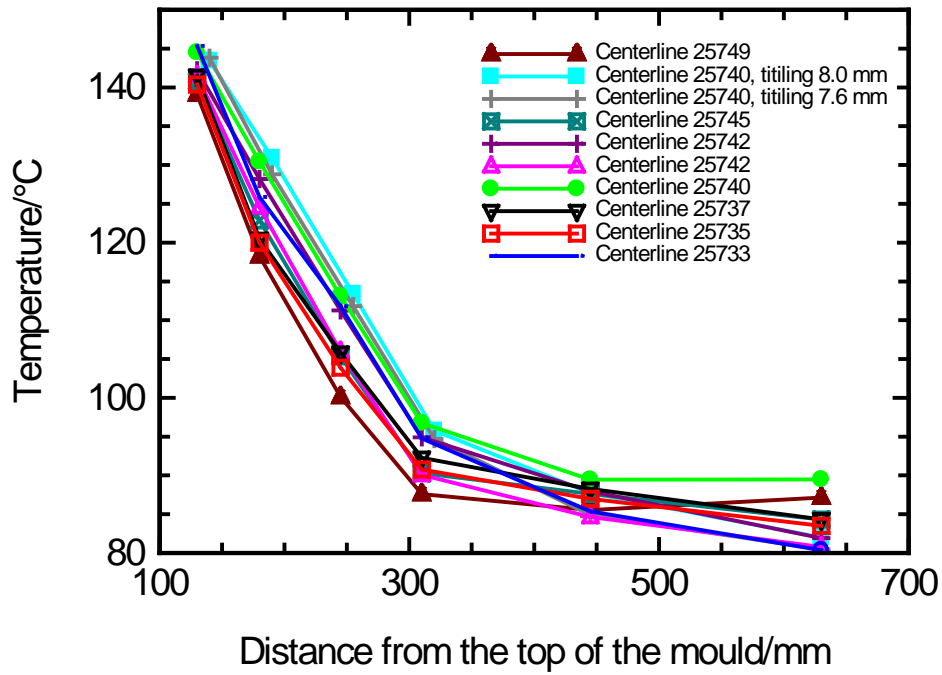


Figure 97. Summary of the centreline temperature for all sequences.

Additional photos of micro structure shown with ruler (with millimetre scale) have been carried out for sequence 25735-6. These are shown in Figure 98 -100. All these samples were centred around the half thickness of the slab i.e.  $290 \text{ mm}/2 = 145 \text{ mm}$  (at the convex nose of the "gull-wing").



Figure 98. Microstructure photo of sample number 1 (sequence 25735-6).



**Figure 99.** *Microstructure photo of sample number 2 (sequence 25735-6).*



**Figure 100.** *Microstructure photo of sample number 3. (sequence 25735-6).*

The pictures with the ruler show:

- An extremely fine structure on first part down to 1 mm depth (good thermal contact).

- From about 1 to about 11 mm depth a coarse structure (poor thermal contact, at the mid section of the mould (convex nose or “gull-wing”).
- From about 11 mm to 24 mm a fine structure (thermal contact again).
- From about 24 mm depth, a coarse structure (mould exit).

A rough estimation can, however, be used using the thumb rule [ref. 13]:

$$\text{Shell growth} = 25.3 \cdot \sqrt{\frac{\text{Distance from meniscus}}{1000 \cdot V_C}}$$

where the distance from meniscus is expressed in the unit mm and the casting speed  $V_C$  is expressed in unit m/min (The casting speed was 0.78 m/min). The shell growth from this rule of thumb is shown in Figure 101:

- “Rule of thumb” in this case correctly calculates shell thickness to 24 mm at the end of mould, 785 mm high (steel level 80 mm below upper part of the mould).
- Same equation estimates that start of fine grains at 11 mm happens at 230 mm below upper part of the mould (at third thermocouple) which is not correct. It rather happens at 310 mm (fourth thermocouple).

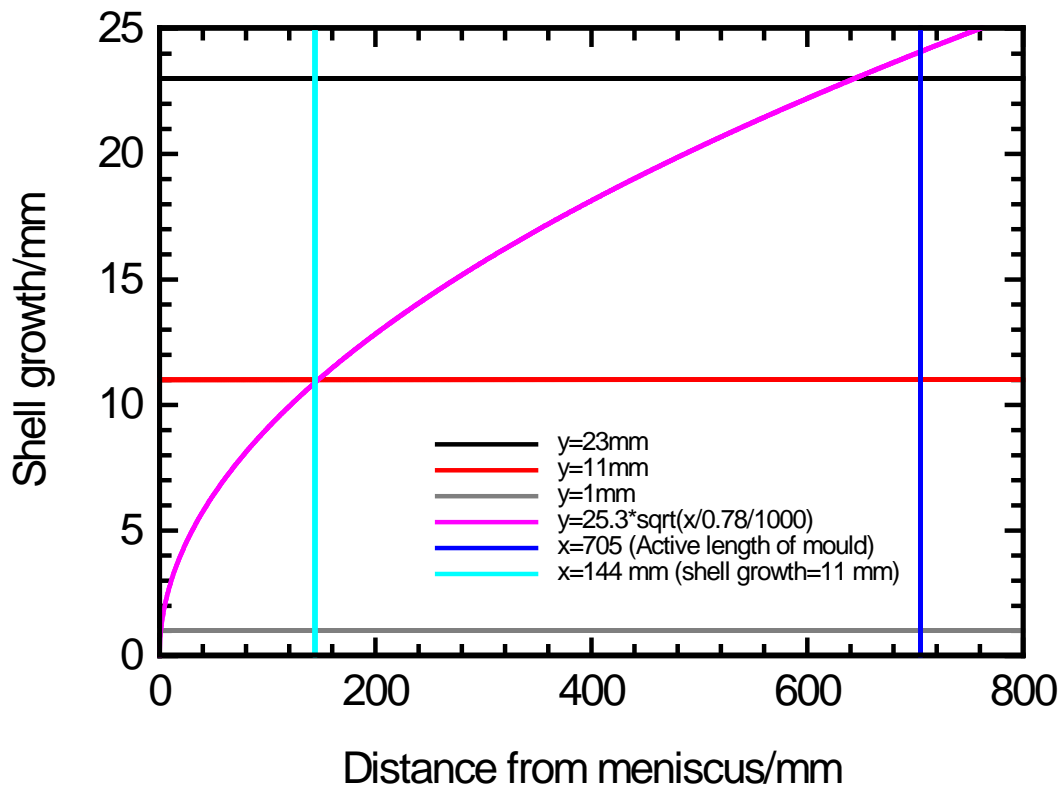


**Figure 101.** Shell growth in the mould as function of distance from meniscus.

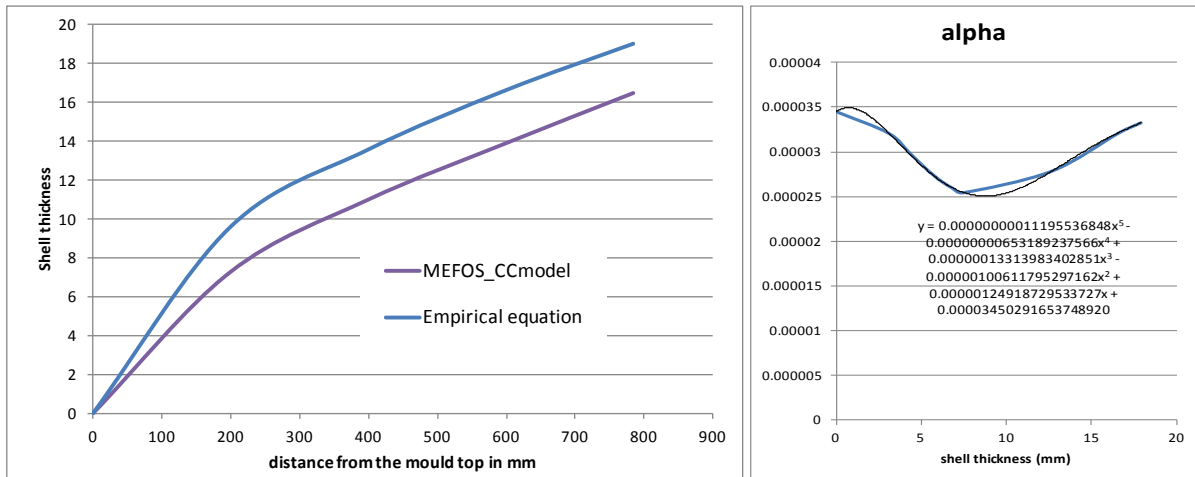


**Figure 102.** Shell growth in the mould as function of distance from meniscus for MEFOS CC model and thermal expansion coefficient as a function on shell thickness.

The change in contact conditions at approximately 11 mm show 2 different shrinkage slopes during shell formation. This agrees well with the predictions of the empirical equation and MEFOS CC model (although it predicts a lower thickness). The most likely reason for the loss of contact in the upper part of the mould is the comparatively low taper of the convex nose (gull-wing) of the design. This should be removed.

## 7.5. Plate quality results

Results from Oxelösund experiment with 290 mm thick using a "gull-wing" – mould, week 27 in 2013 was summarized. The corner cracks are the dominant cause of failure, and they increased by the experiments. The plate surface quality result is shown in Table 11. The differential mould water temperature is given in Table 12. The results indicate clearly that the mould loses the cooling efficiency the narrow faces at the trial due to "gull-wing" body. The plate results in Table 11 confirm this, by showing somewhat increase in fails.

**Table 11.** Plate surface quality results.

Week	Category	Index of Plate with surface code	Expected Index (Same result/ grade as during week 1 to 26)
1 to 26	References	10,34	
27	Experiments	13,15	11,04

**Table 12.** Mould water temperatures.

Week	Category	Average WideFace (°C)	Average NarrowFace (°C)	Average (NarrowFace)/(Wide Face)
1 to 26	References	4,77	4,75	99,58 %
27	Experiments	4,65	4,40	94,63%

## 7.6. Conclusions

The average temperature of the thermocouple measurement of the centreline positions and near the corner positions is summarized for the heats in Figure 103. The error bars correspond to the standard deviation of the average.

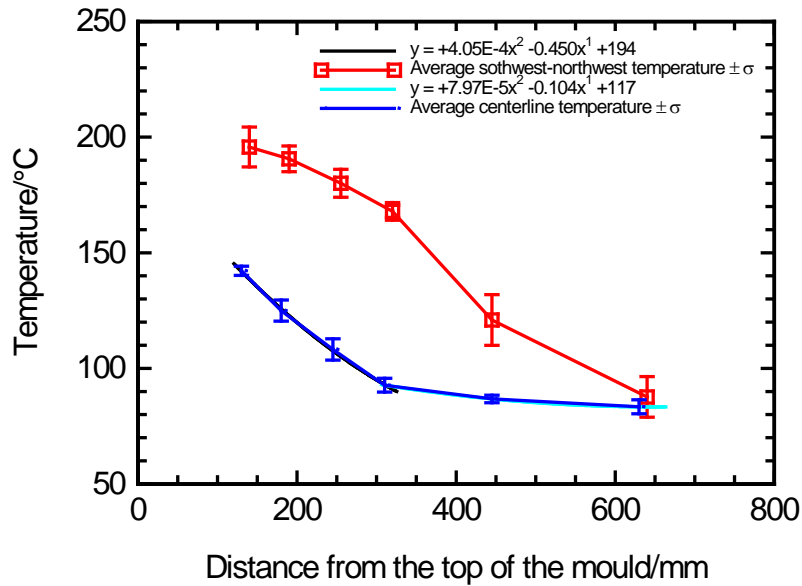


**Figure 103.** Average temperature of centreline and near corner positions of the experiments.

The first row of thermocouples, which correspond to 130 mm and 140 mm from the top the mould, has now been recalculated to the same distance as the positions of the thermocouples near the corner. Figure 104 show the difference between the average temperature of the centreline positions and positions near corner of the experiments carried out.

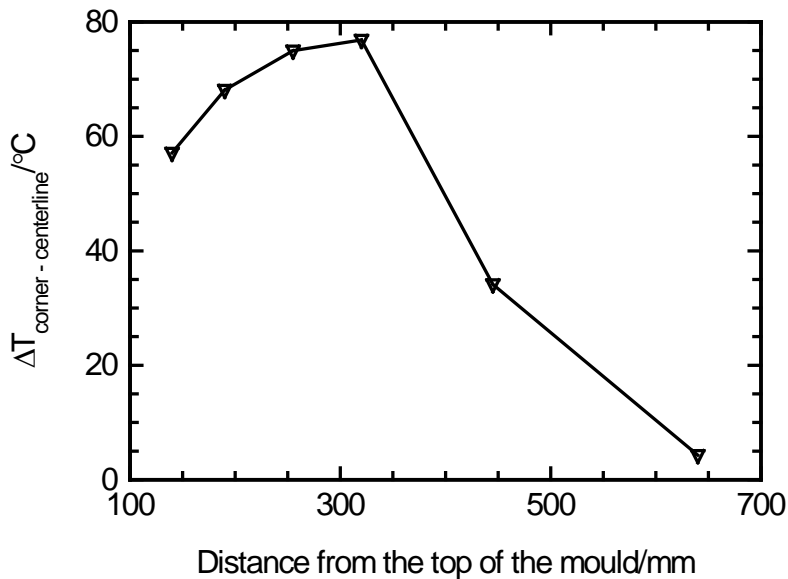


**Figure 104.** Difference between average temperature of centreline and near corner positions of the experiments.

The convex nose or “gull-wing” shaped part of the mould is between the top of mould to about 390 mm distance. Figure 104 indicates clearly that the difference is about 57°C at 140 mm and the difference increases with the distances from the top of the mould up to 320 mm, where the largest value occurs. These differences are not desirable. It concerns both magnitude and the tendency that it increases with the distances from the top of the mould.

In the flat region of the mould which is below 390 mm to the end of the mould, the difference decrease with the distance down the mould and the difference is about 5°C at a distance of

640 mm from the top of the mould. This minor difference means also that the corner losing thermal contact at the end of the mould, especially at the south west/lower corner due to the bending operation.

Additional photos of etched corner of sequence 25735-6 have been analysed. These photos are shown in Figure 105-106. The corresponding temperature measurement near the corner (39 mm) is shown in Figure 107, conclusions:

- At the north upper side corner, Figure 105, the structure is fine grained at the wide side part of the corner but coarse grains come quite near to the corners, 10-20 mm, at narrow side part of the corner.
- At the south lower side of the corner, Figure 106, coarse grains longer from the narrow side, approx. 30 mm. This can be due to better contact on the south side in the upper part of the mould (see Figure 107).

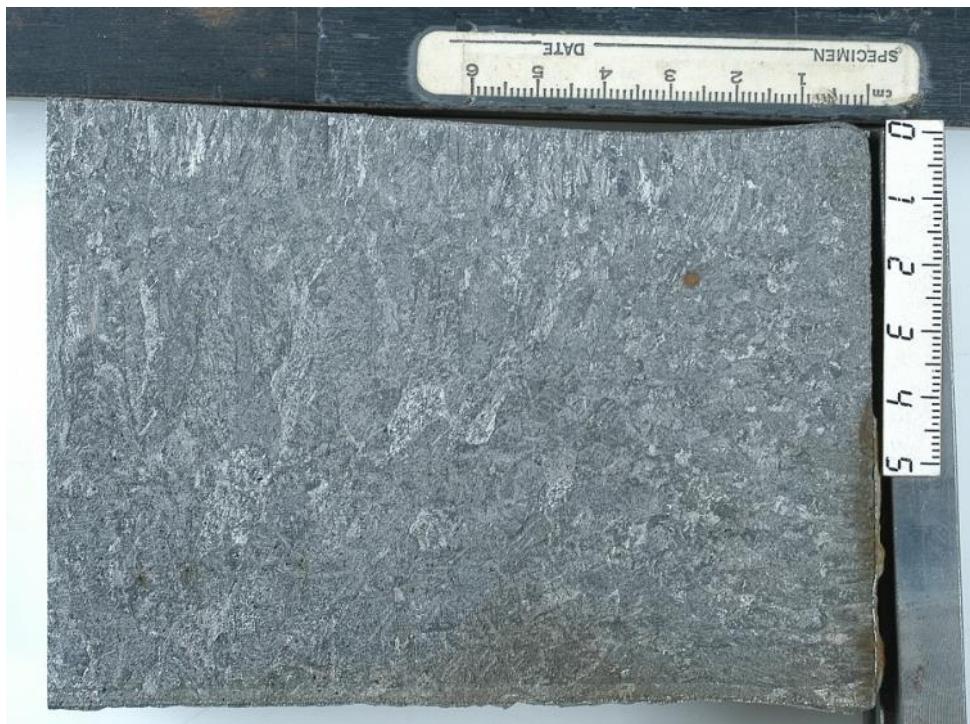


**Figure 105.** *East narrow side north/upper corner with a ruler for sequence 25735-6, narrow side horizontal.*



**Figure 106.** East narrow side south/lower corner with a ruler for sequence 25735-6, narrow side horizontal.

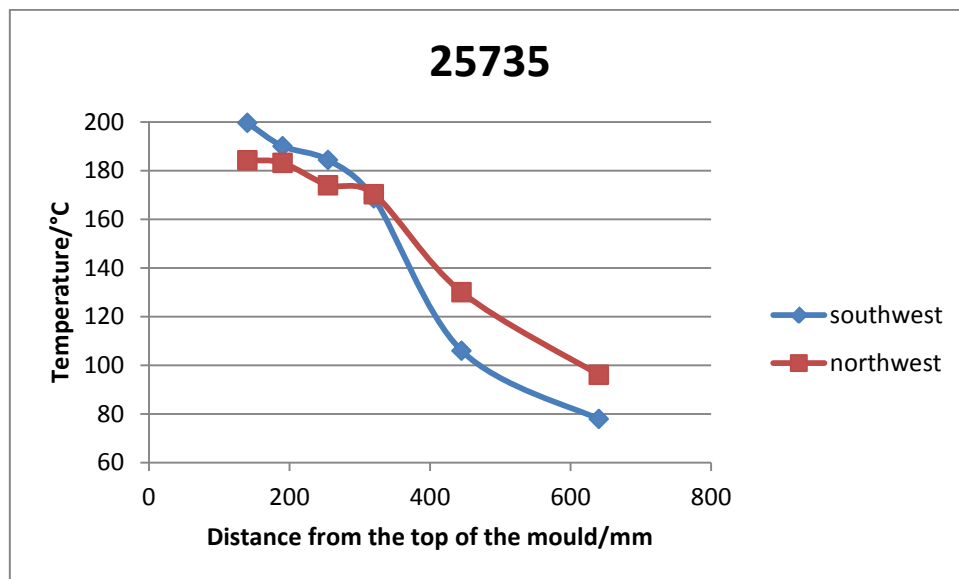


**Figure 107.** Average temperature near corner (39 mm) versus distance from the top of the mould.

A comparison with previous measurement in the soft cooling project of centerline positions is shown in Figure 108.

The depth in the copper plate of thermocouples is larger in this project, which means that values are lower than the previous measurements.

### Centerline:

It is possible to make different probable interpretations of the measured temperatures in the mould. From the middle (about 300 mm) to the end of the mould, the temperature curves of the centerline are roughly parallel to each other (slope of  $-0.03^{\circ}\text{C}/\text{mm}$  and  $-0.04^{\circ}\text{C}/\text{mm}$ ). That means there is no significant difference between the lower part of the mould and the previous reference mould.

In the upper part of the mould there is difference in peak value ( $142^{\circ}\text{C}$  and  $156^{\circ}\text{C}$  of the soft cooling project) at the meniscus, but the peak is not maintained in the same way ( $-0.12^{\circ}\text{C}/\text{mm}$ , between 130 mm to 190 mm of soft cooling project). Instead there is a more pronounced decrease with a slope  $-0.27^{\circ}\text{C}/\text{mm}$ , which indicate lack of thermal contact, in that part of the mould.

### Corners:

The thermocouples near the corner (39 mm) have a slope of  $-0.16^{\circ}\text{C}/\text{mm}$  between distances of 140 mm to 320 mm. That is near the magnitude of the centerline of the soft cooling project  $-0.12^{\circ}\text{C}/\text{mm}$ . Below 320 mm the slope is  $-0.24^{\circ}\text{C}/\text{mm}$ . That is about 8.5 times larger than the corresponding centerline slope. A possible interpretation is that corner loose thermal contact in the lower part of the mould or that very good thermal contact in the upper part cooled the steel corner in that magnitude, that it is much cooler than the centerline positions. Without modelling tools it is very difficult to determine which case is most probable but we believe in the first explanation, corners losing contact below 32 mm down in the mould.

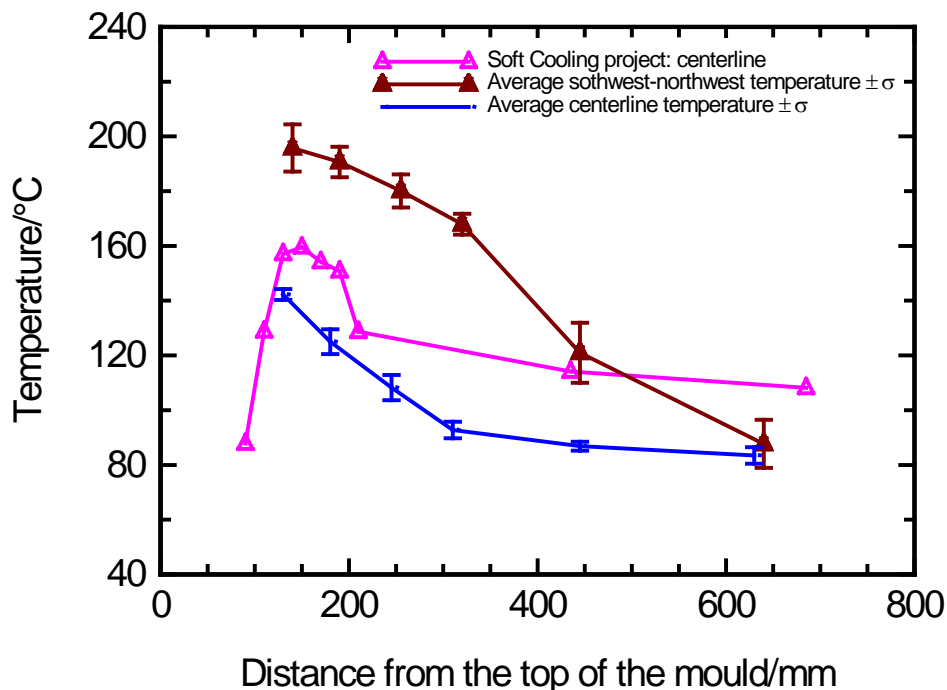


**Figure 108.** Comparison with previous measurement in the soft cooling project of centerline positions.

The final conclusion is that the convex nose or “gull-wing” produces poor thermal contact in the upper part of the mid of the narrow face. No numerical evaluation has been made to investigate the reason for this but lack in taper in relation to nearby parts can be one reason.

The recommendation for further work is to remove the convex nose or “gull-wing” curvature at the upper part of the mid of the narrow face according to Figure 109. New experiments to investigate whether the thermal contact will be improved have been proposed based on a new design with a “flat nose”.

The tilt of the narrow sides during casting should also be considerably higher than the maximum 8 mm used in this trial.

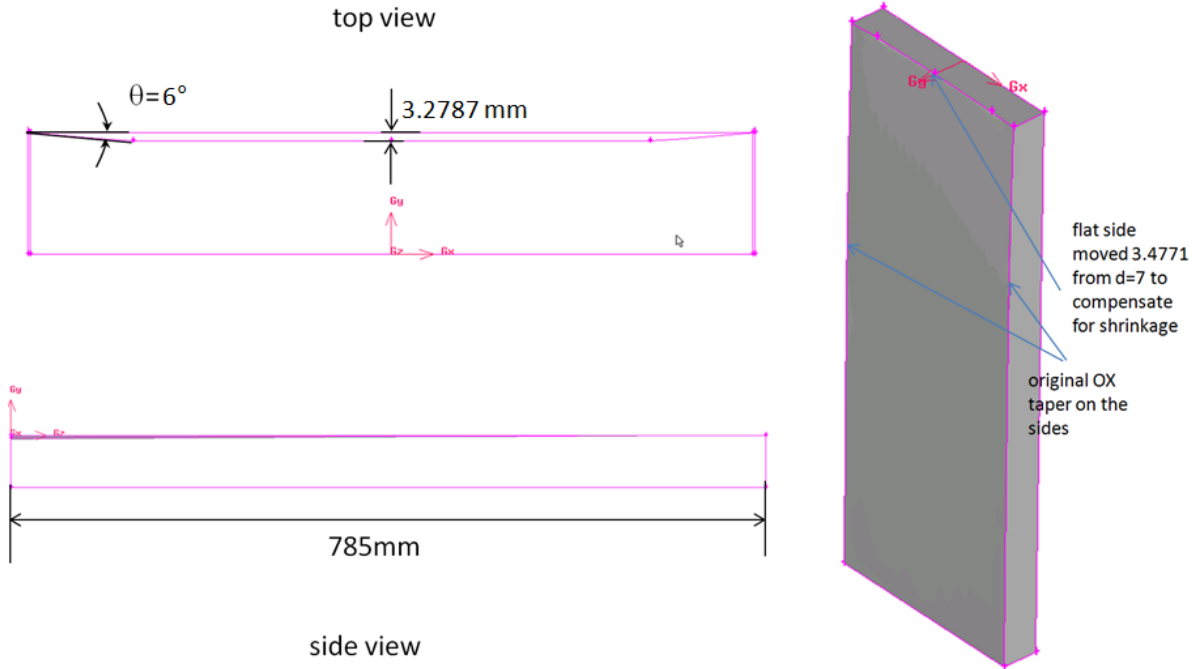


Figure 109. New proposed mould design.

**8. POTENTIALS OF ENERGY SAVINGS BY USING OPTIMISED CC MOULDS**

The total potential for reduced energy consumption, for crack sensitive steel grades, is about 75 GWh/year of which 15 GWh/year, could be reached by optimisation of CC moulds. By reducing the number of cracks surface grinding can be reduced (lower electrical consumption) and also fewer rejects needed (lowering the need for production of new material) which results in an overall higher productivity. Conversion to continuous casting for steel grades which are currently produced by ingot casting could achieve an additional reduction of energy saving of 20 GWh/year. Another possible future outcome of the project is the possible development of new grades with high market potential since some of these are very difficult to cast in ordinary CC moulds.

The project did not reach the expected results regarding improved surface quality but it built a strong competence base of CC mould optimisation regarding design methodology, instrumentation of moulds and ways to analyse the plant results. This competence base will be used for future work to optimise the CC moulds which has become ever more important due to the strong development of new, more advanced steel grades at SSAB EMEA and SMT.

With the continued work of CC mould optimisation 80 % of the potential energy savings are estimated to be achieved after 5 years of the project closure, while 100% is estimated after a

10 year period. A successful project which includes implementation can be carried out without any large investments at SSAB EMEA, Oxelösund and Sandvik Materials Technology.

## **9. SUGGESTIONS FOR FURTHER RESEARCH AND IMPLEMENTATION EFFORTS**

Although the optimized mould for SSAB EMEA did not meet the required expectations, there are ideas on how to proceed further. The design work for both SSAB and SMT has clearly shown that it is far more complex to construct an optimized mould than expected. The way forward is to consider only one design feature at a time. The following actions are proposed to address the shortcomings of this project:

- Additional calculations and adjustments of the delivered mould design for SSAB Oxelösund (there are possibilities to produce an improved mould and in the long term it should be possible to meet the energy goals).
- Test in full scale production of the proposed new parabolic shape of fix- and loose side on SMT plate mould 365x265 mm.
- Restricting the current design only to the corners and parabolic taper everywhere by removing the “convex” part, or nose, in the current experimental SSAB Oxelsösund design would improve the thermal contact in the mid of the narrow side.
- Further development should also include larger total tilting of the narrow sides.
- Design of an optimized mould shape that fully accounts for the shrinkage of slabs and blooms should be carried out in a stepwise manner.
- There is probably an interaction between shape changes in the mould. With new settings or new features, there might be a need for adjusting previous settings.

## **10. ACKNOWLEDGEMENTS**

This work was financially supported by the Swedish Energy Agency and Jernkontoret Technical Area 24, and in kind contribution by SSAB EMEA Oxelösund and Sandvik Materials Technology. We would like to thank the chairman Dr. Jesper Janis and Lars-Henrik Österholm, Jernkontoret, for their work within the project and Carl-Åke Däcker for transforming the previous technical report to a final report to Swedish Energy Agency.

## 11. REFERENCES

- [1] JK 2417/90
- [2] Patent WO 96/35532
- [3] Patent WO 96/35533
- [4] Brolund B., Rogberg B., *Kokillutformning lämplig för reduktion av termisk töjning i stelnade strängskal*, JK2430/94, 1997.
- [5] Bruce H., Andersson P., Hertzman S., Wass S., *Design och erfarenheter från fullskaleförsök med IMMODOCO kokill för stränggjutning av blooms*, TO24-144, April 2000.
- [6] Bruce H., Andersson P., Hertzman S., *IMMODOCO kokill för stränggjutning av slabs - design nr 1 och erfarenheter från fullskaleförsök*, TO24-121, Nov 2001.
- [7] Bruce H., Andersson P., Hertzman S., *IMMODOCO kokill för stränggjutning av slabs - design nr 2 och erfarenheter från fullskaleförsök*, TO 24-122, Nov 2001.
- [8] Bruce H., *Driftsförsök med IMMODOCO kokill vid Avesta Polarit - förstudie*, TO24-141, Maj 2003.
- [9] Johansson A., *Kartläggning av hörnvinkelkontraktion vid stränggjutning – examensarbete*, TO24-142, Nov 2003.
- [10] Bruce H., *IMMODOCO – ny kokilldesign – slutrapport inom JK 20405/02*, TO24-154, Dec. 2005.
- [11] Kristiansson J-O., *Stress and strain during solidification*. Dissertation 1983, Chalmers University of Technology, Gothenburg Sweden.
- [12] Däcker C-Å., Eggertsson C., Andersson S.P., Salwén A., *Development of a CC mould with soft cooling properties for casting of crack sensitive steel grades, Final Report*, JK D835, Nov. 2010.
- [13] Mattsson K., SSAB OXELÖSUND, Report 2001-04-01, Identity MS 2001353 U5.

## Projektorganisation och deltagare

### Forskningskommitté

JK 24055

Energimyndighetens projekt 35337-1

### Projektperiod

2012-01-31– 2013-08-31

### Ordförande

Jesper Janis

Outokumpu Stainless AB

### Projektledare

Peter Andersson

Swerea KIMAB

### Forskningschef

Lars-Henrik Österholm

Jernkontoret

### Industrimedlemmar

Arashk Memarpour

Sandvik Materials Technology

Bo Rogberg

Sandvik Materials Technology

Sohrab Azar

Sandvik Materials Technology

Christer Nilsson

SSAB EMEA Luleå

Tomas Sohlgren

SSAB EMEA Oxelösund

### Adjungerade forskare

Peter Andersson

Swerea KIMAB

Carl-Åke Däcker

Swerea KIMAB

Christer Eggertson

Swerea KIMAB

Fatemeh Shahbazian

Swerea KIMAB

Pavel Ramirez-Lopez

Swerea MEFOS





## **DEN SVENSKA STÅLINDUSTRINS BRANSCHORGANISATION**

Organisationen grundades 1747 och ägs sedan dess av de svenska stålföretagen. Jernkontoret företräder stålindustrin i frågor som berör handelspolitik, forskning och utbildning, standardisering, energi och miljö samt skatter och avgifter. Jernkontoret leder den gemensamma nordiska stålforskningen. Dessutom utarbetar Jernkontoret branschstatistik och bedriver bergshistorisk forskning.

# **JERNKONTORET**

Box 1721, 111 87 Stockholm • Kungsträdgårdsgatan 10  
Telefon 08 679 17 00 • Fax 08 611 20 89  
E-post [office@jernkontoret.se](mailto:office@jernkontoret.se) • [www.jernkontoret.se](http://www.jernkontoret.se)

